Politecnico di Torino

Master’s Degree in Geo-Engineering

a.y. 2021/2022

3D AND 2D NUMERICAL MODELS OF MECHANISED EXCAVATION OF OVERLAPPED TUNNELS IN URBAN AREA: SENSITIVITY ANALYSIS OF THE STRESSES AND THE STRAINS IN THE SEGMENTAL TUNNEL LINING VARYING THE EXCAVATION SEQUENCE.

Supervisors:

Prof. Daniele PEILA

Eng. Michele PALOMBA (Systra SWS)

Candidate:

Emanuela Malvaso

INDEX

INTRODUCTION

In the world the increasing need of the improvement of the transportation infrastructures led to the construction of twin tunnels at shallow depths. For this reason, the aim of this thesis is to analyse the interaction between two overlapped tunnels changing the construction process.

The thesis focuses on the project of the metro M5 of Bucharest, designed by the company SYSTRA SWS, in which the work of thesis has been realised.

The subways want to improve the underground network with the aim to reduce the congestion on the surface. This new metro line is characterised by two twin tunnels, which change their relative position along the alignment. Most of the arrangement is in horizontal configuration, however approaching the stations, it becomes offset and then piggyback. The excavation of the tunnels is realised with an Earth Pressure Balance machine.

The study evaluates the acting loads and the resultant deformations on the segmental tunnel lining changing the construction process and the layout of the two tunnels. This aim is fulfilled by numerical FEM analysis in three and two dimensions.

The 3D numerical model is realised with the software MIDAS FEA NX, which is able to simulate the three-dimensional effects of the excavation. Moreover, the 2D numerical model is developed with the software PLAXIS 2D.

As first **in the chapter 2**, the segmental tunnel lining is described considering all the parts and materials which compose it, in order to understand how it responses to the change of the excavation sequence. Moreover, the theory behind the structural behaviour of the segmental tunnel lining of both the tunnels, is highlighted in order to evaluate if the induced forces and moments, can be compared with the resistances of each ring.

In the **chapter 3**, the cases history of already built twin tunnels are summarised to obtain a global view of the practical problems.

The 3D numerical simulations are treated in the **chapter 4**, in which the main steps able to correct design a 3D model is presented. The 3D model allows the most accurate representation of the reality; in particular the excavation process, taking into account the passage of the shield, the installation of the segmental lining and the injection of the grout.

Furthermore, **in the chapter 5** there is the description of the 2D models. In order to simulate the advancement of the machine two different methods are applied: the method of the deconfinement and the method in which an internal radial pressure is applied.

Finally **the chapter 6** presents the results of the analysis and their interpretation.

1. THE PROJECT OF METRO LINE 5 OF BUCHAREST

In the recent years, the city of Bucharest is facing a huge development, caused by increasing population density, growing economic activities and the importance of the city, being the capital of Romania. For these reasons, the city requires an extensive infrastructures fulfilment to increase urban mobility.

The underground existing network is composed by four main lines with a total covered length of 69.25 km, which transports over 650000 passengers per day, as shown in Figure 1. The stations are 51 with an average distance between them of 1.5 km.

Figure 1 Existing underground network

The line 5 of Bucharest connects West to East sides of the city, in particular from Drumul-Taberei district to Pantelimon area. These two zones are served by surface transport, as buses, trolleybuses and tram. This led to high traffic congestions: a technical report on surface transport made in 2015, showed an average value of the commercial speed of about 13 km/h, therefore the travel time exceeded 60 minutes. Regarding the private traffic, the vehicles per day recorded are 30000 and the average velocity is 32 km/h. Hence the need to improve the public transport network occupies a key role for the future of the city, in order to address to the phenomenon of urban congestion.

Summarizing, the scopes of the work are:

- Accessibility;
- Minimum time on the origin-destination route;
- Safety and comfort of the passengers;
- Minimize environmental impacts (noise, pollution, useland…);
- Improve the transport capacity;
- Modernize public transport infrastructures.

1.1 Description of the project

The alignment of line 5 crosses the city of Bucharest in a West-Est direction joining three major areas, as reported in Figure 2: Drumul Taberei district, Bucharest Centre and Pantelimon district. The line 5 Drumul Taberei- Pantelimon includes 22 stations: Valea Ialomitei, Raul Doamnei, Brancusi, Romancierilor, Parc Drumul Taberei, Drumul Taberei 34, Favorit, Orizont, Academia Militara, Eroilor, Hasdeu, Cismigiu, Universitate, Calea Mosilor, Traian, Piata Iancului, Victor Manu, National Arena, Chisinau, Morarilor, Sfantul Pantelimon, Vergului.

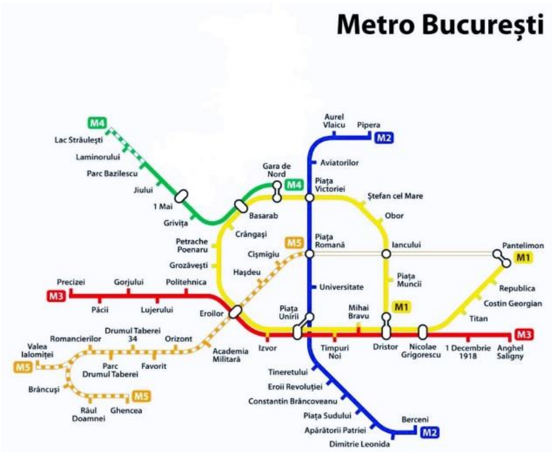

Figure 2 M5 Metro Line

The line 5 allowed the interconnections with the others metro lines, in correspondence of the stations Eroilor, Universitate and Piata Iancului.

The project is subdivided in the construction of three main structures:

- Tunnel, which is constructed with mechanised shield method or with Cut and Cover open excavation;
- Station: open excavation supported by temporary and permanent structures;
- Gallery: it is an extension of the station structures used for manoeuvring and is built in open excavation.

The stations and galleries are constructed by top-down procedure due to lack of space on the surface and time restriction. The overburden of the station is at least 2 meters. The selected construction method involves the execution of diaphragm walls and slabs from top to bottom in order to ensure the stability and sealing of the excavation.

The tunnel is excavated with Earth Pressure Balance EPB machine, which is able to adjust the excavation pressure based on the characteristic of the soil. The operational mode of the machine is Fully Closed mode. The general design aspects are:

- The overburden is from 10 to 14 meters, also reaching 28 meters. In order to guarantee the stability condition, a minimum overburden is considered, as 1.5 times the diameter of the machine;
- The internal diameter of the segmental lining is 5.7 meters;
- The thickness of the segmental lining varies between 25-35 centimetres;
- The width of the segmental lining ranges between 1 – 2 meters.

1.2 Geological and hydrogeological situation

From the geological point of view, the Bucharest area can be classified in seven main layers, starting from surface (in brackets the thicknesses are highlighted), as in Figure 3 :

1. Anthropogenic filling and topsoil (3 – 10 m);

2. Upper clay sandy complex which is subdivided in three subcomplexes: Dambovita-Colentina interfluvial domain (2 – 5 m), Baneasa-Antelimon (10 – 16 m) and Cotroceni-Vacaresti (3 – 6m);
3. Colentina gravel complex (1 – 20 m);
4. Intermediate clay layer (0 – 25 m);
5. Sands of Mostistea (1-25 m);
6. Lake complex (20-50 m);
7. Fraternal complex.

From the hydrogeological point of view, the Dambovita river crosses the route of the future metro in the left side. In addition there is the presence of three main aquifers in a depth range between 4 and 50 meters, as in Figure 3:

- The aquifer of Colentina gravel: it is made up of coarse sediments and it is located at a depth of 15-20 meters. The hydraulic conductivity is about 20 m/day.
- The sands of Moististea aquifer: is located at 20 – 42 meters depth. Its hydraulic conductivity has a value which ranges between 3-15 m/day.
- Fratesti aquifer system: it is a confined aquifer.

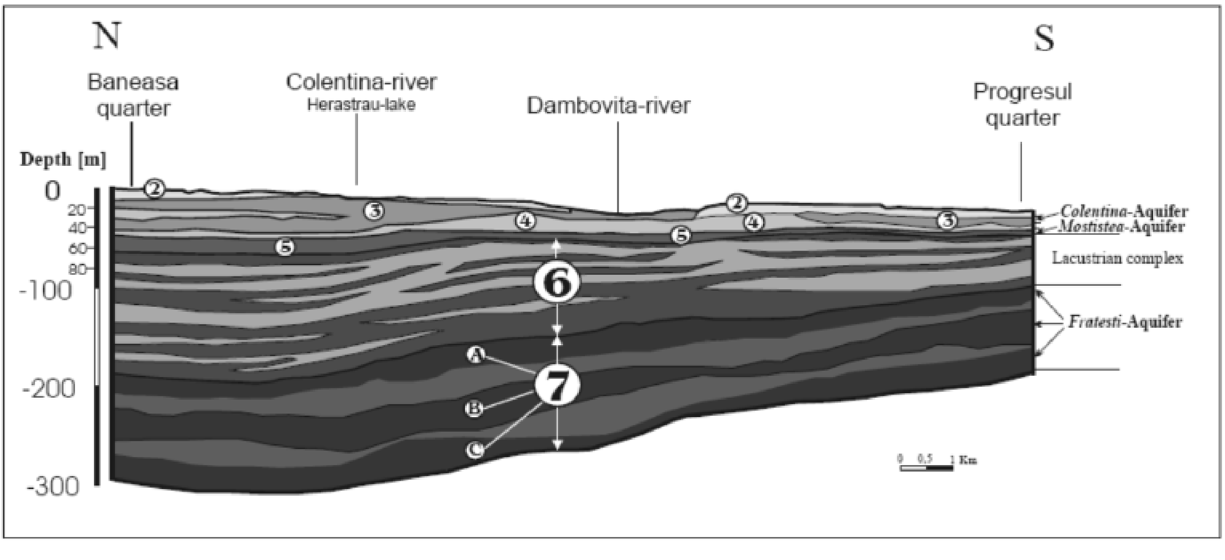

Figure 3 Stratigraphy of the project area

1.3 Earth Pressure Balance

The Earth Pressure Balance Shield Machine, Figure 4, provides support on the face front and on the cavity. The support of the cavity is guaranteed thanks to the presence of the steel shield; on the other hand the face stability is provided with the treated excavated soil. The EPB machine has different advantages with respect to the Slurry Shield or compressed air machine: it is able to better control the surface settlement, it does not require a separation plant for the re-use of the bentonite, leading to the reduction of the needed space on the surface and of the costs.

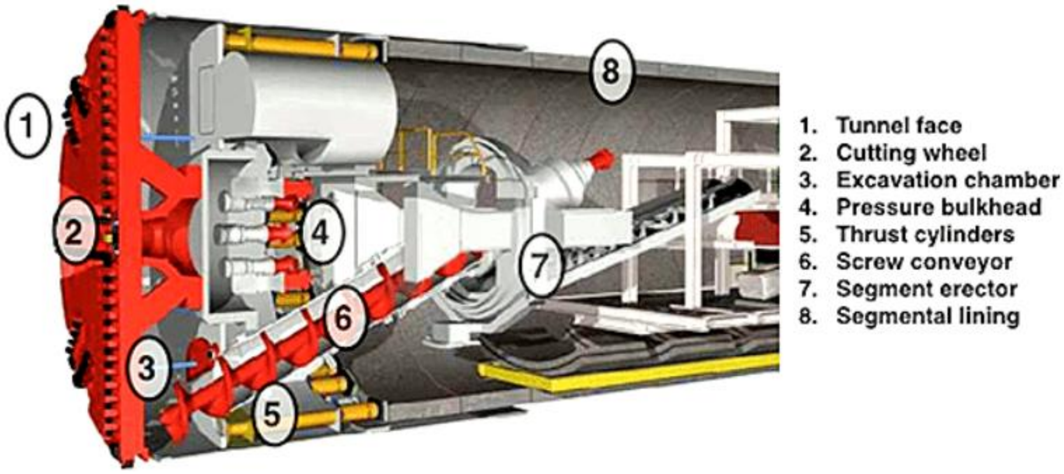

Figure 4 Scheme of Earth Pressure Balance

The excavation of the soil is provided by the rotation of the cutterhead, which has particular cutting wheels based on the type of ground. The advancement of the machine, thanks to the thrust cylinder, will induce an excavated volume, then the material is mixed with conditioning agents and pushed against the soil to be excavated transferring the thrust force from the shield jacks to the tunnel face. The excavated material, after it is modified or conditioned, comes out from the excavation chamber through a screw conveyor. It has two main goals:

- Transport the excavated material from the excavation chamber to the conveyor belt;

- Regulate the pressure inside the chamber to counterbalance the groundwater and ground pressures.

By adjusting the speed of the cochlea, the applied support pressure changes, because the amount of conditioned soil inside the chamber changes. At the end of the screw conveyor there is the conveyor belt. It's important to have a nil pressure at the end of the auger, in order to better lie down on the conveyor belt. Hence, the length and the inclination of the screw help to reduce the pressure, usually 0.2 bar per helix. Once the muck is on the conveyor belt, it arrives outside the tunnel and then it is transported to the surface. The conveyor belt is able to storage and incorporate the belt by advancing, in order to cover the entire length of the excavation from the screw up to outside. It is called extendible conveyor belt and it is possible to incorporate about 400-500 meters**.**

The advancement is mainly guaranteed by the thrust, while the excavation by the torque transmitted at the cutter head.

The thrust force (Σ_W) is applied by the hydraulic thrust cylinders, which are located all around the circumference of the machine. The thrust is transferred from these elements to the conditioned soil through the bulkhead in order to avoid uncontrolled penetration. It depends predominantly on the friction of the shield coat during the passage inside the soil, the maximum applicable thrust force of the single tool and on the requested support pressure. Its maximum value must be limited to avoid the faiulure of segment contact areas where thrust is exerted. Its computation is done as follow:

$$\Sigma_W = \mathrm{W}_M + \mathrm{W}_{Sch} + \mathrm{W}_{BA} + \mathrm{F}_S + \mathrm{F}_{NL} + \mathrm{F}_{SP}$$

Where:

- W_M is the friction of the shield coat;
- W_{Sch} is the thrust resistance of the cutting edge;
- W_{BA} is the maximum tool thrust force;

- F_S is the drag force tailskin seal;
- F_{NL} is the drag force back-up system;
- F_{SP} is the support pressure.

However, the torque (T) is provided by several hydraulic motors, which transmit the rotation to the cutter-head via a gear rim. The torque is empirically evaluated by taking into account the diameter of the machine (D) and a coefficient (α), which has been evaluated studying a huge amount of case histories. A significant variation of this last parameter during the excavation can be evidence of problems, which are occurring in the excavation chamber.

$$T = \alpha * D^3$$

The α coefficient has a high value compared to that one for the slurry machines because of the greater density of the conditioned material, which ranges between 2 – 3 for the EPB and 0.75 – 2 for the slurry.

The EPB machine is equipped with an installation system of the final lining. After completing a cycle of advancement, a ring of lining is installed. There are three existing types of rings:

- Rectangular ring which has all the sides equal;
- Tapered ring that has one side perpendicular and the other inclined with respect to the longitudinal direction;
- Universal ring with both the sides inclined.

Nowadays the most used is the universal ring; the tapering (ΔL) must be evaluated:

$$\Delta L = \frac{R_e - L}{0.8 * R_t}$$

Where:

- R_e is the radius of the ring at the extrados;

- L is the length of the smallest side;
- R_t is the radius of the alignment.

Every ring is composed by pre-casted elements called segments, divided in three families: normal, counter-key and key. Typically, the number of the segment for each ring is six. The thickness of the lining ranges normally from 30 to 70 cm and it can vary depending on soil and water pressures.

The segments are assembled starting from the bottom element up to the key: their installation is made by an erector that works with vacuum. Since they are installed below the shield where the confining pressure is not acting, the stability is guaranteed by elements like connectors, bolts and dowels. Moreover, the water tightness is ensured by the gasket which is a rubber element glued all around the segment.

The segments are produced in a plant close to the construction site in a quantity that guarantees the continuous feeding of the machine.

The main problem with the use of a tunnel boring machine is the formation of an annular void due to the overcut of the cutter head, the conicity of the shield, the thickness of the shield and the thickness of the steel brushes, as shown in Figure 5. If this gap is not filled just after its formation, a ground surface settlement can arise. The dimension of the annular gap ranges between 10 and 20 centimetres.

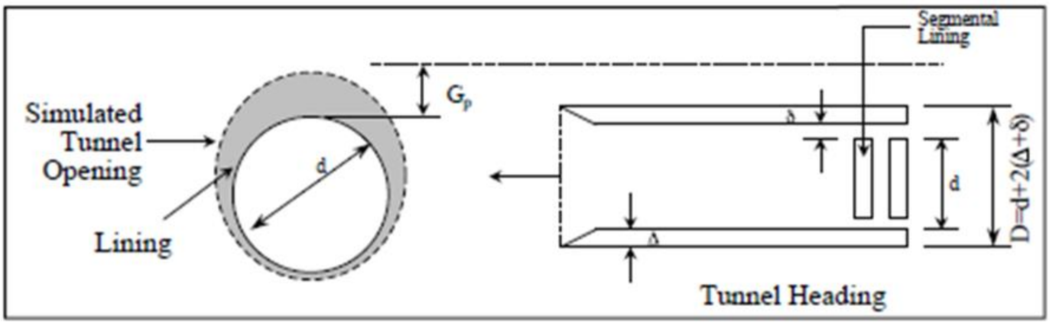

Figure 5 Dimension of the annular gap (Loganathan, et al., 1998)

The solution of this problem is the backfilling. Nowadays, the most used grout for this purpose is the two-component grout. This material is characterised by two parts: the component A and the component B. Water, cement, bentonite and retarding/fluidifying agent compose the first one, while the second one is only an accelerator. This innovative solution led to a series of advantages:

- It reduces the vertical displacement whatever the soil is;
- it is able to enter in the gap with small energy reducing the load on the coatings due to the small viscosity;
- the storage capacity is high due to the presence of the retardant;
- the mechanical performances are developed in a few seconds after the injection;
- the permeability is very low due to the presence of the bentonite;
- the resistance to the water washout is very high due to the almost immediate gelification;
- low risk of blockage of the injection pipes thanks to the absence of aggregates and the use of bentonite;
- very easy transport and pumpability because the low viscosity and great volumetric stability;
- the practicability in the use of this material in relation to the reduction of the operative action to install it.

The implementation of this grout is in continuous during the advancement with an injection from some grouting ports on the tail skin at a pressure greater than that of the excavation in order to minimise the immediate displacements.

The Earth Pressure Balance machines nowadays are the most used machines in the world for the projects in shallow tunnel in urban area. When the soil has stiff consistency (Ic>1), high cohesion and low permeability it is possible to work without support pressure. The conditioning can be obtained only with water for soils falling in Area 1, as Figure 6 . If the material is coarser and it falls in Area 2, as in Figure 6, the foam is added. When the soil becomes coarser and more grained like in Area 3, the soil is conditioned with foam, water and, if necessary, with bentonite, filler and different types of additives like polymers and anti-clogging, as in Figure 6. The limits of application are determined by the permeability and the groundwater pressure: in fact, the permeability should not exceed the 10^{-5} m/s.

Moreover, the diameter of the chips should be limited to avoid damages to screw conveyor, since in EPB machines, the crusher is absent.

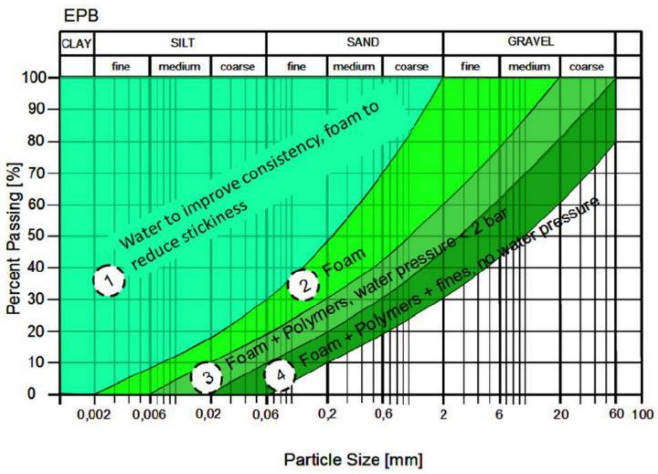

Figure 6 Application ranges of the EPB shield (DAUB, 2016)

The cutterhead of the machine has large percentage of openings: the higher is this value, the lower is the amount of cutting tools. The selection of the cutting tools is based on the type, the resistance and the abrasiveness of the encountered soil and on the content of clay or quartz. On the periphery of the circular head there are also the overcutting tools, which permit an over-excavation in order to help the shield to pass easily and to not block inside the above and bottom soil. On the face there are also different nozzles to spray the conditioning agents, which allow to mix the soil ahead of the face and then to enter in the chamber.

To support and provide the rotary movement to the cutting head, several hydraulic motors work in parallel in order to transfer the motion to the head. This part is always filled with grease because it avoids the entrance of particles inside the gear, which can be seriously damaged.

On the upper part of the EPB the air lock is fundamental when it is necessary to enter in the working chamber by the personnel. This part allows the acclimatization to the pressure in the chamber, in entrance, or to the atmospheric pressure at the return. The presence of the air lock is fundamental for avoiding health problems during the permanence of the personnel, because inside it they are exposed to a gradually increase of pressure.

2. SEGMENTAL TUNNEL LINING

2.1 Introduction

The segmental lining has to withstand different functions in terms of construction and operation phase.

- Operational constraints: to act as permanent lining and to support varying the environment condition. Regarding the cover action it has to consider mainly that the lining has to prevent the water or any type of fluid inflow, but also the leakage from the tunnel itself. The lining has to provide support for permanent service and for mobile or fixed equipment;
- Construction constraints: it has to offer immediately support, especially in longitudinal direction in order to help the penetration of the ground. During this stage the lining has to be able to support all the back-up equipment and construction plant in the machine.

The segmental lining follows different stages: manufacturing, transportation, installation and the final service condition. The production and transportation include: the demoulding, the storage on the surface, transportation inside the machine and the handling through the ring erector. During the construction stages on the installed ring is applied the thrust of the jacks for permitting the advancement of the machine, then the grouting pressure both primary and secondary. Finally the main service condition includes the support of the ground, of the groundwater and of the surcharge on the surface.

In the Table 1, some examples of loads during the life of the segments are presented with the factors of safety (ACI-544.7R, 2016), (ITA Working Group 2, 2019).

Table 1 Loads on segments

LOAD CASE	LOAD FACTORS
Demoulding	1.4*W
Storage	1.4*(W+F)
Transportation	1.4*(W+F)
Handling	1.4*W
Thrust jack forces	1.2*J
Tail skin grouting	1.25*(W+G)
Secondary grouting	1.25*(W+G)
Earth pressure and groundwater	1.25*(W+WA)+1.35*(EH+EV)+1.5*ES
Longitudinal joint bursting	1.25*(W+WA)+1.35*(EH+EV)+1.5*ES
Additional distortion	1.4*M

Where:

- W: self-weight of the segment;
- F: weight of the segments placed above;
- J: TBM jacking force;
- G: grout pressure;
- WA: groundwater pressure;
- EH: horizontal ground pressure;

- EV: vertical ground pressure;
- ES: surcharge load;
- M: additional distortion effect.

2.2 Segmental ring geometry

The precast concrete lining comprises a sequence of rings, placed at the rear of the TBM shield. These rings are divided into different sectors, called segment. The design of the segmental tunnel lining starts with a first attempt of the thickness, width and length of the segments and considering different loading cases. The final designed geometry, compressive strength and the amount of reinforcement are specified in order to ensure that the lining satisfied all the serve conditions.

Internal diameter of the bored tunnel : the intrados is evaluated considering the needed internal space based on the utilization of the tunnel(e.g. railroad or subway tunnel). For example in the double railroads, the intrados has to take into account the track structure, drainage system, emergency walkways.

Thickness of the segmental lining ring: the thickness has to be able to resist to all the loading cases and service condition. Basing on ACI, AFTES, if the internal diameters are greater than 5.5 meters, the thickness is 18-25 times the diameter; if the internal diameter is between 4 and 5.5 meter, the thickness can be in 15-25 times the intrados. (ACI-544.7R, 2016), (AFTES, 2005).

Length of the ring: it ranges from 0.78m up to 2.50m. The choice of the length must take into account different considerations like:

- if the length is shorter, it is easier the transportation and erection processes, it is better for construction of the curves and reduces the length of the shield tail;

- if the length is larger, it reduces production costs, the number of joints (so it is stiffer), number of bolts and gasket length, increasing the speed of advancement.

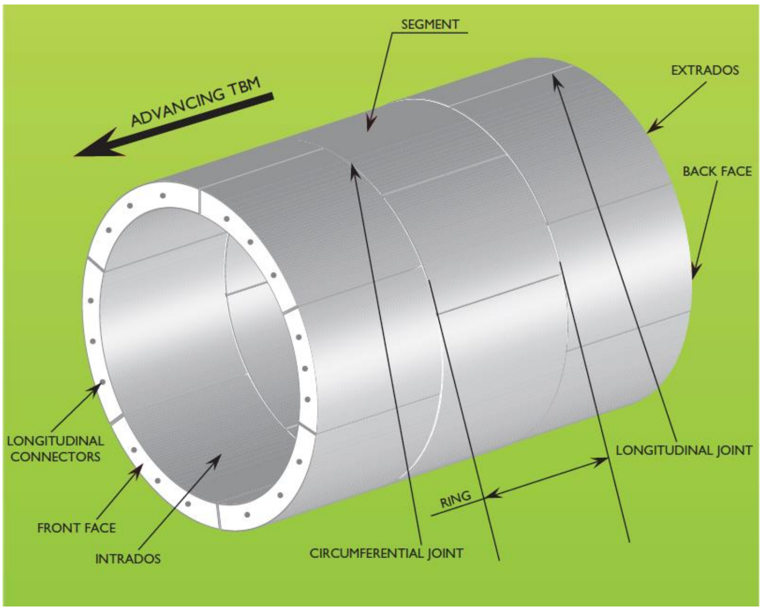

Figure 7 Nomenclature of the ring, (Guglielmetti, 2007)

Universal rings: the main advantage is that only one type of formwork is required for straight and curved pathways. The tapering k can be calculated :

$$k = \frac{\phi_A * b}{R}$$

Where:

- k: tapering, it is the difference between minimum and maximum width of the single segment;
- ϕ_A is the outer diameter of the segment;
- b is the mean ring width;
- R is the minimum curve radius.

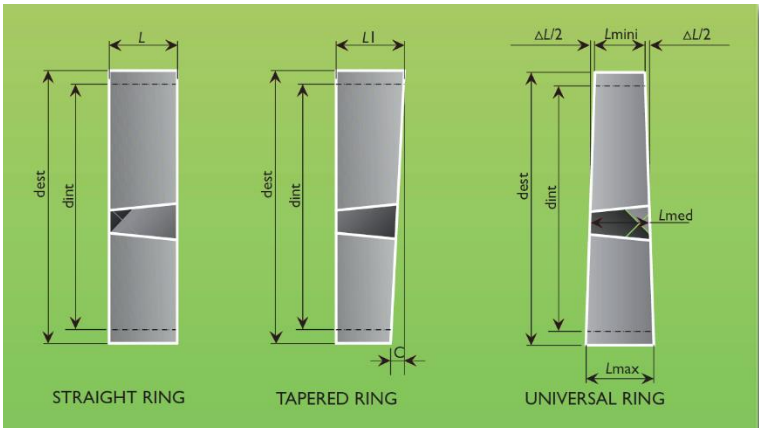

Figure 8 Various type of geometry ring (Guglielmetti, 2007)

When the machine has to follow a straight path, the rings are rotating of 180° every round, while during the curves the ring are partially rotating or putted the minimum faces in the same side.

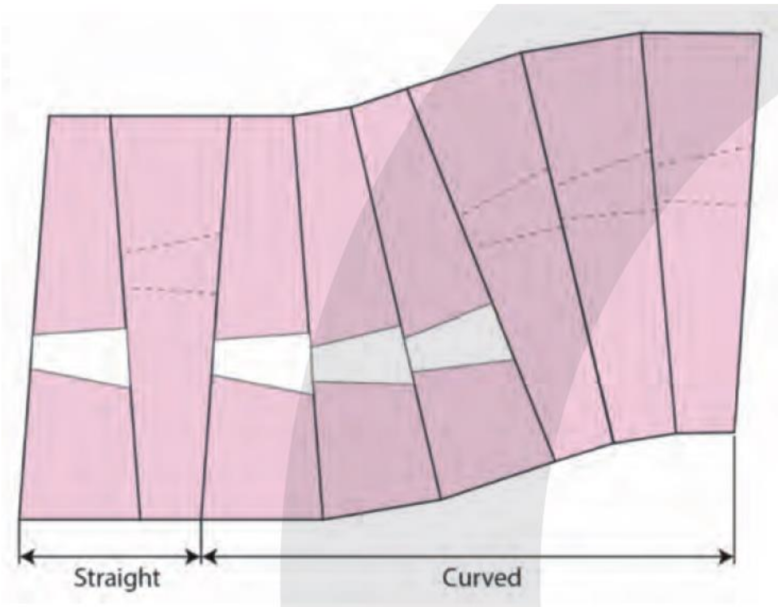

Figure 9 Representation of pathways, (ITA Working Group 2, 2019)

Slenderness ratio λ: it is important to determine the length of the segment. If the number of segments and the thickness of the ring increases, the slenderness and the flexural stresses reduce. The number of segments depends also on the position of the thrust jacks. Usually 6m diameter has 5+1 segments (1 key). If the diameter is higher than 6m, the number is 7 segments with a larger key.

Geometry of the segment during advancement (ring by ring):

In each ring three different types of segments are present: the key segment, the counter-key and the remaining ones. The key segment is the smallest one and has a shape of trapezoid . Its aim is to transfer uniformly the loads inside the rings. On the two sides of the key, there are the two counter-key, which have one side coincident with the key and the others parallel to the advancement. The remaining segments can be (Maidl, et al., 2011):

- Hexagonal: each element act as key. In this case the gaskets are not effective used, so the waterproofing of the lining is not satisfied;
- Rectangular : adequate watertightness but if dowels are pre-inserted it is difficult to place other segments without impacting on the gasket on the adjacent segment;
- Trapezoidal: half of the segments are installed as counter key and the others half as key segments. The disadvantage is that high thrust jack's forces are applied to the counter key while the key segment is installed;
- Parallelograms or rhomboidal: shape of parallelograms with counter key and key in the shape of trapezoid. The first to be installed is the counter key and then the parallelogrammical segment. This system allows continuous erection, improves sealing and permits faster operation during the connection with dowels.

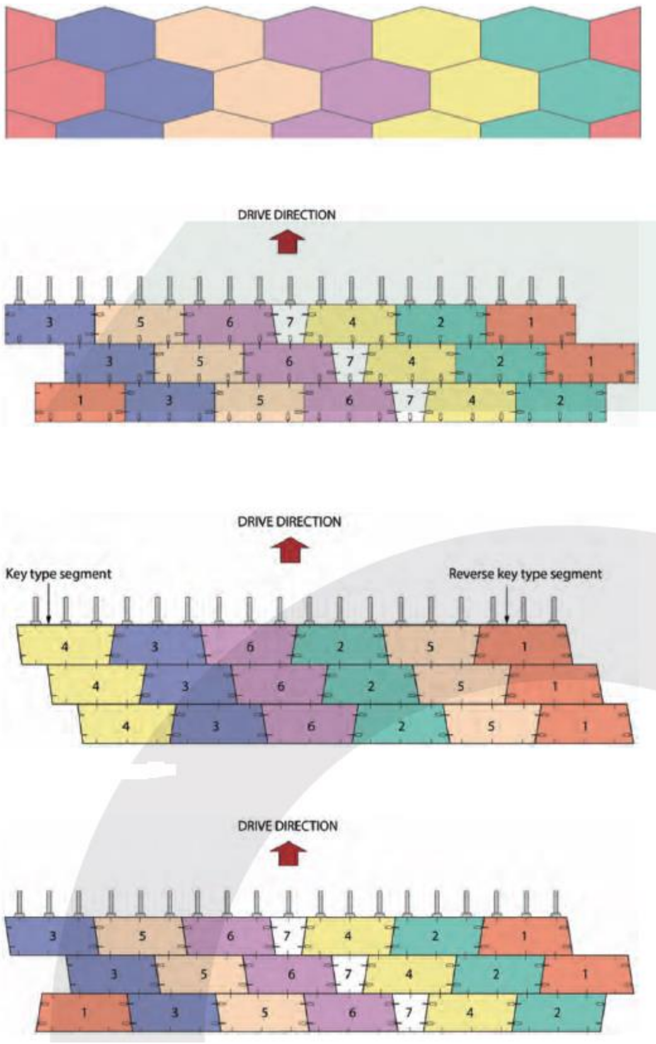

Figure 10 Types of segments (ITA Working Group 2, 2019)

Geometry of the joints: two types of joints are present in the lining: one is the longitudinal, created between two segments and the other, called circumferential, placed between two rings, Figure 11. They are zones subjected to a high concentration of loads. They reduce, in general terms, the stiffness of the ring lining, which is no more considered as continuous system.

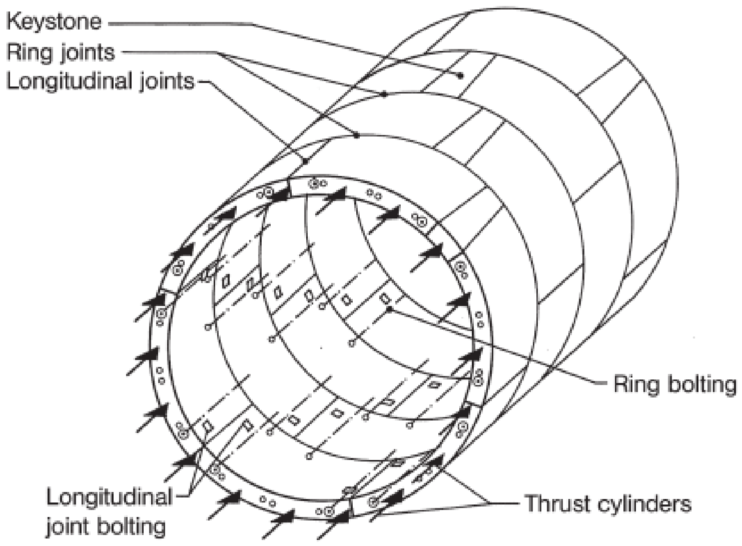

Figure 11 Joints (Maidl, et al., 2011)

The longitudinal joint run parallel to the tunnel axis. They transfer axial ring forces, bending moment and shear forces from external loading. By a structural point of view, these zones are modelled as hinges, due to the limited capacity to transfer bending moments. Longitudinal joints can have three main different surfaces: two flat contact surfaces, two convex contact surfaces and convex/concave contact surfaces (Maidl, et al., 2011).

- FLAT CONTACT SURFCES: they transfer axial compression, shear forces and bending moments. The rotation occurs at the contact surface thanks to compression strain;

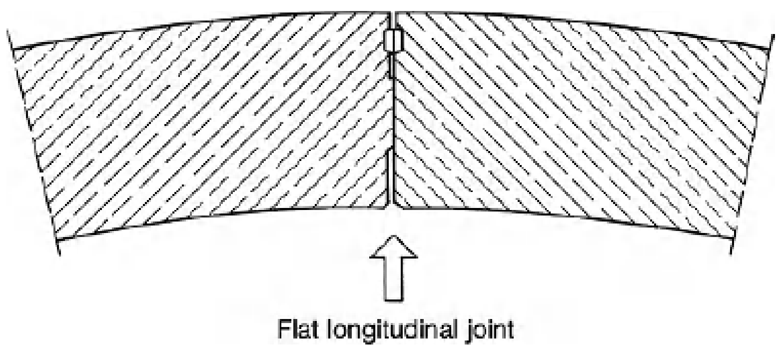

Figure 12 Flat contact surfaces (Maidl, et al., 2011)

- TWO CONVEX CONTACT SURFACES: if the compression forces acting at the contact surface are very high, two convex surfaces are recommended. The radius of the curvature has not to be too high, otherwise the rotation capability of the segments is limited, and at the same time not too small else the contact surface become small and not able to transfer the loads;

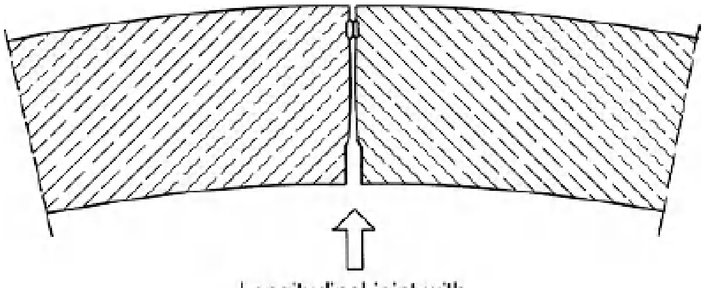

Figure 13 Two convex contact surfaces (Maidl, et al., 2011)

- CONVEX-CONCAVE SURFACES: these surfaces permit high rotation of the segments and in order to ensure this fact, the radius of curvature is large.

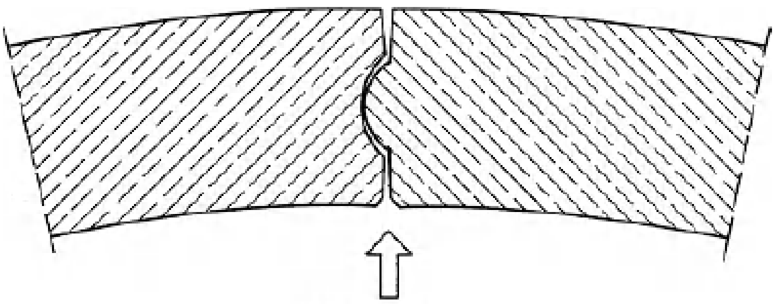

Figure 14 Convex- convex surfaces (Maidl, et al., 2011)

(Maidl, et al., 2011)

During the construction of the ring, the thrust jack forces are applied to the ring joints, through a pad, to increase the support area. In order to avoid high stresses and consequently formation of cracks, intermediate spacers, Figure 15, made of rubber bitumen, are glued in every ring joints, in order to form a virtual column.

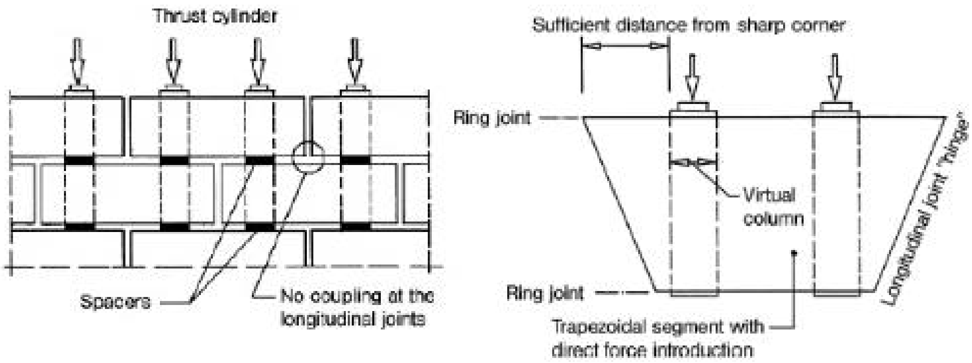

Figure 15 Rubber biutmen spacers (Maidl, et al., 2011)

2.3 Segmental lining design:

2.3.1 Production and transient stages

The production of the segments occurs in special precast concrete plant. When the project of a tunnel is larger, it is better to adjust and consider a production facility directly on site. The supply of segments is a fundamental part of the entire project, since they are always requested during all the time of the construction. The mixture of concrete is poured inside a steel formwork, in which there are already the steel reinforcement cage.

2.3.1.1 Demoulding

After six hours of curing, the segments is extracted from the formwork. It is important to consider the strength when the segment is lifted, typically by a vacuum erector. In the design this phase is modelled as a cantilever beam loaded by its weight, (ACI-544.7R, 2016).

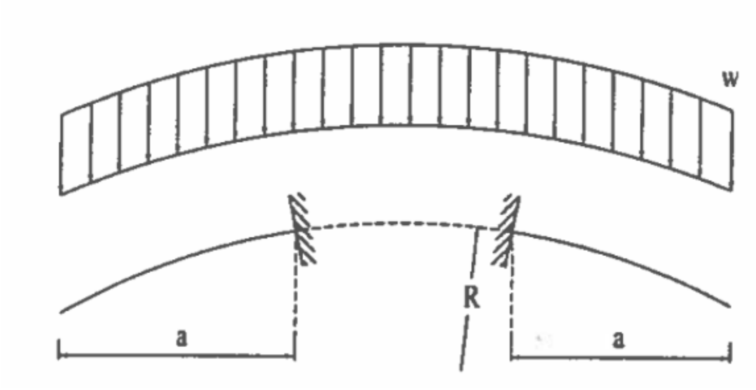

Figure 16 Stripping in the segment manufacturing plant and forces acting on the segments, (ACI-544.7R, 2016)

2.3.1.2 Segment storage

After the stripping, the segments are stored in order to reach the required strength before the transportation in the tunnel. Usually, a complete ring is piled up. In this stage it is important to consider the bending moment and shear forces acting on the piled segments. This is modelled as a supported beam under its weight, and two forces on the stack support which represent the upper segments. Two different cases are analysed, considering the same eccentricity of 100 mm, but applied once on left and once on right side of the applied force F, (ACI-544.7R, 2016).

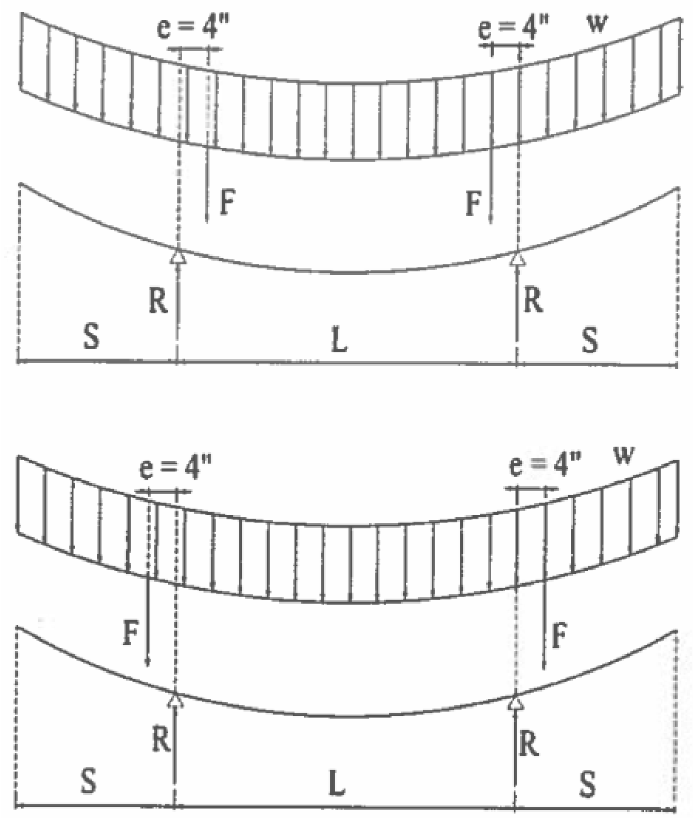

Figure 17 Segment piled up and forces acting on the bottom segment, (ACI-544.7R, 2016)

In these first two stages, demoulding and storage, the verification is that no cracks occur, and they define the minimum strength of the segment and the bearing points.

2.3.1.3 Segment transportation and handling

The segments are transported to the construction site and finally to the trailing gear on the TBM. The modelling is the same as the storage.

The handling is performed thanks to special device, like lifting lugs or vacuum lifters.

Finally the maximum bending moments generated in the different stages of the segments are summarised in Table 2, (ACI-544.7R, 2016), (ITA Working Group 2, 2019):

Table 2 Maximum Bending Moments

LOAD CASE	MAXIMUM BENDING MOMENT
Demoulding	$W*a^2/2$
Storage	$W*(L^2/8- S^2/2)+F_1*e$
Transportation	$W*(L^2/8- S^2/2)+F_2*e$
Handling	$W*a^2/2$

Where : a,L,S are geometrical distance shown in the Figure

F_1 is the weight of all segments completing a ring, without considering the bottom one;

F_2 is the weight of all segments placed in transport, excluding the bottom one.

2.3.2 Construction stages

The construction stage is the most important in term of structural dimension of the segment. In particular, the three phases to be considered are the application of the thrust jack force, the back-up load of the equipment and the final grout-injection pressure.

2.3.2.1 Thrust jack force

When the machine stops for the installation of the ring, only the thrust jacks, related to the single segment to be installed, are retracted while the others apply the force to the previous ring. When the new segment is placed, the jacks are immediately pushed against it. It is noteworthy that along the ring, the applied pressure is not homogenous, but the lower groups of jacks have to counterbalance the tendency of the machine to go down due to its weight; hence, the bottom segments have to resist to higher jack pressure, respect to the upper ones, (Guglielmetti, 2007).

The possible configuration of the jacks can be of three types: French, German or Japanese type, (AFTES, 2005), (DAUB, 2014). With French configuration, the force is applied close to the longitudinal joint and by using the bituminous pads in order to uniformly distribute the loads, as in Figure 18. Instead, with German type, the actions are directly applied on the longitudinal joints, as in Figure 19. In the Japanese configuration the jacks are positioned on the entire segmental length, as in Figure 20. When selecting the number and position of thrust jacks, two considerations can be done: the jacks require scarce space in the TBM, so it is beneficial to minimise the number of them. Moreover, by limiting the number, the jack forces are more concentrated, so this can be a disadvantage, (Blom, 2002). By inserting the jack shoe, the concentration of forces can be mitigated.

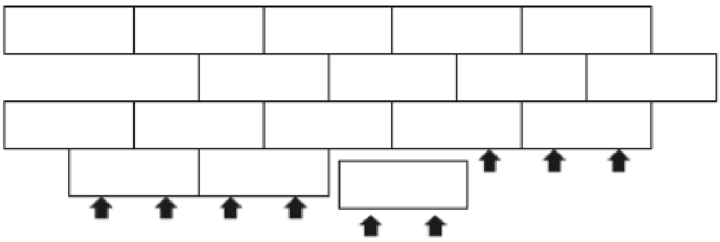

Figure 18 French configuration, (Blom, 2002)

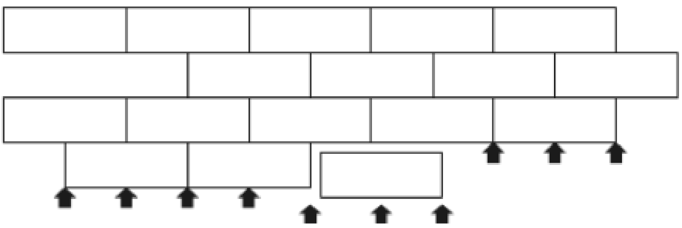

Figure 19 German configuration, (Blom, 2002)

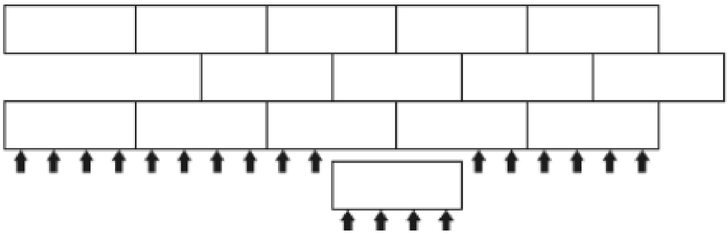

Figure 20 Japanese configuration, (Blom, 2002)

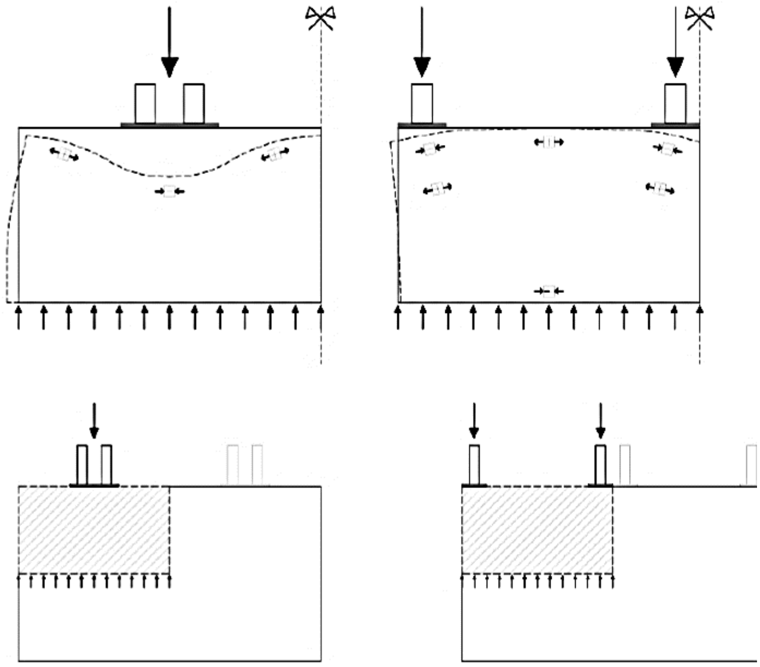

Figure 21 Distribution of stresses by the TBM jacks: French (left) , German (right) (ITA Working Group 2, 2018)

The installation step does develop high compression stress on the concrete behind the jacking pads, which can be calculated thanks to (ITA Working Group 2, 2019):

$$\sigma_{c,j} = \frac{P_{pu}}{a * h_{anc}}$$

Where:

- P_{pu} is the force applied by the jacks on each pad;
- h_{anc} is the length of the contact area between pad and the reduced depth of cross section;
- a is the transverse length of contact zone between jacks and the segment face.

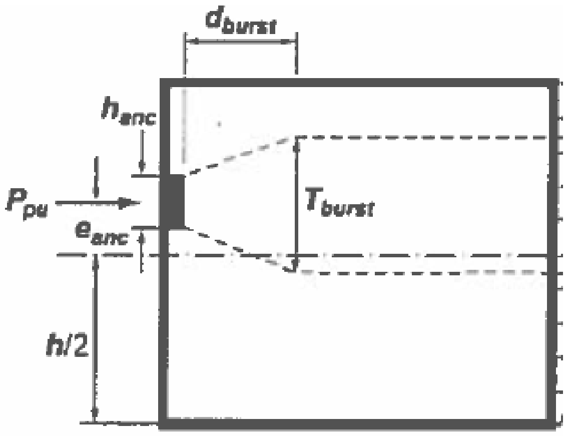

Figure 22 Bursting tensile forces and corresponding parameters, (ACI-544.7R, 2016)

Moreover, as shown in Figure, tensile stresses due to thrust forces arise perpendicularly to the loading direction. Bursting tensile stresses develops at a certain distance from the jacks, due to the spread of compression stresses in concrete.

Spalling tensile stresses develop in the circumferential joints, due to the interaction between two adjacent jacks.

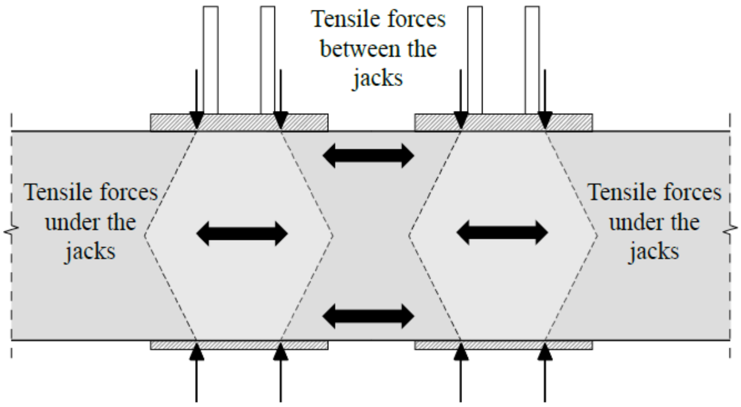

Figure 23 Tensile forces in the segment ,(ITA Working Group 2, 2018)

Bursting tensile stress may be evaluated by means of analytical equations, Iyengar diagram or FEM models.

Equations: the used theory is that for post-tensioned anchorage zones of prestressed concrete sections. It is possible to calculate the bursting tensile force based on the thrust jack force and the distance when it is maximum.

In the tangential direction, (ACI-544.7R, 2016) proposed the formula for the bursting tensile force:

$$T_{burst} = 0.25 * P_{pu} * (1 - \frac{h_{anc}}{h})$$

$$d_{burst} = 0.5 * (h - 2 * e_{anc})$$

DAUB, recommends similar equations for the forces develop in the circumferential joints:

$$T_{burst} = 0.25 * P_{pu} * (1 - \frac{h_{anc}}{h - 2 * e_{anc}})$$

Where:

- P_{pu} is the force applied by the jacks on each pad;
- h_{anc} is the length of the contact area between pad and the reduced depth of cross section;
- h is the depth of cross section;
- e_{anc} is the maximum eccentricity of the pad with respect to the centroid of the cross section.

If a FRC type of segment is used, the 28-day specified residual tensile strength of the segment is evaluated thanks to the maximum bursting stress developed in the radial and transverse directions, (ACI-544.7R, 2016).

Tangential direction $\sigma_p = \frac{T_{burst}}{\phi * h_{anc} * d_{burst}}$

Circumferential direction $\sigma_p = \frac{T_{burst}}{\phi * a_l * d_{burst}}$

ϕ is a reduction factor used with FRC concrete. It is equal to 0.7

It is important to notice that only a part of the circumferential segment is in contact with the jacking pads, so the allowable compressive strength has to be reduced in a partially loaded part. (DAUB, 2014) (Iyengar, 1962) recommends this formula:

$$f'_{co} = 0.85 * f_c * \sqrt{\frac{a_t * (h - 2 * e_{anc})}{a_l * h_{anc}}}$$

- a_t is transverse length of stress distribution zone at the centreline of the segment under thrust jack forces;
- a_l is the transverse length of contact zone between jacks and the segment face.

Iyengar diagram (Iyengar, 1962): the tensile stress along x direction, generated as a response of the applied thrust pressure, is a percentage of the total compressive stress. Beta is the dimension of the loaded surface, the different curves, on the graph, represent how the stress changes inside the segment, varying the dimension of the stress zone.

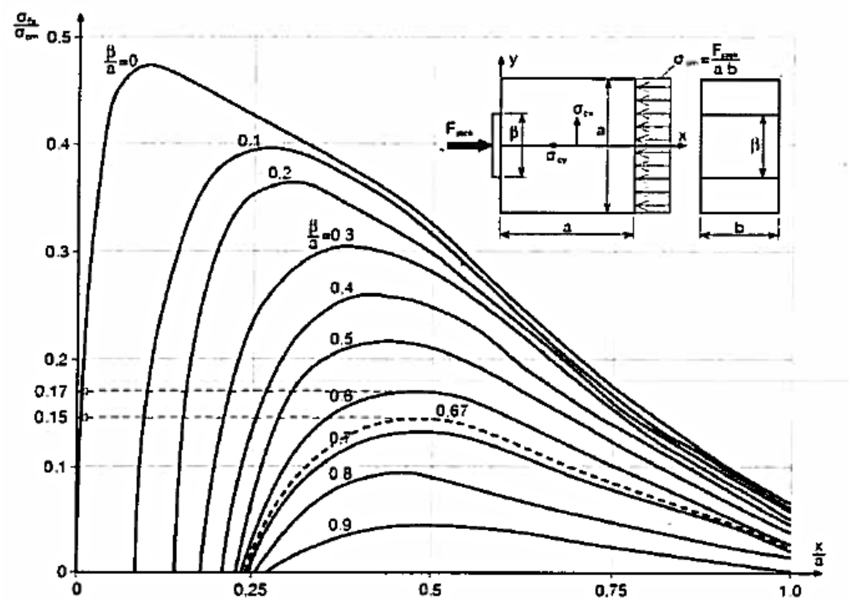

Figure 24 Iyengar diagram, (ACI-544.7R, 2016)

FEM models: Bakhshi and Nasri have modelled two adjacent rings, taking two segments. The jacking forces are applied along the contact area between the jacking pads and the segment face. The results, as shown in the Figure 25, demonstrate that the spalling tensile stresses between jack pads, and the bursting tensile stresses under the jacking pads are significant. Based on that, the segments and the reinforcement have to be designed in order to withstand these high tensile stresses.

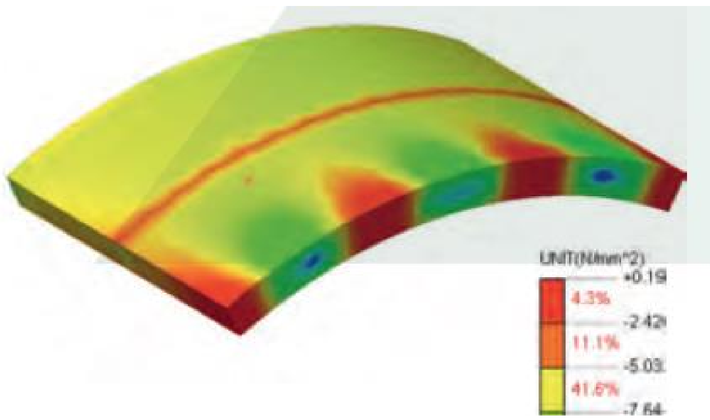

Figure 25 Typical bursting and spalling tensile stresses developed in segments in FEM analysis (Bakhshi, et al., 2013)

Longitudinal joint bursting load: Bursting tensile stresses can develop along the longitudinal joints similar to that one on the circumferential joints. The normal forces in this case are the result of the external acting loads, as the ground pressure, groundwater pressure and surcharge load and the gasket pressure. According to (DAUB, 2014) (AASHTO, 2010), the bursting tensile forces, spalling and secondary tensile force are calculated along the longitudinal joints.

$$F_{Sd} = 0.25 * N_{Ed} * (1 - \frac{d_1}{d_s})$$

$$F_{Sd,R} = N_{Ed} * \left(\frac{e}{d} - \frac{1}{6}\right)$$

$$F_{Sd,2} = 0.3 * F_{Sd,R}$$

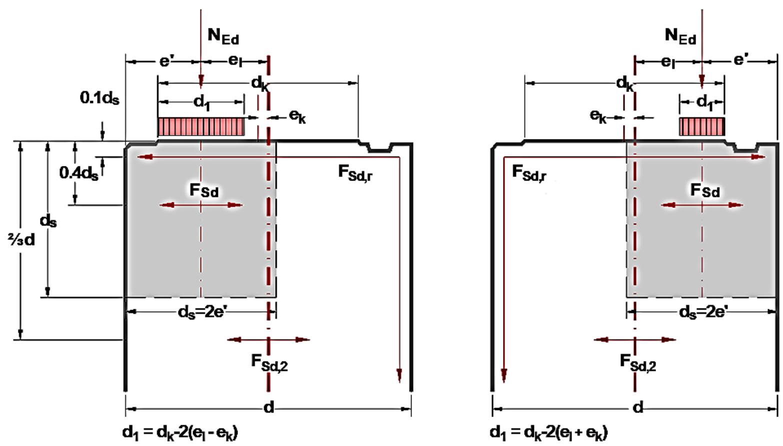

Figure 26 Segment joint with load eccentricity and split tensile stress, (DAUB, 2014)

2.3.2.2 Tail Skin Back-Grouting Pressure

The annular gap, created between the rings and the ground, is caused by several factors: the overcut of the ground in front of the machine, the conicity and the thickness of the shield, the presence of wire brush at the end of the shield. This gap is filled with two-component grout, injected at high pressure, which apply a load on the lining during the advancement of the machine. The load is considered in transversal direction respect to the tunnel direction, so a single ring is considered. The load applied by the grout is radial, from the minimum at the crown up to the maximum at the invert and the value is based on the face pressure. At this moment, the total forces applied on the ring are the grouting pressure and the weight of the ring itself. A second injection of grout is performed after different ring in order to fill the upper part void, created due to the gravity.

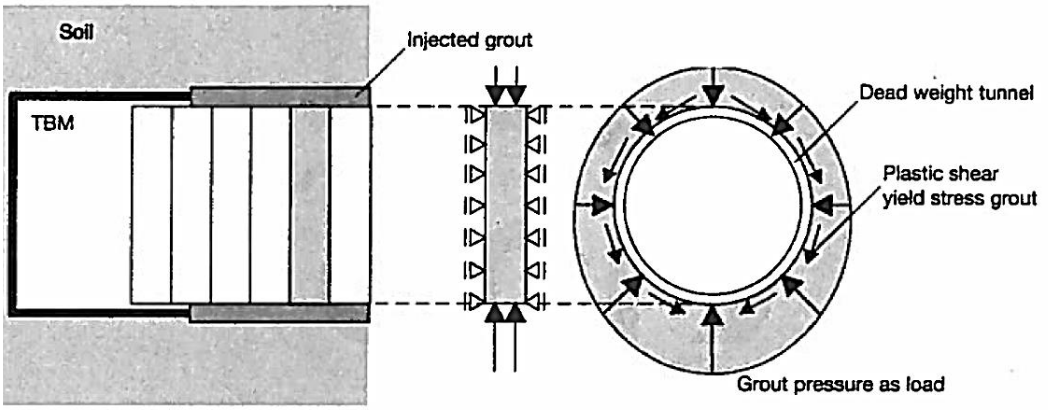

Figure 27 Forces of back-filling of tail-skin void, (ACI-544.7R, 2016)

2.3.2.3 TBM Backup Load

This load is applied on the lining behind the shield. Punching shear has to be considered with the assumption that the load is applied uniformly. The forces in this final stage are considered in long term, like groundwater, surcharges on the surface, fire, explosion and external loads depending on the utilization of the tunnel.

2.3.3 Final Service Stages

The precast concrete segments during the final service stage have to be designed to withstand with different loads, like ground pressure, water pressure, its weight, surcharge. The methods for analysing the actions during the serviceability of the tunnel are traditional elastic equations, beam-spring model and numerical analysis. According to (AASHTO, 2010), the loads factors are presented in Table 3.

Table 3 Loads factors for Final Service Stages

	w, WAp		EH, EV		ES	
	Maximum	Minimum	Maximum	Minimum	Maximum	Minimum
ULS	1.25	0.90	1.35	0.90	1.50	0.75
SLS	1.0		1.0		1.0	

Where:

- w: self-weigth;
- WAp: groundwater pressure;
- EV: vertical ground pressure;
- EH: horizontal ground pressure;
- ES: surcharge load

2.3.3.1 Elastic Equation

The applied forces are: in the vertical direction there are water and ground pressure uniformly distributed; on the lateral sides there are again water and ground pressures with trapezoidal shape and a triangularly distributed horizontal ground reaction. It is fundamental to consider a reduced bending rigidity in the lining, because the ring is not continuous, but is made with different segments. Hence, in order to take into account the effect of longitudinal joints, a reduced moment of inertia is considered, considering the relation of Muir (Miur Wood, 1975):

$$I_m = I_j + \left(\frac{4}{n}\right)^2 * I$$

Where:

I_j is the moment of inertia of the joints;

I is the moment of inertia of the ring without joint;

n is the number of joint.

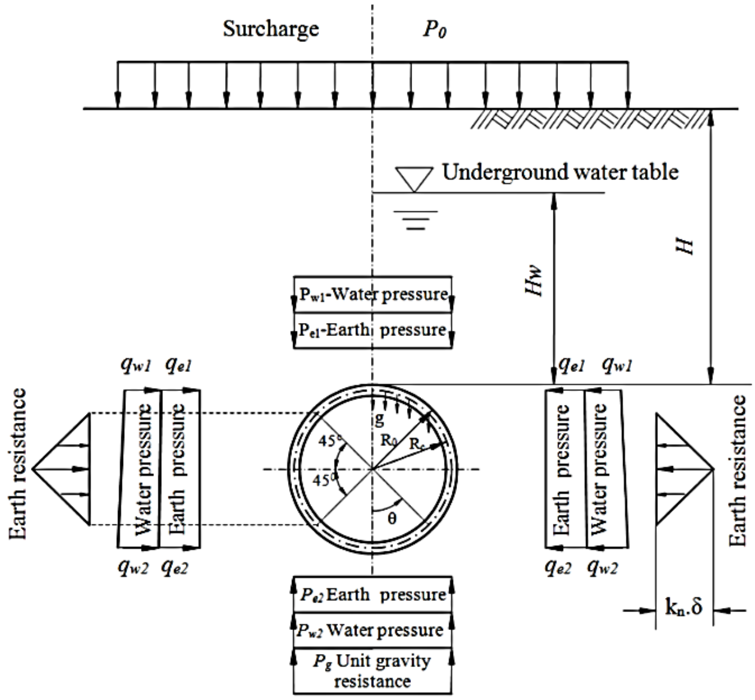

Figure 28 Distribution of loads used in elasti equations method, (JSCE, 2007)

For the radial subgrade reaction modulus can be used the formulas proposed by (DAUB, 2014) and (AFTES, 1993).

$$k_{rAFTES} = \frac{E_S}{R * (1 + \nu)}$$

$$k_{rDAUB} = \frac{E_S}{R}$$

Where:

- E_s is the stiffness modulus;
- R is the outer diameter of the lining.

In the Table 4, (JSCE, 2007) proposes elastic equations in order to calculate the forces.

Table 4 Elastic equations

Load	Bending moment	Axial force	Shear force
Vertical Load **$P = p_{w1} + p_{e1}$**	$(1-2*S2)*P*R_c^2$	R_c*P*S2	$-S*C*P*R_C$
Horizontal Load **$Q = q_{w1} + q_{e1}$**	$(1-2*C2)*Q*R_c^2$	R_c*P*C2	$-S*C*Q*R_C$
Horizontal triangular load **$Q' = q_{e2} + q_{w2} - q_{w1} + q_{e1}$**	$(6-3*C-12*C2+ +4*C3)*Q'* R_c^2/48$	$(C+8*C2-4*C3)*Q'* R_c/16$	$(S+8*C*S-4*S*C2)*Q'* R_c/16$
Soil Reaction **$P_k = k*\delta_h$**	**$0<\theta<\pi/4$** $(0.2346-0.3536*C)* R_c^2*k*\delta$ **$\pi/4<\theta<\pi$** $(0.3487+0.5S2+0.2357*C3) * R_c^2*k*\delta$	**$0<\theta<\pi/4$** $0.3536*C* R_c*k*\delta$ **$\pi/4<\theta<\pi$** $(0.7071*C+C2+0.7071S2*C) *R_c*k*\delta$	**$0<\theta<\pi/4$** $(0.3536*S)* R_c*k*\delta$ **$\pi/4<\theta<\pi$** $(S*C-0.7071*C2*S) * R_c*k*\delta$
Dead Load **$P_g = \pi*g$**	**$0<\theta<\pi/2$** $(3/8*\pi-\theta*S-5/6*C)* R_c^2*g$ **$\pi/2<\theta<\pi$** $[-\pi/8+(\pi-\theta)*S-5/6C-1/2\pi*S2]* R_c^2*g$	**$0<\theta<\pi/2$** $(\theta*S-1/6*C)* R_c*g$ **$\pi/2<\theta<\pi$** $[-\pi*S+ \theta*S+ \pi*S2-1/6*C)* R_c*g$	**$0<\theta<\pi/2$** $(\theta*C-1/6*S)* R_c*g$ **$\pi/2<\theta<\pi$** $[-(\pi- \theta)*C+ \pi*S+ \pi*S*C-1/6*S]* R_c*g$
Horizontal Deformation at spring Line **δ_h**	$\delta_h=[(2*P-Q')+ \pi*g]* R_c^4/[24*(E*I/h+0.045* R_c^4*k)]$		

Where:

- R_c is the radius of the middle line of the tunnel lining;
- g is the gravity;
- $S = \sin\theta$; $S2 = \sin^2\theta$; $C = \cos\theta$; $C2 = \cos^2\theta$; $C3 = \cos^3\theta$

2.3.3.2 Beam-Spring Model

According to (JSCE, 2007) and (AASHTO, 2010) the lining is modelled in the cross section, like series of curved beam, jointed with the longitudinal joints. The ground is represented as springs in the radial, tangential and longitudinal directions. In this model the longitudinal joints and a reduced bending rigidity are used. In the two-dimensional model it is not possible to represent the circumferential joints or the staggered arrangements between the rings. However a so called 'two and a half dimensional multiple hinged segmented double ring beam-spring' is implemented: the segment is curved beams, the longitudinal joints are like rotational springs and the circumferential ones are shear springs. In order to evaluate the internal forces, after modelled in these two possible ways, a conventional structural analysis is used.

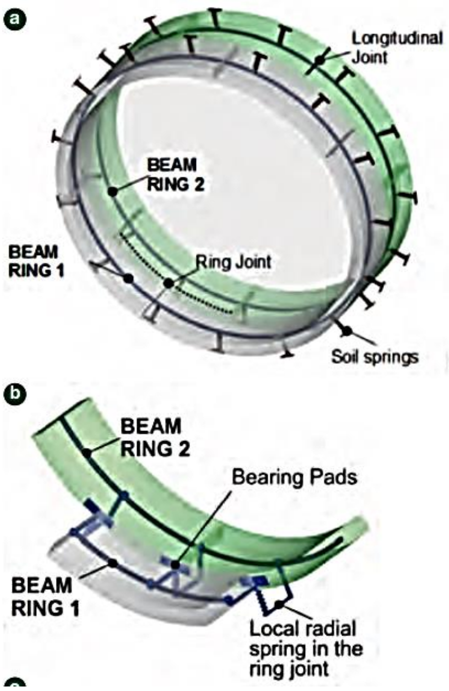

Figure 29 (a) Double ring beam-spring model with radial springs (ground) and joint springs (longitudinal and circumferential joint), (ITA Working Group 2, 2019)

2.3.3.3 Loads Due To Additional Distortion

This distortion is the difference between the movement of left and right sides f the tunnel, or between the crown and the invert. It can be caused during the assembly of the segments under their weights or during the construction of adjacent tunnel. It is possible to use the formula proposed by (Morgan, 1961) to calculate the additional distortional bending moment.

$$M_{distortional} = \frac{3 * EI * \delta}{2 * R^2}$$

Where:

- δ is the maximum radial distortion;
- R is the tunnel radius;
- I is the second moment of inertia and can be used the reduced one of (Miur Wood, 1975).

2.4 Requirements for concrete and reinforcement

Concrete segments are reinforced with steel bars:

- Transverse: perpendicular to the tunnel axis in order to resist to moment and forces, with typical diameters from ϕ10 to ϕ16;
- Longitudinal: parallel to the tunnel axis, required for minimum temperature and shrinkage phenomena;
- Joint reinforcement (place close to the joints in order to resist bursting and spalling stresses,ϕ6 and ϕ16).

An alternative to reinforced concrete is the use of Fibre Reinforced Concrete FRC, which has a lot of advantages: as first it reduces the human error and increases the worker safety, because it is not necessary the assembly of the cages. The FRC improve the behaviour of the concrete after the formation of the cracks, because the fibres generate a post-cracking residual tensile strength. With the uniform distribution of fibres, the cracks result smaller and so the durability of the concrete increase. It is known that by increasing the width of the cracks, several problems rise on the concrete because aggressive agents enter, like corrosion of steel reinforcement or carbonation.

Figure 30 Conventional segment reinforcement (left) and segment with steel fibers (rigth) (DAUB, 2013)

2.5 Gasket

The gasket is a system that guarantee the waterproofing of the tunnel. They are placed between segments in the longitudinal and circumferential joints. They are positioned around the individual segments in the extrados sides. If it is necessary, the gasket can be inserted in the intrados in order to increase the watertightness.

The two main materials used for the gasket are EPDM (Ethylene Propylene Diene Monomer, not resistant with presence of hydrocarbons) and CR/SBR (Chloroprene Rubber/Styrene Butadiene Rubber, not well in acidic environments). In different position, a layer of hydrophilic seal increments the sealing performance during the days.

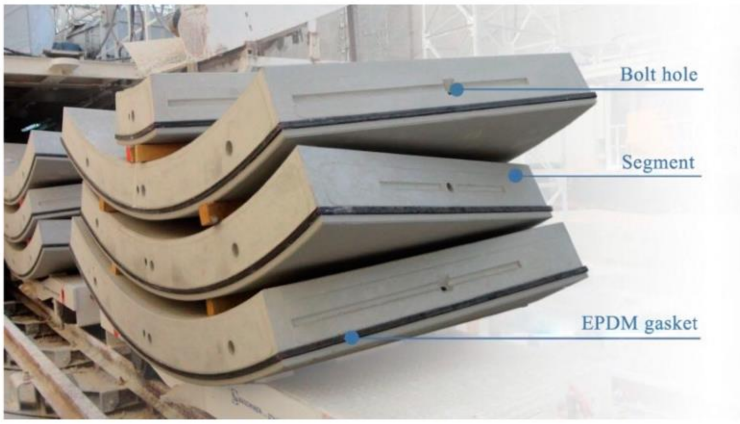

Figure 31 Gasket

The main properties of the gasket are the hardness of the rubber component, tensile strength and elongation.

The main parameter to take into account in the choice and design of the gasket is the resistance to the groundwater pressure. The watertightness is performed by compression of the gasket made by thrust jacks, during the assembly, and by acting stresses, in long term. There are two different types of seals:

- Compression seal, which is basically the simple compression performed by the connector;

- Compression seal with swelling element: on the side in which occurs the sweeling in the presence of water, a particular element is inserted. This last can withstand high water pressure, but it is important to protect it because can swell not intentionally.

As time goes on, the relaxation of the rubber increases, so it is important to verify the material with special tests, like aging test, considering a design life of the tunnel equal to 100 years. Most of the specification required that after 100 years, the minimum residual compressive stress has to be 60% of the initial one. The width of the gasket profile depends on the segment thickness, which is a function of the tunnel diameter.

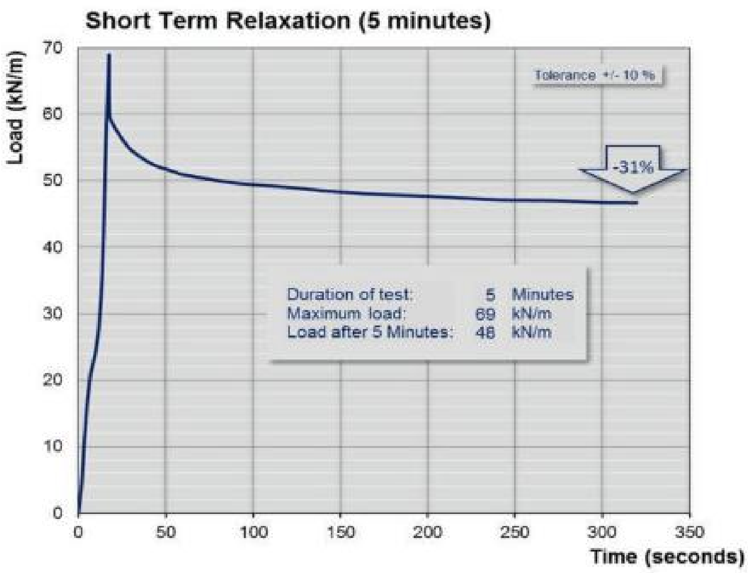

Figure 32 Aging test for gasket

The main problems related to the gasket are the chipping, breaks of the gaskets or detachment of the concrete cover. This area is weaker because there is no reinforcement, so when the gaskets are compressed by the thrust jacks, they transmit tensile stress in the concrete. If this force is higher than the concrete strength, this last breaks.

Figure 33 Example of corner's breaking, (ITA Working Group 2, 2018)

Different solutions in order to reduce this high level of compression in the edges and in the cover of concrete are proposed:

- One solution is to install the gasket at a certain distance from the extrados in order to dissipate the stress.
- Another innovative solution is to create an asymmetric profile of the segment, close to the installation of the gasket, so that, even if the two adjacent gaskets are compressed, a minimum gap remains, avoiding hypertension.

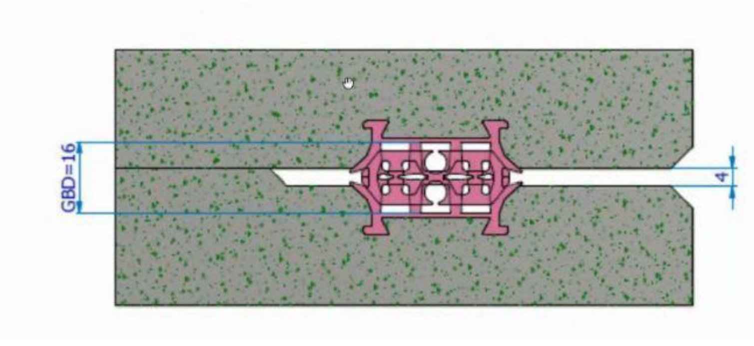

Figure 34 Asymmetric gasket

- The third solution is to design a shallower groove of the gasket. In the image the force R is that one develops during the compression of the gasket, p is distribution of R along the groove and P1 and P2 are the spalling forces. P1 and P2 depend on the depth of the groove, because the greater is the depth and the greater is the generated spalling force. By assuming the same corner (a=b), the P2 has not enough space to dissipate and so damage the concrete. Hence reducing the groove depth, the edge spalling effect is reduced

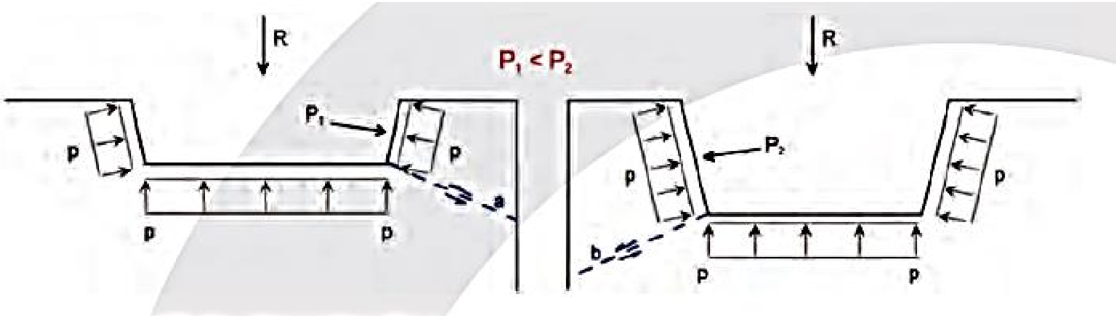

Figure 35 Re-distribution of impact force R in a shallow and deep gasket groove(ITA Working Group 2, 2019)

In the design and in the choice of the type of gasket, two distances have to take into account, which are the gap and the offset, as shown in the Figure. These are unavoidable and moreover are defined by the projects. Usually the maximum values defined in the projects are 5 mm for the gap and 10 mm for the offset.

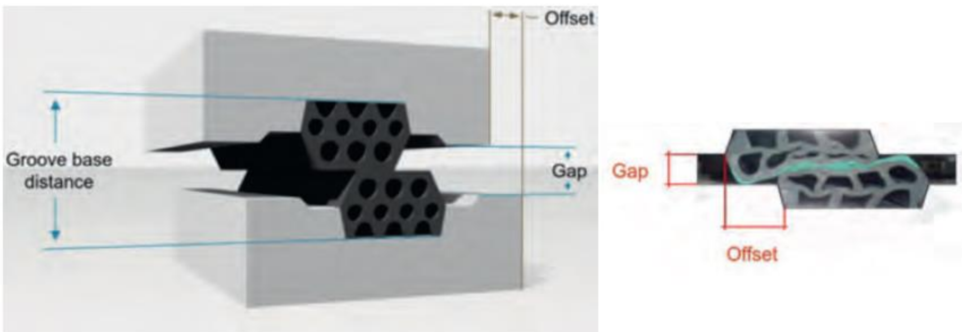

Figure 36 Gap opening and offset before and after compression (ITA Working Group 2, 2019)

The possible causes for excessive gaps and offsets are:

- Factors related to the installation of the segments: in case of universal rings, some rings can be installed in certain position not allowed by the ring design and so the connection system may not maintain the required gaps and offsets.

- Incorrect size of the bituminous pads: if they are present, for the correct distribution of the thrust force, they can cause excessive gaps, especially if they are wide or with low compressibility.
- Excessive thrust of the gasket: when they are compressed, the gaskets exert tensile stress which tend to open the joints. If this force is not balanced by the connection system, excessive gap and offsets are generated.

In order to contain these distances, the selection of the connections is fundamental. The connection system has to be designed taking into account the pull-out resistance. The pull-out resistance has to resist to the ejection of the segment from the connections itself. If this resistance is not sufficient, the gap increases.

Finally when the test of watertightness of the gasket is performed by the producers, the gaps and the offsets vary with different values in millimetre. The final result of the test is a diagram, which correlates the gap, the offset and the resisting water pressure of the gasket . The test starts with a fixed value of water pressure, varying the distances, until the leakage occurs. Obviously, by increasing the distances, the watertightness decreases.

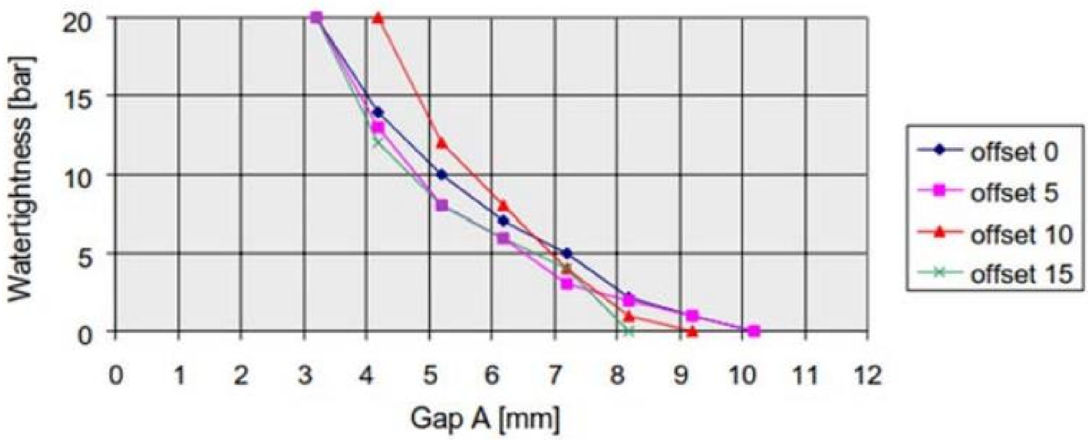

Figure 37 Typical watertightness-gap diagram, (ITA Working Group 2, 2019)

2.6 Connections

The connections between segments in the same ring and between different rings are divided in three categories: joint connection with bolts, dowels and guiding rods.

2.6.1 Bolts

Bolt should be installed both in the radial and circumferential joints. They also help in compressing the gaskets in the short-term. Hence, they can be removed and utilized in other sections. First all the ring is placed and then the bolt is inserted and tightened. The insertion of bolts requires special inclined holes, called socket, and grooves already designed in the mould. The installation requires special personnel who have to insert them.

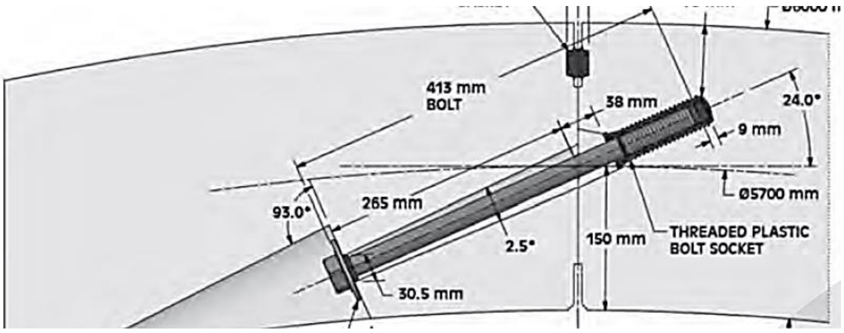

Figure 38 Bolt connection in longitudinal joints (ITA Working Group 2, 2019)

2.6.2 Dowel

They are inserted into the segment during ring assembly by the erector. The dowels and sockets are made of plastic material and with core of steel. The dowel connections are used between ring in circumferential joints. They are designed to resist to the short-term relaxation of the gasket. Modern dowels have higher shear resistance and are less susceptible to humidity.

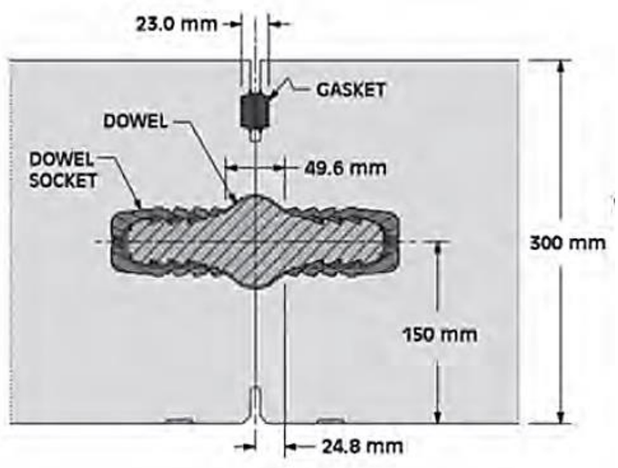

Figure 39 Dowel connection in circumferential joints

2.6.3 Guiding rods

Movable device that provides guidance and allow to centre during installation. It absorbs also shear forces in longitudinal joints.

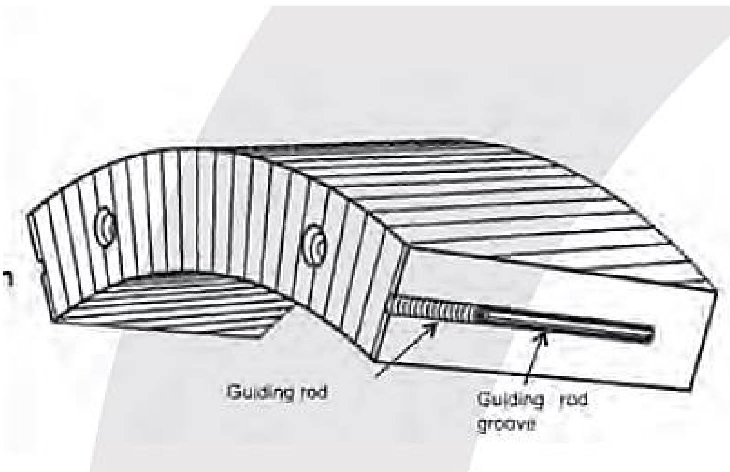

Figure 40 Guiding rod

2.7 Actions and combinations

The design of the segmental lining is carried out according to the EN, 1992-1-1:2004, both for Ultimate Limit State ULS and for Serviceability Limit State SLS. In general the actions are permanent G, variable Q or accidental. In the tunnel the permanent loads are:

- Dead weight of the structure and the weight of fixed equipment;
- The ground surrounding the tunnel;
- Loads of structure close to the tunnel;
- Hydrostatic and hydraulic pressures;
- Annular gap back grouting pressure.

In the tunnel the variable loads are:

- Loads on the ground surface: for example regarding the weight of a building there are interpretations in the different recommendations, because can be considered permanent or variable. Usually a standard value of 10-15 MPa for each floor is considered;
- Loads induced during constructions, like the thrust cylinders;
- Actions induced by temperature variations;

The limit state design method establishes that the ‘characteristic’ values must be re-calculated taking into account the partial coefficients, in order to have the final ‘design’ values. The partial coefficients reduce the resistances of the materials and amplify the actions and loads applied on the structure.

2.7.1 Ultimate Limit State

The study of the Ultimate Limit State expresses the limit of acceptability for the constructions where the resistance forces are greater than the acting forces.

The design resistances of the materials, must be evaluated from the reduction of the characteristic strength of them, by using the partial factors:

- Reinforced concrete for the linings: $f_{c,design} = \frac{fc,k}{1.5}$
- Reinforced steel bars : $f_{y,design} = \frac{fy,k}{1.15}$

Concerning the combinations and the partial factors for the actions and loads in the tunnel design:

$$1.35 * G_{max} + G_{min} + \gamma_{Q,1} * Q_{k,1} + \sum_{i\geq 1} \gamma_{Q,i} * Q_{k,i} * \Psi_{0,i}$$

- 1.35 is the partial factor coefficient suggested by (EN, 1992-1-1:2004) for the unfavourable permanent actions;
- Gmax is the total unfavourable permanent actions;
- Gmin is the favourable permanent actions (like water in some cases. If unfavourable it is multiplied by 1.35);
- Qk,1 is the variable actions, like road, rail..;
- $\gamma_{Q,1}$= 1.5
- $\sum_{i\geq 1} \gamma_{Q,i} * Q_{k,i} * \Psi_{0,i}$is the accompanying variable actions;

In the tunnel design the largest contribution are the permanent actions, so usually the variable loads can be neglected.

2.7.2. Serviceability Limit State

The Serviceability Limit State is the verification that, stresses on concrete and steel, crack opening and deformations, do not overpass the specified service requirements.

As in (EN, 1992-1-1:2004), the limit of crack openings for the reinforced concrete structures, exposed to soil or ground water, has not to exceed the value of 0.20 mm.

The partial factors for stress limits in SLS are:

- Limit of compressive stress for concrete: $\sigma_c = 0.6 * fc,k$
- Limit of tensile stress for steel reinforcement: $\sigma_s = 0.8 * fy,k$

Regarding the combinations and the actions, in SLS the equation is reduced in:

$$G_{max} + G_{min} + \sum_{i\geq 1} Q_{k,i} * \Psi_{0,i}$$

2.8 Structural Fire Protection

The protection against the fire is always to be considered in the design of a tunnel, associating all the protection measures to be installed inside the tunnel, like escape routes design, smoke removal and so on. It is important to guarantee adequate serviceability service during and after a fire, such as water tightness or immediate deformations.

It has noticed, (Maraveas, et al., 2014), that the features of fire inside a tunnel are different from that occur in a buildings, especially the severe rise of the gas temperature, up to 1000°C in a few minutes. This affects the structural integrity of the lining, which tends to explosive spalling, which is the burst out of the concrete accompanied by release of energy. This phenomenon occurs for two reasons:

1. If the content of moisture inside the concrete is high and, after the heating there is an increase of the pore pressure, resulting in develop of tensile stress;
2. There is the development of high compressive stress on to the heated surface, because it is not permitting the thermal dilation due to the other cooler surface.

If spalling occurs, the cover of the segment breaks and so the reinforcement is no more protected. This led to an increase of heat velocity and a faster degradation of the rest of the segment, in all the components. A suggestion can be to design a greater thickness of the lining, such as 60-70 millimetres, (Maraveas, et al., 2014).

Moreover, two main solutions are proposed to be the most effective, (Maraveas, et al., 2014): thermal barriers and the addition of Polypropylene fibres. The thermal barriers are external insulation that minimize the heating rate and the temperatures on the concrete surface. This solution is the most effective, but the costs are very high compared to the PP addition. The PP fibres increase the permeability of the concrete and practically reduce the spalling phenomenon. There are several regulations and guidelines regarding the properties of the PP fibres (Yang, et al., 2020) concrete to be inserted.

3. TWIN TUNNEL

The option to build twin tunnel is growing over the years due to the high traffic demands in urban area and so the need of development new infrastructures, which do not affect the ground surface services. Three main layouts are designed and constructed, such as horizontal, overlapped or offset twin tunnels. The variables that impact on the results for the selection of the optimum layout are mainly the distance between the two tunnels, the construction sequence, in particular what is better to construct before than the other.

The most used is the horizontal layout, since it reduces the ground surface settlement. However, when there is the constraint of small space on the surface for the construction site in the proximity of the stations, as the project studied in this thesis, it is necessary to overlap the tunnels. The overlapped position affects the ground surface settlements, which means damages on the buildings and infrastructures on the surface, and the response of the segmental lining in terms of internal stress and deformations.

The following studies summarised the interaction of twin tunnels with different configurations, focused on the concrete lining.

3.1 Study of the construction sequence of overlapping tunnels by the Shield Tunnelling method: a case study of the longest overlapping tunnel in China

In the Research made by (Yang, et al., 2020) they studied the Tianjin Metro Line 5. In particular they analyse the radial stress on the tunnel lining and the deformation of the lining, caused by the two construction sequences. They conclude that the construction sequence has little effect on the radial stress, but this does not apply for the lining deformation. In fact, if the lower tunnel is constructed first, its final deformation, after the construction of the upper up, is similar to floating of about 8 mm. Instead if the upper tunnel is built before than the lower, at the final stage, the first tends to move down of about -10 mm. Under this consideration, they suggest constructing the lower first and then the upper one.

3.2 Monitoring of three-dimensional additional stress and strain in shield segments of former tunnels in the construction of closely spaced twin tunnels

In the paper of (Gao, et al., 2016) it was analysed the effects of the construction of a new parallel tunnel close to an existing one. They studied the effects on the segmental lining of the former tunnel changing the construction phases of the second one: in particular when the face of the new tunnel is far from a selected monitoring section, then when it approaches and finally when the machine passes the section. They explain that the soil mass around the new tunnel tend to move towards the oldest ones, exerting an additional earth pressure. This led to additional stresses, like radial, circumferential and axial, on the segmental tunnel lining. The circumferential and axial additional stresses were found after 1-2 days of the passage of the excavation face. In particular, in monitored a section they found, the circumferential tensile stress reached the tensile strength of the concrete, so this latter maybe was cracked.

3.3 Three- dimensional numerical simulation of mechanized twin stacked tunnels in soft ground

The paper presented by (Do, et al., 2014) investigates the interaction among three different construction sequences of two overlapped tunnel: excavation of upper tunnel first, excavation of lower tunnel first, both at a distance of ten diameters and simultaneous excavation. Regarding the response of lining, they evaluate the normal displacement, the normal forces and the bending moment inside it. They find interesting conclusions:

1. The normal displacements in the lower tunnel are smaller than those developed in the upper tunnel in all the three conditions;
2. The normal forces induced in the lower tunnel are greater than that induced in the upper tunnel: they suggest that depends on the fact that the lower tunnel is at a great depth and so the weight of the ground is higher;
3. The bending moment in the lower tunnel is smaller than that of upper tunnel probably due to a homogenous distribution of the external loads acting on the lower one;
4. The maximum effects of the interaction between the overlapped tunnels occurs during the passage of the machine of the new tunnel, considering all the three sequences.

3.4 Effect of lining thickness on the behaviour and on the distance between two adjacent circular tunnels

The Research made by (Wael Abd Elsamee, 2019) study the effects of the lining thickness and the distance between two parallel tunnels on the total displacement in soil, total stresses in soil, deflection of the crown point, bending moment and shear forces in the lining. Results concerning the part related to the segmental lining are presented:

1. Deflection of the crown point: it decreases with increasing of thickness of lining and spacing of tunnels;
2. Bending moment: it increases as the thickness increases; this is due to the flexural rigidity which is directly proportional to the thickness of the segments. Hence the segments can support higher moments. Instead by increasing the distance, the bending moments is reduced;

3. Shear force: the results are equal to those ones of the bending moment, so it increases with increasing of the thickness and decreases with increasing of spacing.

The author finally proposed an optimum thickness of the lining equal to 0.030 times the diameter.

4. THREE-DIMENSIONAL FEM ANALYSIS WITH MIDAS FEA NX

The tunnels have been modelled with the software MIDAS FEA NX. This software allows non-linear geotechnical and structural FEM analysis. The powerful of the tool is that it is possible to define all the construction stages, starting from the geo-static condition up to the complete excavation in three dimensions.

The selected constitutive soil model for better representation of the soil behaviour is the hardening soil. The first difference from Mohr- Coloumb model is the hyperbolic relationship between the vertical strain ε1 and the deviatoric stress q, as shown in Figure 49. In practice, when the soil is subjected to primary deviatoric loading, its stiffness decreases, and irreversible plastic strains develop.

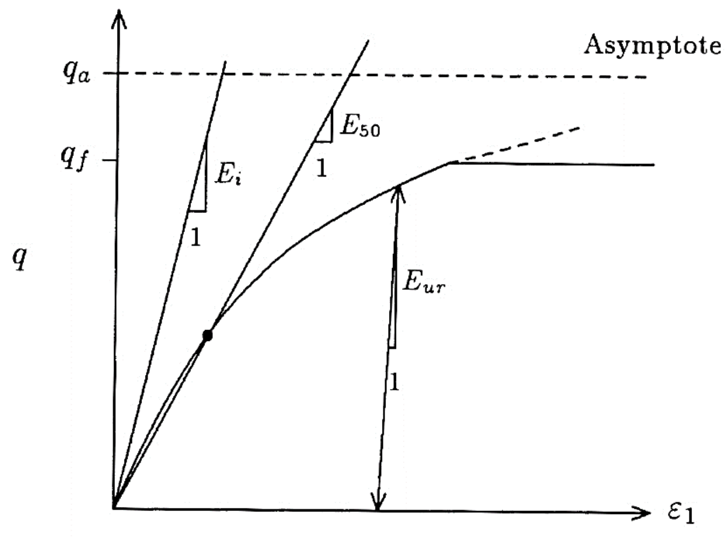

Figure 41 Hyperbolic stress-strain relation for a standard drained triaxial test

$$\varepsilon_1 = \frac{q_a}{2E_{50}} * \frac{(\sigma_1 - \sigma_3)}{q_a - (\sigma_1 - \sigma_3)}$$

In which:

- $q_a = \frac{q_f}{R_f}$
- $q_f = \frac{6 \sin \varphi}{3 - \sin \varphi} * (p + c * cot\varphi)$ and $R_f = \frac{q_f}{q_a}$

The relation of the ultimate deviatoric stress q_f derives from the Mohr- Coloumb criterion, which involves the strength parameters of cohesion c and friction angle φ. R_f is the failure ratio, usually equal to 0.9.

Another important advantages of this model, is that it describes the dependency of the stiffness on the stress level. In fact, it is observed that the stiffness of the soil increases with the increasing of the stress level.

The main parameters of the Hardening soil model are:

- Secant triaxial deformation modulus E_{50}: the E_{50} is used instead of the initial modulus E_i for small strain because the E_i is more difficult to determine experimentally.
- Triaxial unloading/reloading modulus E_{ur}.
- Power m for stress level dependency of stiffness;
- Tangent stiffness for primary oedometer loading E_{oed}.

4.1 Geometry of the model

The model is carried out from the design project of the fifth line of the metro of Bucharest. All the project data have been made available by the company SYSTRA SWS. The geometry considers the tunnels from the chainage 6+694.00 meters up to the chainage 7+040 meters, with a total considered length of 346 meters. The project foresees two twin tunnels which travel almost with a horizontal alignment, till the approaches to the metro-stations, in which they are in vertical. This implies that one of the tunnels has to move, reaching with the other first the offset configuration and finally the vertical one.

The Figure 42 highlights the alignment of the tunnels: the blue is upper one, which has a constant depth along the longitudinal direction; while the red is the tunnel that moves in the three dimensions, lowering and turning to the right.

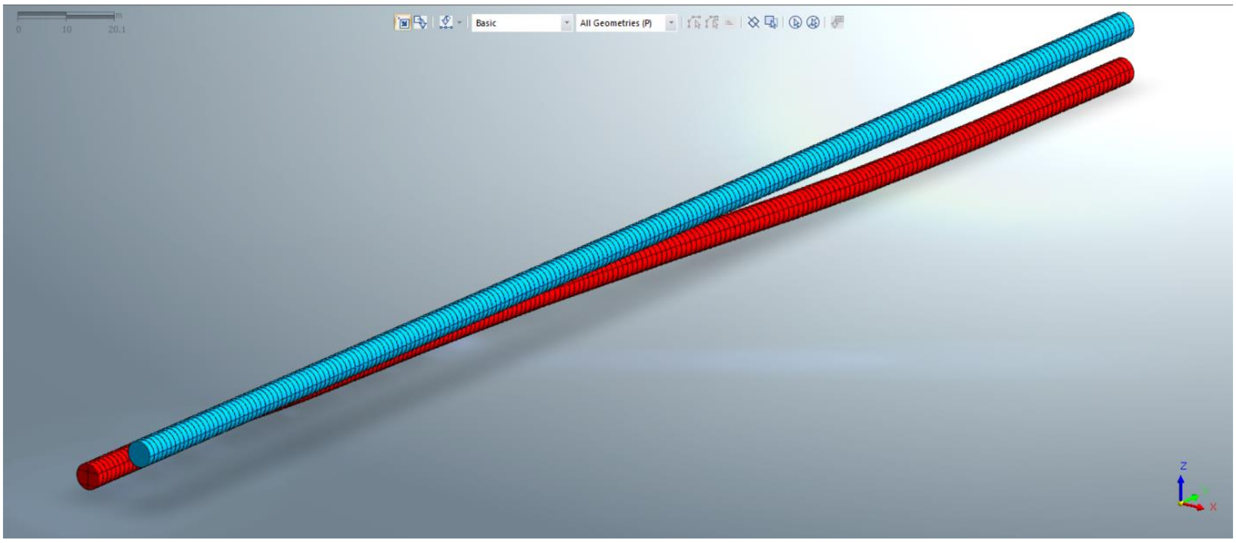

Figure 42 Geometry of the M5 in 3D

The model on FEA NX considers the unusual condition of the entire pathways of the two tunnels, in particular when they are in the vertical configuration, with the coordinates from 6+980 meters up to 7+040 meters. So the geometry is reduced with a total length of 60 meters, in order to prevent problem on the boundary condition and to permit a correct analysis of the selected 60 meters. The vertical arrangement is reached when the tunnels approach the metropolitan stations.

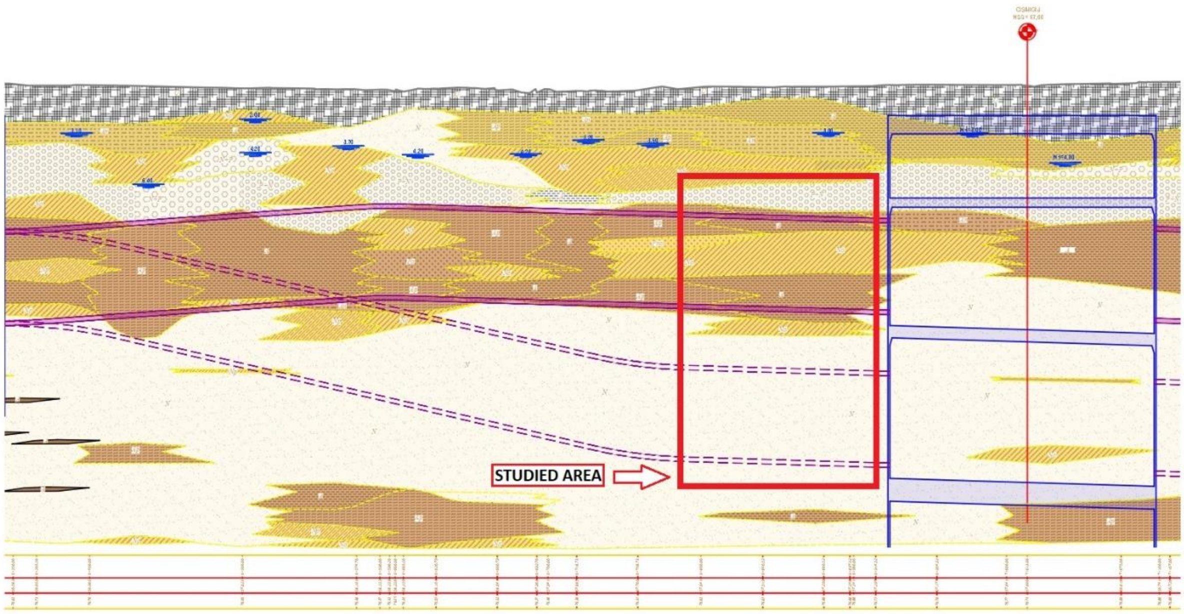

Figure 43 Longitudinal section of the project

4.1.1 Geometry of the ground

The ground is a parallelepiped with a depth of 45 meters and a horizontal dimension of 120 meters, as in Figure 44.

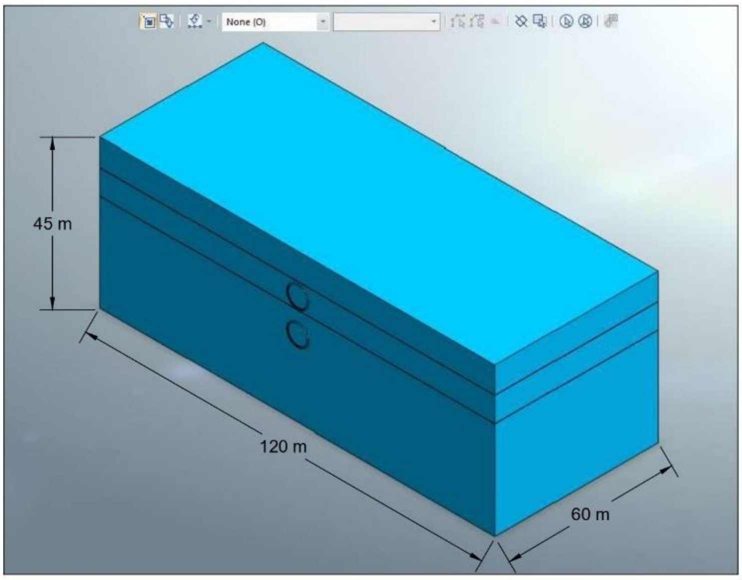

Figure 44 Dimensions of the model in MIDAS FEA NX

The groundwater level is positioned to a depth of 3 meters from the ground-surface. The real stratigraphy is presented, with seven different layers, as reported in Table 5 and in Figure 45. The Table 5 shows the survey's results, performed by SYSTRA SWS, in order to assess the properties of the zone interested by the construction of the tunnels. The soil is simulated with the hardening behaviour.

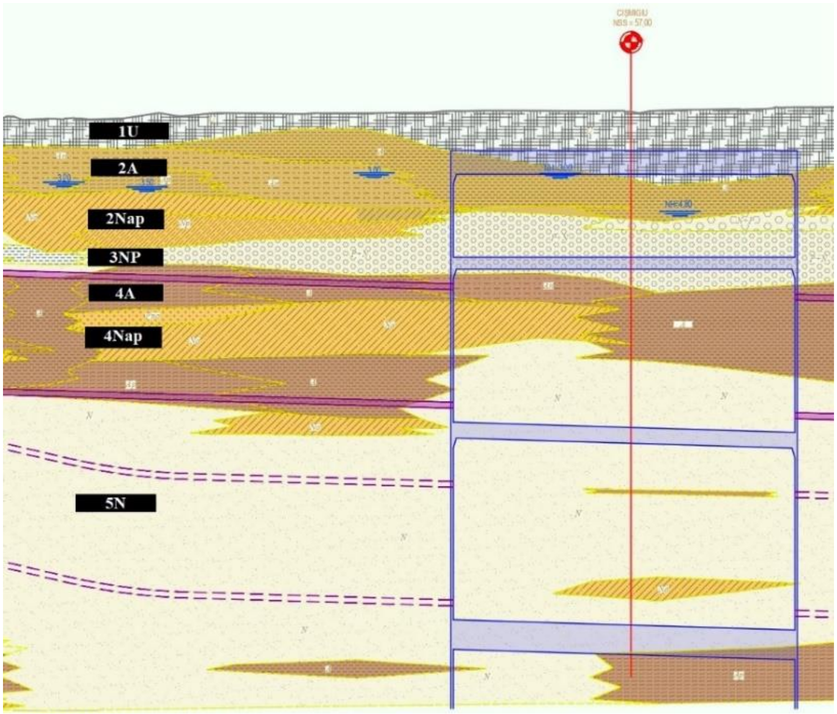

Figure 45 Stratigraphy of the ground

Table 5 Properties of the layers

Layer code	Thickness [m]	γ [kN/m³]	E [kN/m²]	c' [kN/m²]	ϕ [°]	k_0 [-]	k [m/s]
1U	1.5	18	8000	1	20	0.53	1.0E-09
2A	2.5	20	11000	40	17	0.50	1.0E-09
2Nap	2	20	11000	5	20	0.49	1.0E-05
3NP	2	21	20000	0	28	0.49	1.0E-04
4A	1.5	20	15000	55	16	0.43	1.0E-09
4Nap	3	20	15000	5	25	0.49	1.0E-05
4A	3	20	15000	55	16	0.43	1.0E-09
5N	29.5	21	25000	0	30	0.49	1.0E-04

An assumption is made on the layer 4: originally it was divided in three different layers, which the first and the third were undrained and in the centre, there was a drained one. The problem arises because the upper tunnel crossed among these three layers and so in the program FEA NX was not possible to consider this configuration. So in practice, the final hypothesis was to merge the three layers in one single (called, layer 4) with the characteristics of the drained one, in order to consider the worst condition for the calculation.

In the Table 6 the dimensions of the stratigraphy and the geotechnical parameters are shown.

Table 6 New layers

Layers	**Top [m]**	**Bottom [m]**	**Thickness [m]**	**γ [kN/m^3]**	**c' [kN/m^3]**	**k [m/s]**	**k_0 [-]**	**φ' [°]**
1	0	8	8	20	5	10^{-9}	0.50	22
2	8	15.5	7.5	20	5	10^{-5}	0.50	16
3	15.5	45	29.5	21	1	10^{-4}	0.50	30

Layers	**E_{50} [kN/m^2]**	**E_{oed} [kN/m^2]**	**E_{ur} [kN/m^2]**	**m [-]**
1	12500	12500	37500	0.6
2	15000	15000	75000	0.7
3	25000	25000	125000	0.5

4.1.2 Geometry of the tunnels

The twin tunnels have an internal diameter equal to 5.7 meters and an external diameter of 6.3 meters. The internal diameter simulates the intradox of the concrete lining, while the external diameter represents the shield of the machine. Between them, the annular gap of 0.15 meters is filled by the grout. The upper tunnel crosses the new layer 2, while the bottom one is in the new layer 3.

The chainages in which the two tunnels are in vertical arrangement are between 6+940 m and 7+040 m. The coordinates are shown in the Table 7.

Table 7 Chainage of the tunnels in vertical alignment and their coordinates

	BOTTOM TUNNEL			**UPPER TUNNEL**		
CHAINAGE [m]	**x [m]**	**z [m]**	**y [m]**	**x [m]**	**z [m]**	**y [m]**
6+980	0	23	40	0	33	40
7+000	0	23	60	0	33	60
7+020	0	23	80	0	33	80
7+040	0	23	100	0	33	100

Regarding the up tunnel, in the model, has a constant depth equal to 12 meters, calculated in the centre of it up to reach the ground-surface. The bottom tunnel is a depth of 22 meters. Hence the tunnels have a vertical distance of 3.4 meters, evaluated on the external diameter.

In the model the tunnels are composed by four parts:

- 'Bottom_in' or 'up_in': they represent the excavated soil;
- 'Bottom_grout' or 'up_grout': these parts have double function: firstly they represent the excavated soil, but after the passage of the EPB, their properties are changed with grout property. This change is a powerful tool of FEA NX, in which it is possible to transform the property of the material when it is necessary;
- 'Bottom_shield' or 'up_shield': the shield of the EPB is taken as 6.6 meters, taking into account also the overcutting of the machine;
- 'Bottom_lining' or 'up_lining' ;

The lining is modelled in two different ways: with a 3D element and a plate inserted inside the 3D one. This plate allows to have the results as forces M, N and T.

The geometry of the tunnels is subdivided every 1.5 meters, in order to simulate the advancement of the machine and the fact that at each stage, a single ring of lining is placed. Hence the selection of 1.5 meters takes into account the length of the ring.

In the table the parameters of the components of the tunnels, which are inserted in the model, are presented.

	Model behaviour	**Unit weight [kN/m^3]**	**Modulus of elasticity [kN/m^2]**	**Poisson ratio [-]**
Shield of the EPB	Isotropic – Elastic	24	209000000	0.15
Precast concrete lining	Isotropic – Elastic	23.53	31938000	0.2
Grout (Shah, et al., 2017)	Isotropic – Elastic	24	15000	0.3

Before performing the mesh, another important tool of FEA NX is used: all the solids (layers of the ground and upper and bottom tunnels) are connected each other with the AUTOCONNECT function. This last permits the creation of the shared faces among all the solids and in practice they became interconnected.

4.2 Mesh of the model

4.2.1 Size control

Before starting the process of creating the mesh, the first step is to control the edges of the model, in order to create a dense mesh where we want, for example around the tunnel. In the model, three different size controls are used:

1. Interval length on the ground: the number of spacing among the nodes is defined. This option is used on the edges of the ground, with a distance of four;
2. Interval length on the 'hole' of the tunnels: in this zone the mesh has to be denser, so the size control on the voids is equal to one;
3. Linear grading on the front and on the behind views of grounds: this option permits to generate a mesh denser close to the tunnels and coarser as the distance increase.

4.2.2 Mesh generation

In the software FEA NX it is possible to create two types of mesh: tetrahedral and hexahedron centred hybrid shape. The second one is an advantageous shape because it combines pyramid and tetrahedron on the hexahedron base, hence it fits better the different shape.

All the parts of the tunnels and of the soils are created with the tetrahedral shape, because it creates a thick mesh with a lot of nodes.

The Figure 46 and Figure 47 show the resultant mesh. The different colours in Figure 46 represent the three different layers while in Figure 47 every ring of 1.5 meters.

The Figure 48 is a zoom on the different parts of the tunnel: the central pink is the soil, the bottle-green is the lining, the light green is the grout and finally the external pink is the shield.

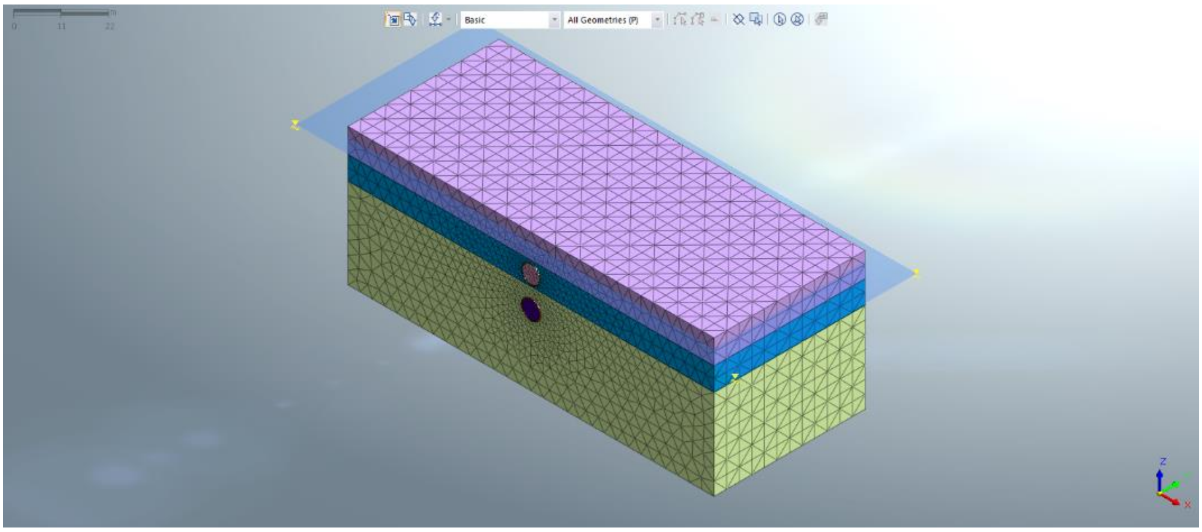

Figure 46 Mesh generation of the soils

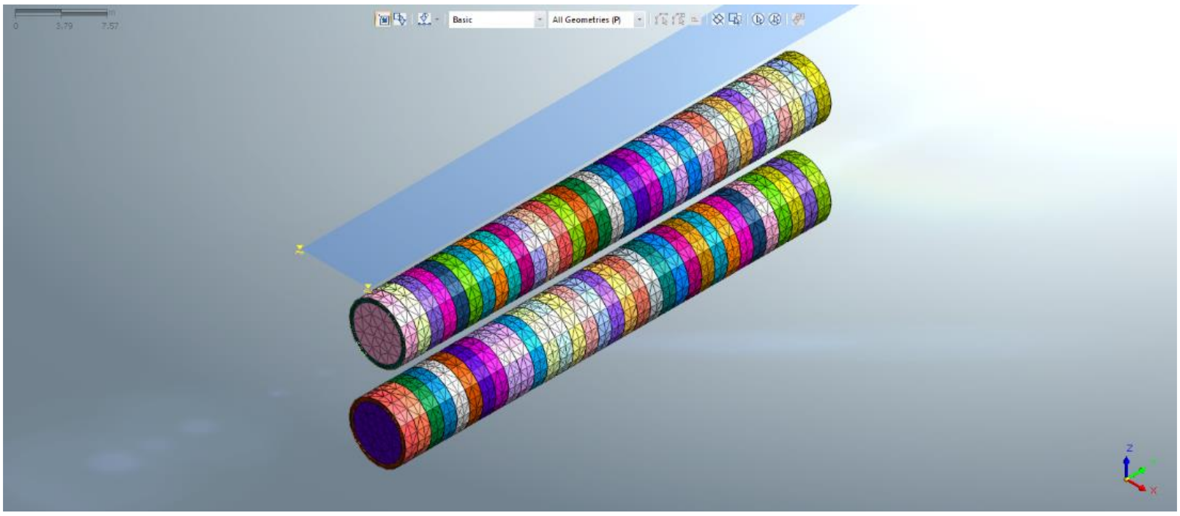

Figure 47 Mesh generation of the tunnels

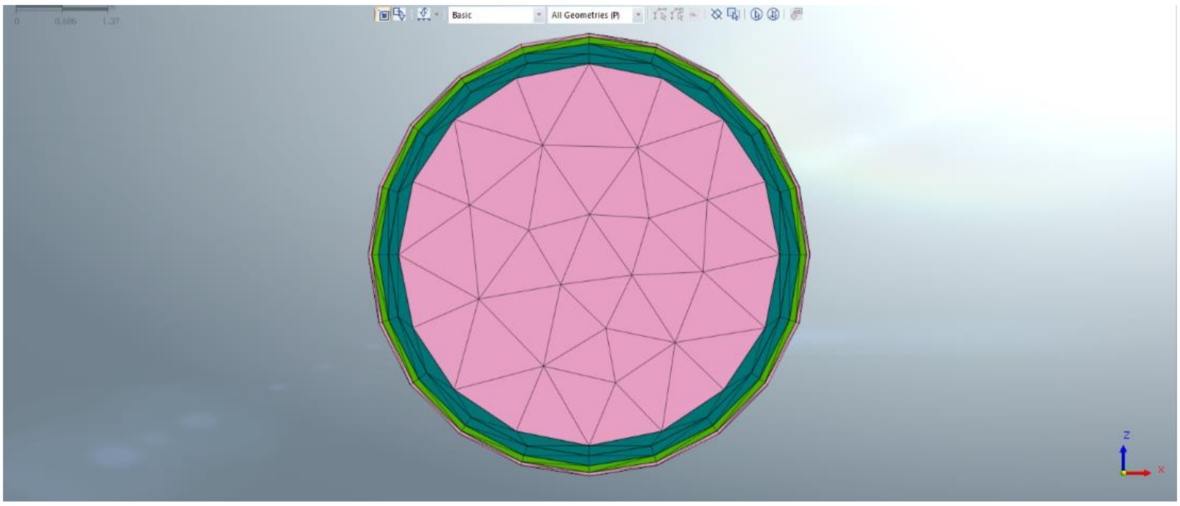

Figure 48 Detail of mesh generation of the tunnel components

The mesh set can be renamed to order all the single rings based on the y-coordinate, so the first ring will be at zero meter, while the last ring will be at 100 meters. This option is useful for the construction stages, because the software will excavate in an orderly way following the advancement of the project.

4.2.3 Boundary conditions

The constraint conditions are assigned to all the mesh sets. It is selected the automatic method for creating the constraints. With this method, the program sets:

- In x direction, the displacements are constrained in left and right sides;
- In y direction, the displacements are constrained in front and back sides;
- In the plane x,y, the displacements are fixed in the bottom part.

4.3 Static Load Analysis

Self-weight: The self-weight is calculated takes into account the volumes, the densities and the gravitational acceleration of the elements. The only input for the model is the vertical direction of the weight, in this case the z one.

4.3.1 Equivalent geo-mechanical parameters

Before starting to calculate the pressure to applied, it is important to specify the parameters; in particular, being the soil not uniform, but made of different layers, all the mechanical characteristics have to be 'homogenised', based on the distance from the tunnels, Figure 49. The equivalent mechanical parameters are calculated, as follow:

$$Param_{eq} = \frac{\sum_{i=1}^{n} t_i * w_i * param_i}{\sum_{i=1}^{n} t_i * w_i}$$

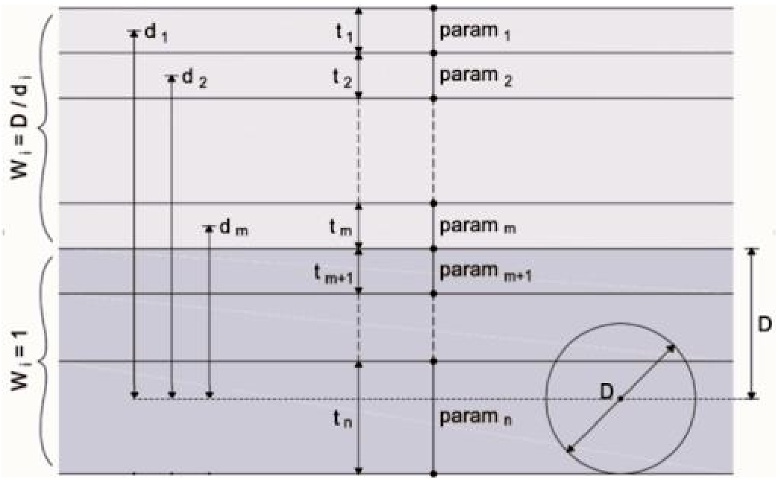

Figure 49 Scheme for the equivalent parameters

The Table 8 shows the results for the bottom tunnel.

Table 8 Bottom tunnel

γ_{eq} [kN/m^3]	c'_{eq} [kN/m^3]	φ' $_{eq}$ [°]	$k_{0,eq}$ [-]
20.55	3.56	27.18	0.49

The Table 9 shows the equivalent parameters for the upper tunnel, so the equivalent parameters are weighted on one single distance D.

Table 9 Upper tunnel

γ_{eq} [kN/m^3]	c'_{eq} [kN/m^3]	φ' $_{eq}$ [°]	$k_{0,eq}$ [-]
20.01	9.57	22.88	0.50

4.3.2 Support pressure on the face

4.3.2.1 Minimum support pressure

The face of the excavation has to be supported by applying a pressure from the machine, to counter-balance the trapezoidal pressure of the soil and the trapezoidal pressure of the groundwater, present above the tunnels.

The support pressure has been calculated with the method of (Anagnostou, et al., 1996a). The failure mechanism is the creation of a wedge ahead of the tunnel face, above which a prism extends from the crown of the tunnel up to the surface, as in Figure 50.

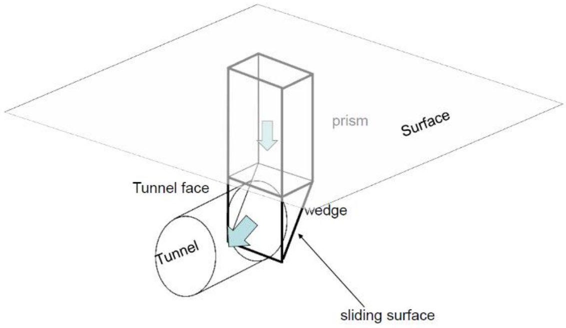

Figure 50 Scheme of Anagnostou and Kovari

It is important to notice that this method has strict hypothesis to be applied:

- the soil has to be in drained condition, otherwise the results will appear inconsistent because the soil will be always stable, without requiring support pressure;
- The different layers have to be homogenised, looking like a single homogenous soil;
- The different geometric parameters have to be take as reported in the paper and as shown in the Figure 51;

The resultant pressure refers to the minimum pressure, in order to stabilize the soil front, following the proposed failure mechanisms which can occur in the tunnel front. The final support pressure s' is a function of:

- the tunnel diameter D;
- the overburden H;
- the piezometric head in the chamber $h_{f;}$
- the elevation of the water table h_0;

- the effective shear strength parameters (cohesion and friction angle equivalents);
- the submerged unit weight of the soil;
- four dimensionless parameters, extracted from four different nomograms (F_0, F_1 , F_2 and F_3), as represented in Figure 51 .

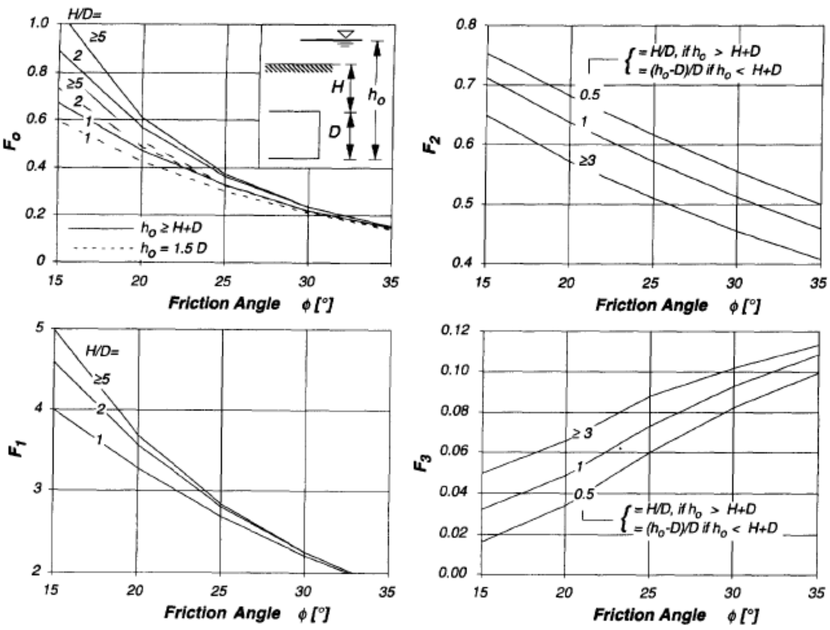

Figure 51 Nomograms of the four dimensionless parameters

$$s^{A\&K}(kPa) = F_0 * \gamma'_{eq} * D - F_1 * c'_{eq} + F_2 * \gamma'_{eq} * \Delta h - F_3 * c'_{eq} * \frac{\Delta h}{D}$$

In this analysis the piezometric head h_f in the chamber of the machine, is equal to that ahead of the face h_0, in order to avoid the entrance of the water.

However, in this approach the water load has to be added for the final solution and also in this case two different factors of safety are considered in order to increase the minimum pressure.

$$s_{axis}'(kPa) = s^{A\&K} * 1.5 + \gamma_{water} * \left(h0 - \frac{D}{2}\right) * 1.1$$

The result of this formula is applied on the tunnel axis, hence the pressures on the crown and on the invert are evaluated for all the chainage and the corresponding water level and overburden. To transform the pressure on the axis to the crown and invert, the component of the conditioned soil is considered, with a unit weight equal to 14 kN/m^3.

$$s_{crown}'(kPa) = (s^{A\&K} - \gamma_{cond_{soil}} * R) * 1.5 + \gamma_{water} * (h0 - D) * 1.1$$

$$s_{bottom}'(kPa) = (s^{A\&K} + \gamma_{cond_{soil}} * R) * 1.5 + \gamma_{water} * h0 * 1.1$$

4.3.2.2 Maximum support pressure

The first two problems related to the high applied support pressure is the blow-out of the medium and the break-up of the overburden that affects the surface. The maximum pressure is considered as the minimum between the total load acting on the machine and the operational limit of the machine itself. (DAUB, 2016) recommends that this maximum pressure has to be smaller than the 90% of the total vertical stress applied on the tunnel crown. In this approach the maximum pressure that can be applied by the machine is 500 kPa.

$$\sigma_{v,axis}(kPa) = 0.9 * (\gamma'_{eq} * H + \gamma_{cond\_soil} * \frac{D}{2})$$

$$\sigma_{v,crown}(kPa) = 0.9 * (\gamma'_{eq} * H)$$

$$\sigma_{v,bottom}(kPa) = 0.9 * (\gamma'_{eq} * H + \gamma_{cond\_soil} * D)$$

Finally, it was selected a reference pressure for all chainages of the bottom tunnel:

- Pressure on the axis: 225 kPa;

The same procedure is applied for the upper tunnel:

- Pressure on the axis: 135 kPa;

4.4 Construction stages

The advantage of the 3D numerical models is the simulation of the construction phases of the tunnel. It is possible to model the passage of the TBM shield, the installation of the segmental lining and the injection of the grout. All the construction stages can be easily defined in MIDAS FEA NX by “removing” or “activating” parts of the model.

The first analysis starts with the upper tunnel, which is excavated first, and after the final installation of the last ring, the bottom tunnel excavation begins. The construction sequences are summarised (Figure 52), remembering that each stage covers only 1.5 meters, equal to the ring length:

- I.S. : this acronym means Initial State, hence the condition of the soil before starting the excavation. In this phase the only stresses are the weight and the water pressure and all the solids, have to be activated with initially soil characteristics;
- S1: The internal parts of the tunnel are removed, and the soil starts to be excavate, which are called “up_grout”, “up_in” and “up_lining3D” in the model, as explained in the chapter 4.1.2. Simultaneously, the shield “up_shield” is activated in order to prevent the collapse of the void and to apply the support pressure on the face “FU”.

This first step S1 is repeated up the total length of the shield (1.5 meter * 8 stages = 12 meters);

- S9: After the shield, immediately there is the installation of the rings (“up_lining3D” and “up_lining2D”) and the injection of the grout (“up_grout”) around them. These last three parts are activated while the shield starts to be removed.

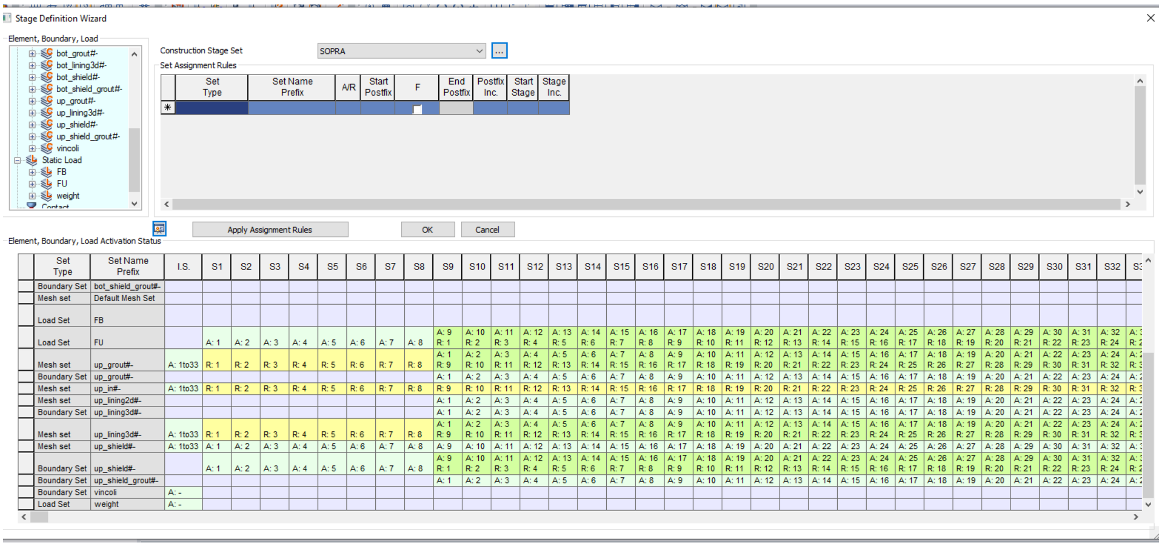

Figure 52 Construction Stages Definition

5. TWO-DIMENSIONAL FEM ANALYSIS WITH PLAXIS2D

PLAXIS2D is a two-dimensional FEM software. The first difference with the 3D is that it possible to draw, analyse and study planar sections. Hence the longitudinal component is not considered; however, it is possible to simulate the three dimensionality of the problem, analysing different transversal sections or applying an internal radial pressure, e.g. at the face front of the tunnel or when the lining is installed. The other differences are the easier creation of the model and the faster velocity on the calculations. This allows the interpretation of the results and, if necessary, the change of some parameters in a short time.

Initially three different arrangements of the tunnels are analysed, resuming the initial project of the Bucharest metro line: horizontal, offset and vertical layouts. After that, a second different analysis is performed considering only the piggyback configuration, which is the most particular and unusual one.

5.1 Geometry of the model and mesh generation

The stratigraphy is considered with its different soil layers, as reported in Table 5, hence no simplification is made, differently to the 3D model. The sizes of the 2D model are taken as those of the 3D one, in particular 120 meters in length and 45 meters in height. In PLAXIS2D, it is possible to define the stratigraphy describing the layers of a virtual borehole. In practice, the characteristics like thickness, physical and geo-mechanical parameters are inserted and automatically assigned to the previous defined dimensions of the model. At this step, the water-head is inserted.

The Figure 53 shows the screen of PLAXIS2D for the definition of soil properties.

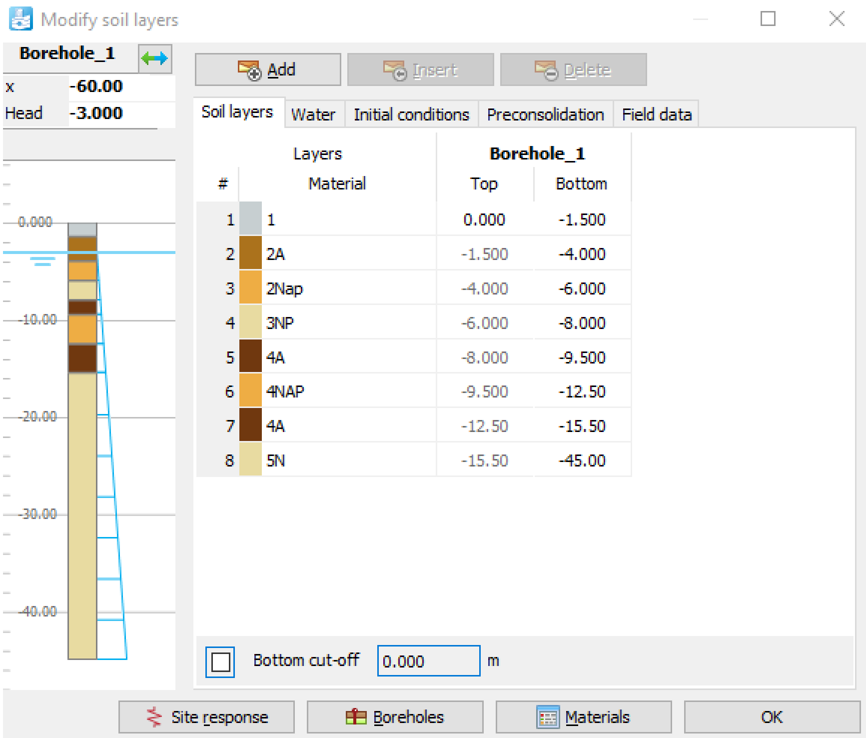

Figure 53 Definition of borehole

The tunnel linings are modelled as plate, with the parameters of the segment reinforced concrete. An important step is the creation of interfaces: these allow the interaction between the tunnel lining and the soil. In this way two nodes are created (Figure 54), one regards the soil and the other the structure: the interaction is like elastic-perfectly plastic springs.

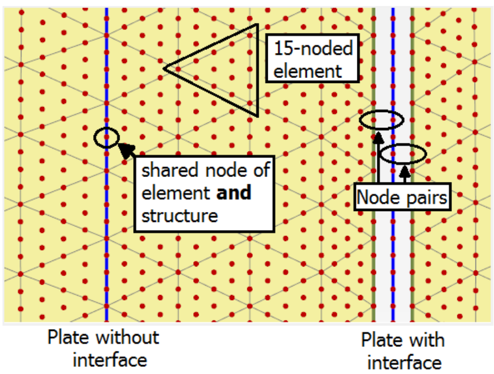

Figure 54 Interfaces

In this model the diameter of the lining is equal to 6.6 meters, so the value of the diameter of the excavation, since in 2D models, the shield and the grout are not simulated.

Horizontal configuration (Figure 55):

- Depth of the crown: 9.7 meters;
- Horizontal inter-axis distance : 13.6 meters;

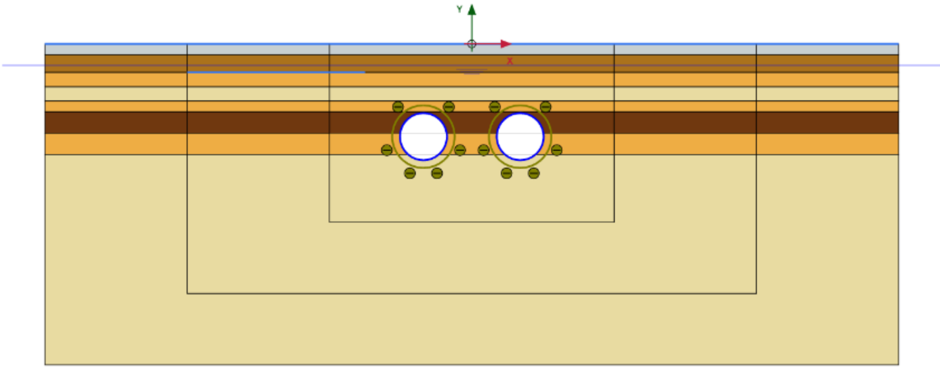

Figure 55 Horizontal configuration

Offset configuration (Figure 56):

- Depth of the crown - tunnel right: 8.7 meters;
- Depth of the crown - tunnel left: 16.2 meters;
- Vertical inter-axis: 7.3 meters;
- Horizontal inter-axis: 13.1 meters.

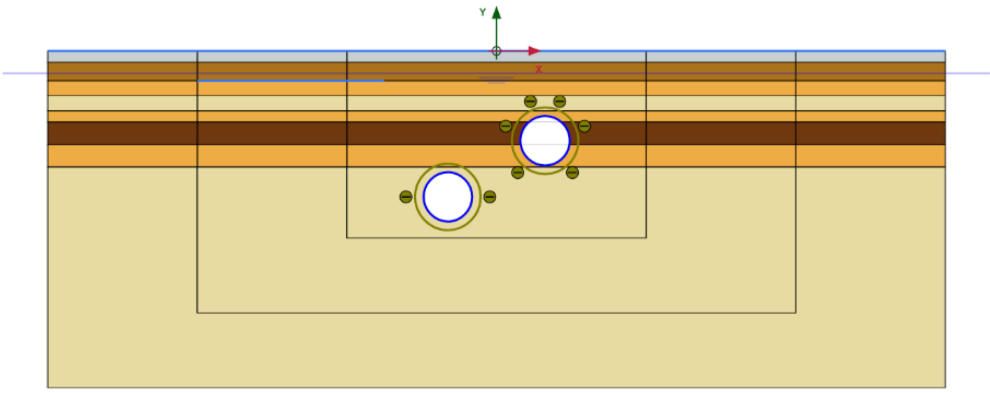

Figure 56 Offset configuration

Piggyback configuration (Figure 57):

- Depth of the crown - upper tunnel: 12 meters;
- Depth of the crown - bottom tunnel: 22 meters;

- Vertical inter-axis: 10 meters;

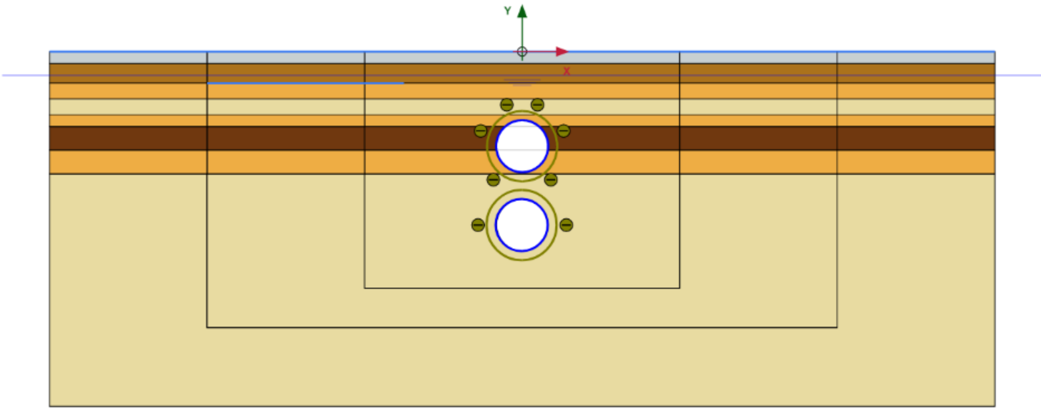

Figure 57 Piggyback configuration

After the definition of the geometry, it is necessary to generate the mesh. On PLAXIS2D it is possible to set a very fine pattern for better results.

In order to not overweight the time calculations, the model is subdivided in three different zones: from far away from the tunnels up to reach the plate of the lining, the mesh appears denser close the tunnels and coarser on the boundary, as shown in Figure 58.

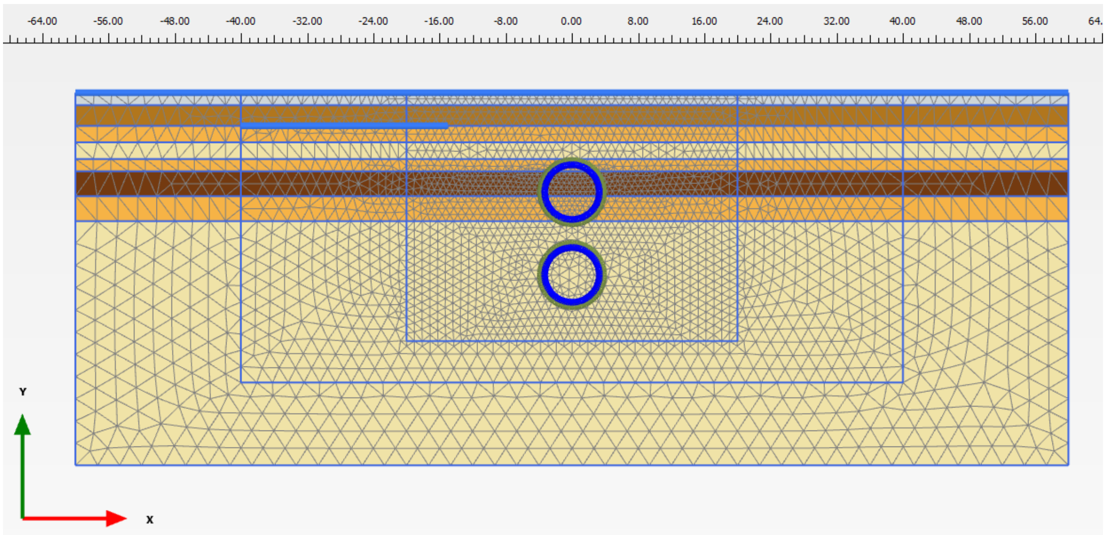

Figure 58 Mesh generation on PLAXIS2D

5.2 Staged construction

Two different types of analysis are performed on PLAXIS 2D: the first regards the comparison among the three arrangements of the tunnels and the second goes in detail with the vertical layout. In PLAXIS the excavation simulation can be done in two different ways:

- Application of the deconfinement;
- Application of an internal radial pressure.

The construction stages are the same for each analysis, in particular:

1. Excavation of the first tunnel with the application of one of the two abovementioned methods;
2. Installation of the lining;
3. Excavation of the second tunnel as before.

5.2.1 Construction Stages with the three different alignments

The analysis of the three alignments is performed with the application of the deconfinement on the excavated zone. The idea is to simulate the progressive advancement of the machine towards the studied section by the application of a coefficient (1-β) to the initial stress before the tunnel is constructed.

$$p_f = (1 - \beta) * \sigma_0$$

This coefficient of deconfinement β is introduced by (Panet, et al., 1974).

In practice, when the soil cluster is deactivated, this deconfinement value is applied in order to simulate the reduction of the initial stress due to the creation of the void. When the studied section is equal to the face-front, typical value of the deconfinement is about 28%. It means that only the 72% of the initial stress field acts as support around the tunnel. In the subsequent phases, the pressure has to be reduced up to the section in which the lining is installed. At this point, the deconfinement is maximum (100%), which means that the support pressure does not act anymore, and all the loads are transferred to the lining.

In order to select which is the value to insert as deconfinement, a preliminary analysis is performed by imposing a percentage of volume loss on the surface; in this thesis the two volumes losses supposed are equal to 0.5% and 1%. The volume loss is correlated to the deconfinement in the void: if the wanted volume loss is lower, the deconfinement will be lower and consequently the applied pressure p_f higher.

5.2.2 Construction Stages with vertical alignment

This analysis is carried out by simulating the excavation process thanks to the application of an internal radial pressure. This pressure varies increasing the depth, taking into account the presence of the conditioned soil, which has a unit weight equal to 14 kN/m^3.

Four different values are selected in order to conduct a parametric analysis: these values are chosen between the minimum support pressure required to stabilize the excavation and the maximum applicable one, as mentioned in the 4.3 Static Load Analysis.

The pressures for the upper tunnel are:

- 0.75 bar;
- 1 bar;
- 1.25 bar;
- 1.5 bar.

The pressures for the bottom tunnel are:

- 1.75 bar;
- 2.25 bar;
- 2.75 bar;

- 3.25 bar.

The parametric analysis is designed by fixing the pressure of the tunnel constructed first and varying the pressures related to the other one. In this way it is possible to obtain sixteen pressure combination for each excavation sequence.

In the Figure 59 there is an example of this type of analysis. In particular, the upper tunnel is excavated with 0.75 bar (*0.75_P1*), then the lining is installed (*0.75_P1_Lining*), and the last four steps are related to the excavation of the bottom tunnel, varying the bottom pressure from 1.75 bar up to 3.25 bar (e.g. *0.75_P1-1.75_P2*). After that the pressure of excavation of the upper tunnel is fixed to 1 bar (*1_P1*) and again the bottom is excavated with the four pressures.

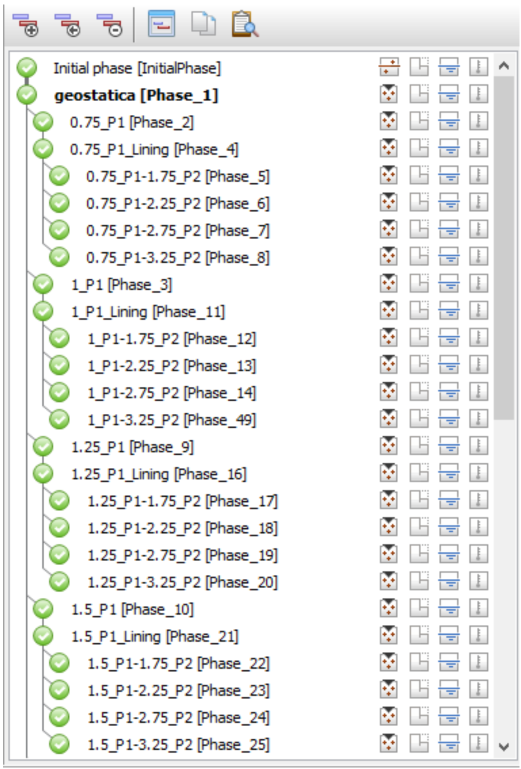

Figure 59 Example of Staged Construction in PLAXIS2D

All this procedure is repeated when the bottom tunnel is constructed first, starting with the application of 1.75 bar and vary the upper from 0.75 bar to 1.5 bar.

6. RESULTS AND INTERPRETATION

After the presentation of all the models, different outputs are extrapolated and interpreted, focusing on the actions and loads resulting in the segmental tunnel lining. The results are extracted on the first constructed tunnel in two different stages: when the first lining is installed and when the second tunnel starts to be excavated. In this way it is possible to examine what can be the effects of a single construction and what are the effects if a second tunnel is excavated.

Summarising three different analyses are performed:

- 3D numerical model with vertical alignment with MIDAS FEA NX: the results are the stresses σ_{zz} and σ_{xx};
- 2D numerical model with horizontal, offset and vertical alignments with PLAXIS2D: the results are the bending moment M and the axial force N;
- 2D numerical model with vertical alignment with PLAXIS2D: the results are the axial force N, the bending moment M, the eccentricity e, the vertical and horizontal ovalization and the relative displacement of the invert of the tunnel.

6.1 3D Numerical Model With Vertical Alignment With MIDAS FEA NX

The first step is the validation of 3D model; this is done with the comparison of the initial stage before the excavations between FEA NX and PLAXIS2D.

Both the software in the initial stage takes into account the geostatic stress as the vertical stress, which considers the stress of soil under its weight, and the initial K_0 condition for the horizontal stress.

In the Figure 60 and Figure 61 the total vertical stress is considered: the 3D model considers the results in the barycentre of the 3D element of the mesh and not on the element edge. This explain why on the ground surface there is a number (20 kPa) and not zero as can be expected and why the two maximum values on the depth of the two models are slightly different.

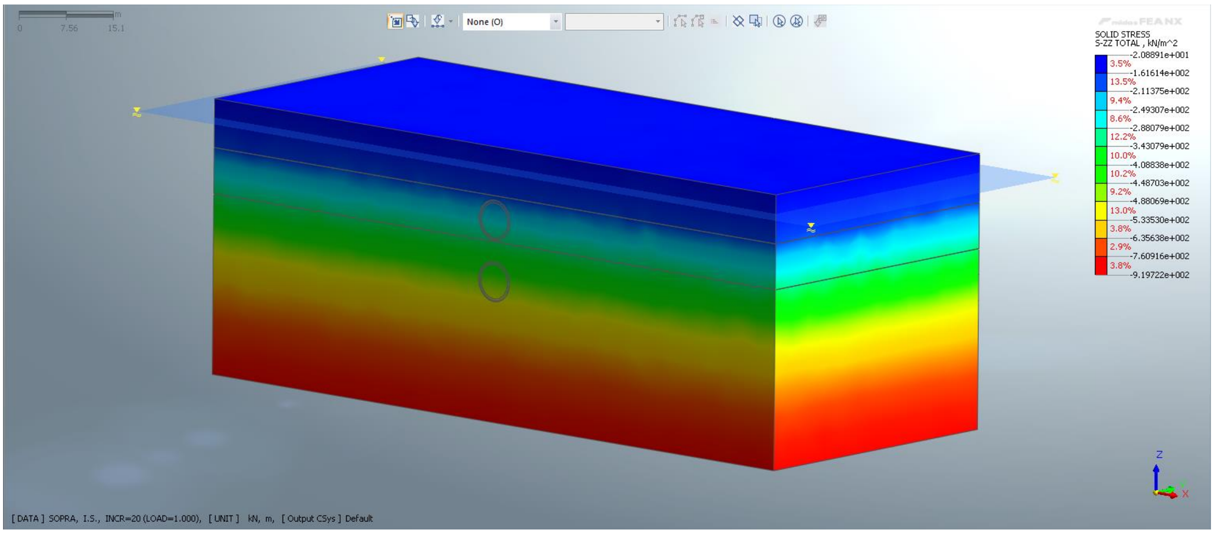

Figure 60 Initial stage - 3D model (MIDAS)

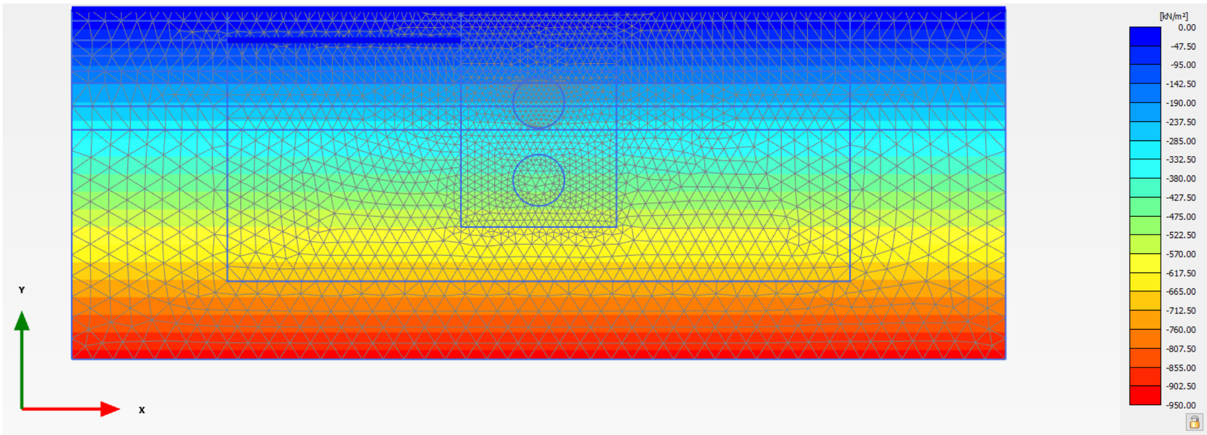

Figure 61 Initial stage - 2D model (PLAXIS)

The outputs of 3D analysis are carried out for the two excavation sequences, upper excavated first and bottom excavated first. They are extracted from the solids "up_lining3D" and "bot_lining3D" as reported in chapter 'Geometry of the tunnels'.

The two extrapolated stresses are chosen in order to be compared to the axial force N: the vertical stress σ_{zz} is the component of axial force calculated on the sidewalls of the tunnel, instead σ_{xx} is the component of the axial force calculate on the invert and on the crown of the tunnel.

Starting from the excavation of upper tunnel first and comparing the horizontal stress σ_{xx} (Figure 62 and Figure 63), it is possible to notice that the excavation of second bottom tunnel does not involve a variations of the stresses on the crow and on the invert.

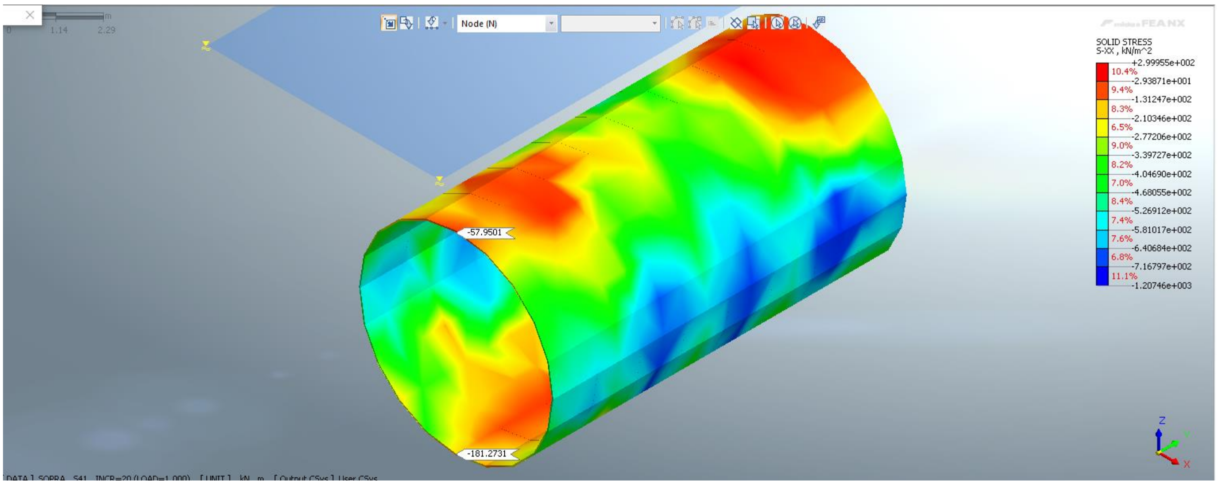

Figure 62 Horizontal stress on the crown and invert for the upper tunnel, 3D model - upper tunnel first

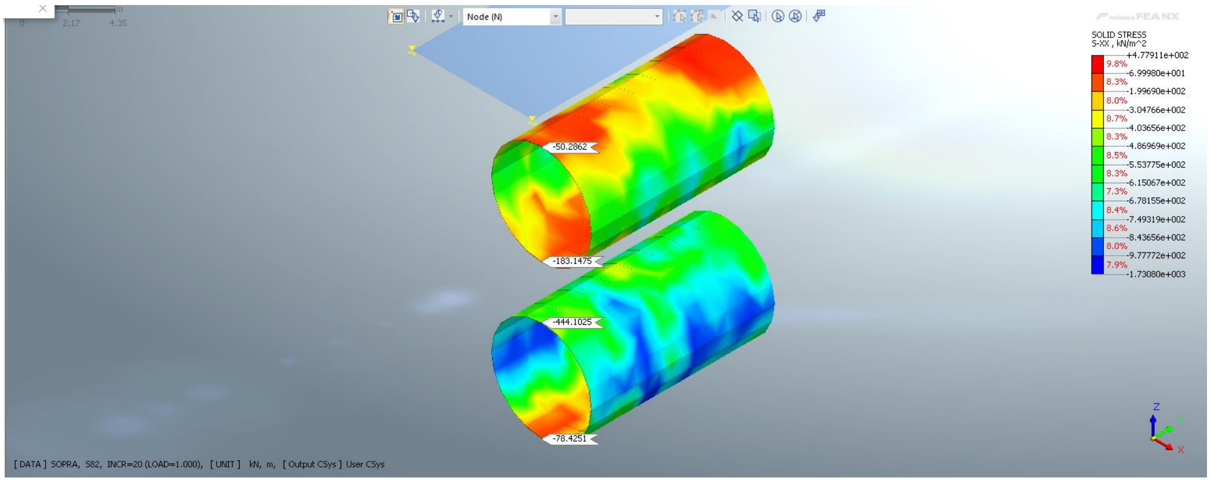

Figure 63 Horizontal stress on the crown and invert for 3D model- Upper tunnel first

If the excavation starts with the lower tunnel, the horizontal stresses on the bottom tube, does not significantly vary, as can be noticed in Figure 64 and Figure 65. Hence, for both the sequence, it is possible to discover that the excavation of a second tunnel, does not imply a variation of the stress state on the crown and invert for the first lining.

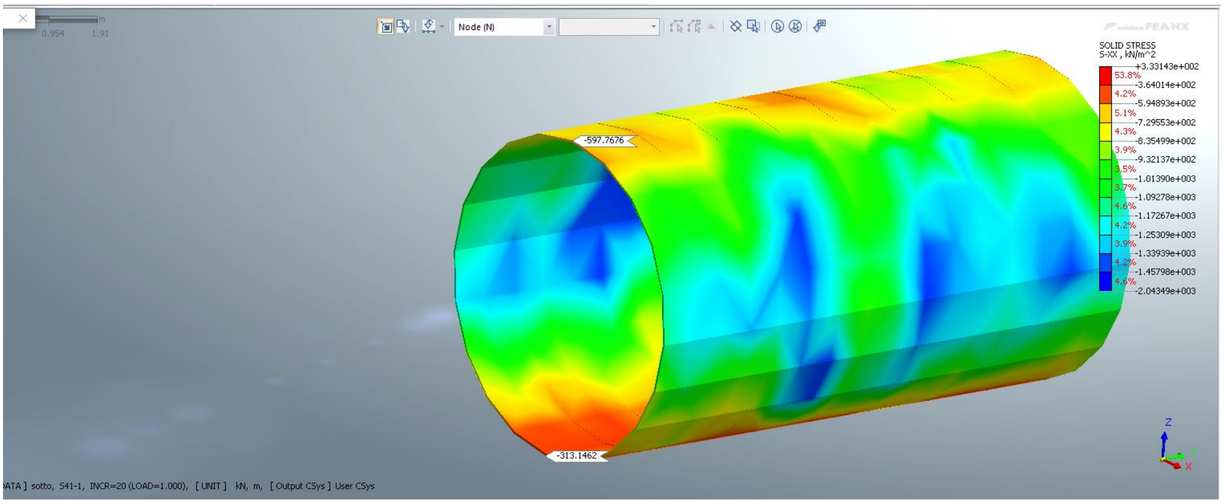

Figure 64 Horizontal stresses on the crown and invert for the bottom tunnel, 3D model- Bottom tunnel first

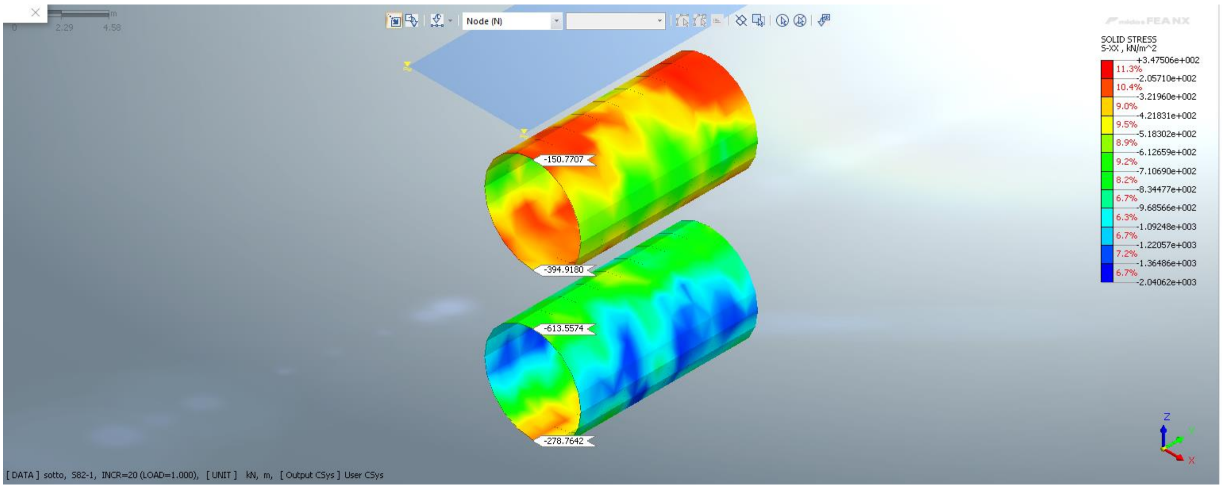

Figure 65 Horizontal stress on the crown and invert for 3D model - Bottom tunnel first

What is important to notice, comparing the Figure 63 and Figure 65, is that the excavation of bottom tunnel first induces in both the tunnel, higher values of compression stresses, which means high axial force in the sections. The higher is the axial force and better the ring works, being a compressed circle. Moreover, lower value of compressive stress means it moves away from the tension zone of the interaction diagram M-N, which can be induce damages especially in the joints.

The vertical stresses σ_{zz} on the sidewalls are evaluated, and the results are plotted in Figure 66 and Figure 67. It is possible to establish that the sidewalls are not affected by the excavation sequence, in fact the values regarding each tunnel do not change. Obviously, the bottom tunnel, in both the excavation sequence, exhibits higher values compared to the upper tunnel, due to higher depth.

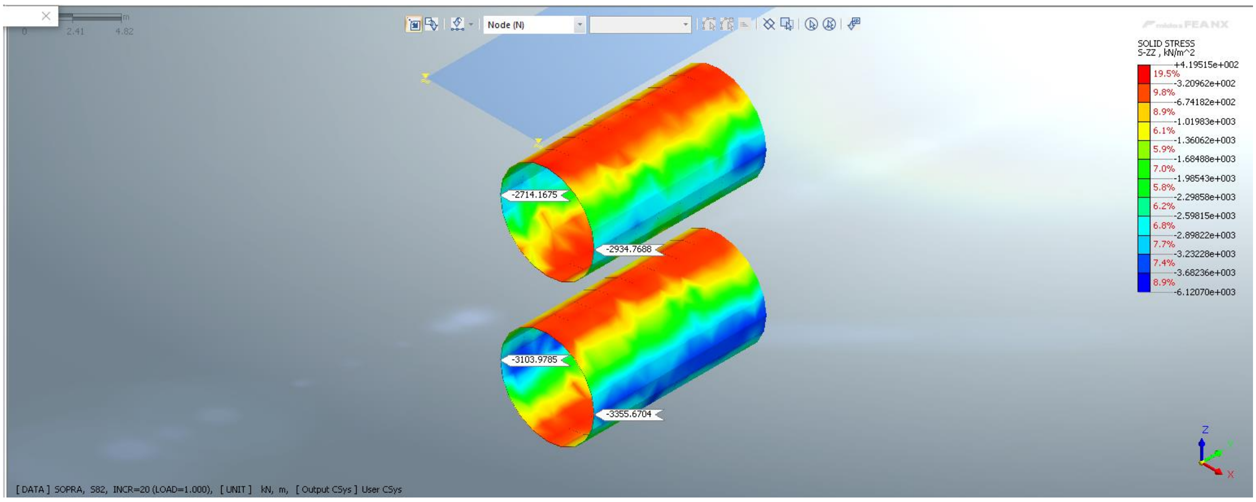

Figure 66 Vertical stress of the sidewalls for 3D model - upper tunnel first

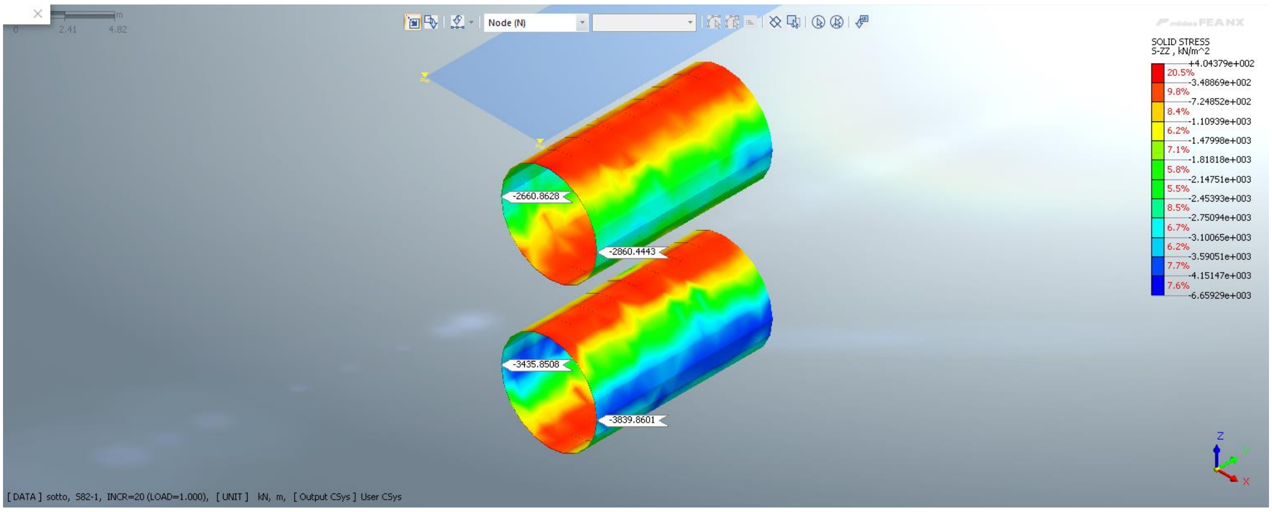

Figure 67 Vertical stress of the sidewalls for 3D model- bottom tunnel first

The complexity of the 3D FEM model, in which all the details have been properly modelled, such as the applied face pressure, the shield and the segmental lining, may lead to possible misinterpretation of the achieved results. Hence more simplified 2D models have been also performed in order to cross-check the general results and tunnel behaviour, confirming the assessments presented so far.

6.2 2D Numerical Model With Horizontal, Offset And Vertical Alignment With PLAXIS2D

The first two-dimensional analysis is a comparison among the three different layouts in order to observe some effects regarding the lining. Moreover, two different volume loss on the surface are fixed and this is correlated to how much loads, the lining takes. The first volume loss is equal 1%, which implies less deconfinement than the case with the volume loss equal to 0.5%.

Starting with the horizontal alignment, the maximum values of bending moment and axial force are when the excavation of the second tunnel starts and with a total volume loss equal to 0.5%. However, the results between the two volume losses are not so different, as in Figure 68.

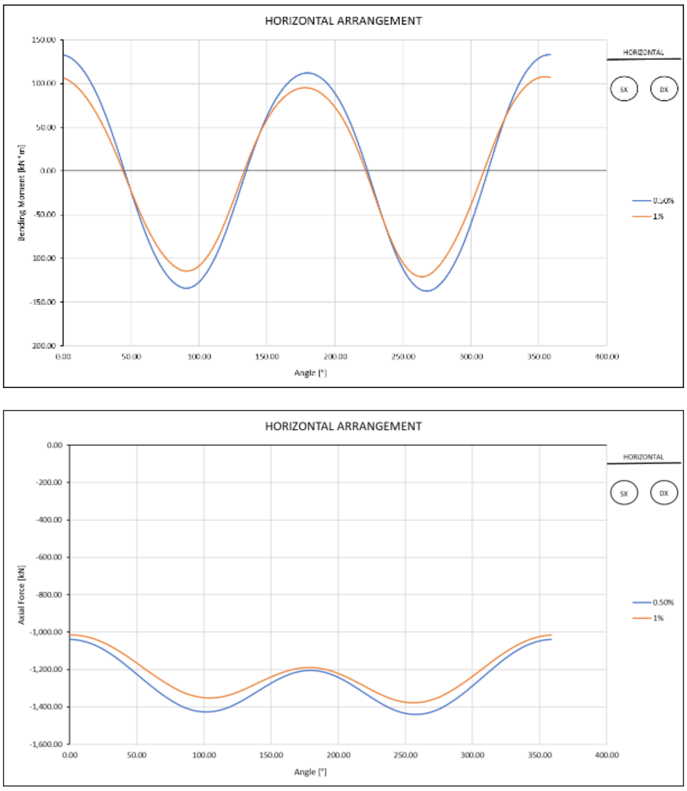

Figure 68 Bending Moment and Axial force - Horizontal layout

The offset configuration has the same principles of the horizontal layout, with an addiction analysis regarding the excavation sequence between starting first the left tube and the other with starting of the right tube. As previous, the worst condition is for the lowest value of the volume loss, because the lining has more loads, as in Figure 69. The bending moments and the axial force are maximum when the left tunnel starts before.

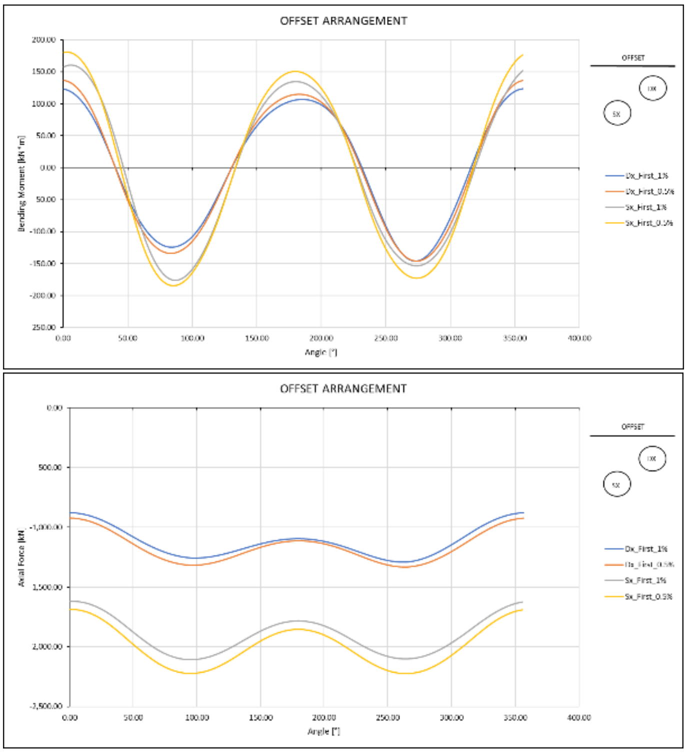

Figure 69 Bending Moment and Axial force - offset layout

Finally the vertical arrangement is analysed. The maximum value is when the bottom tunnel is constructed first with a volume loss of 0.5%, in correspondence of the installation of the lining. The excavation of the upper tunnel reduces the stresses around the soil, so the axial force and bending moment reduce.

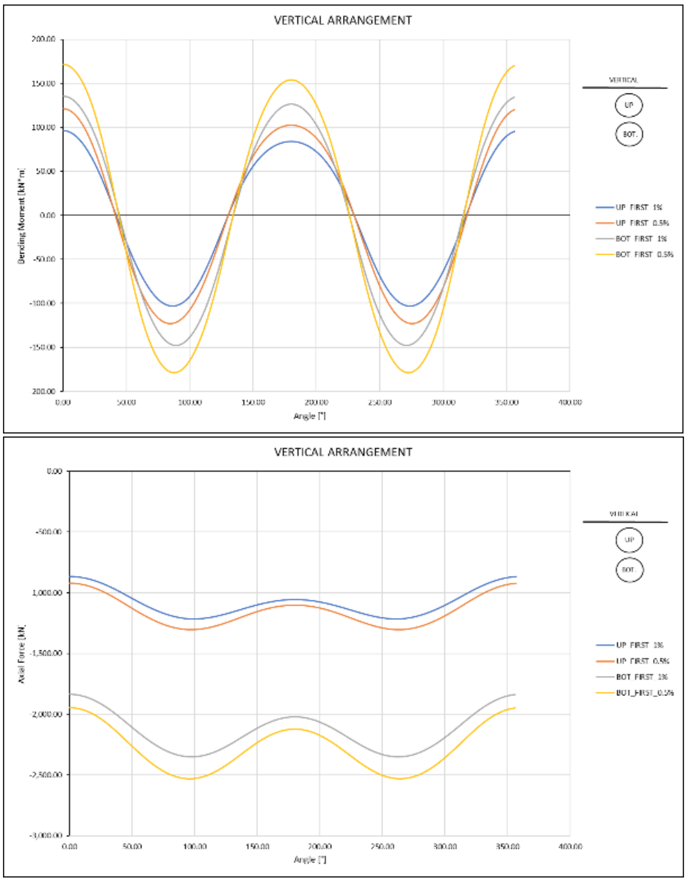

Figure 70 Bending Moment and Axial force - Vertical layout.

At the end, all the maximum values are plotted together for the three arrangements, in order to understand which one reproduce the higher actions. However the results for the volume loss equal to 1% (Figure 72) are showed and it is possible to demonstrate that they present lower values comparing with the results of volume loss equal to 0.5% (Figure 71). In general, the horizontal configuration has the minimum values for both bending moment and axial force. Concerning the moments, there are no difference between vertical and offset regarding the trends, except for the maximum value belonging to the offset configuration. Instead, the maximum axial force pertains to the vertical configuration when the bottom tunnel is excavated first.

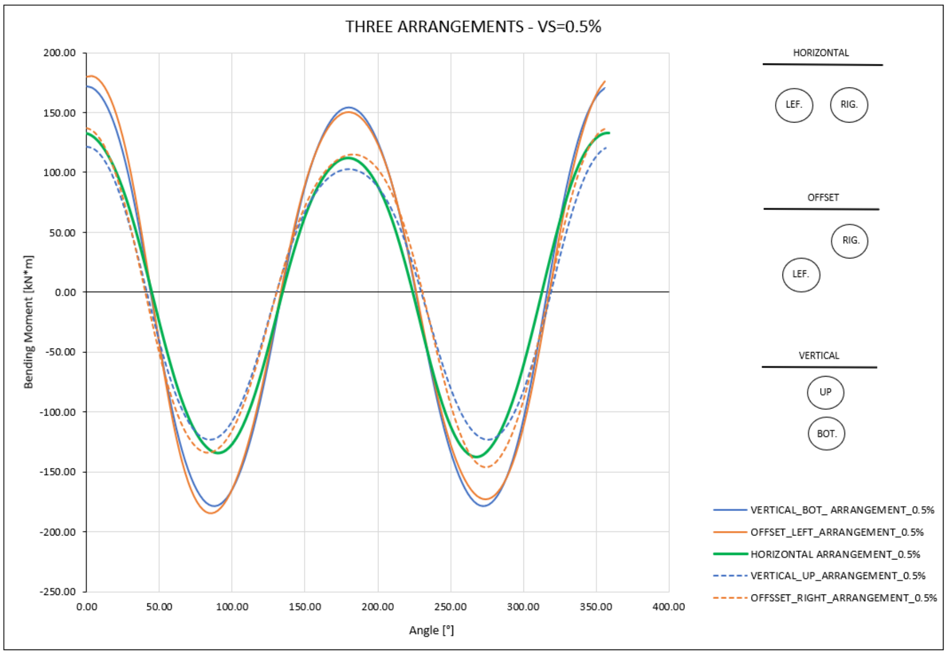

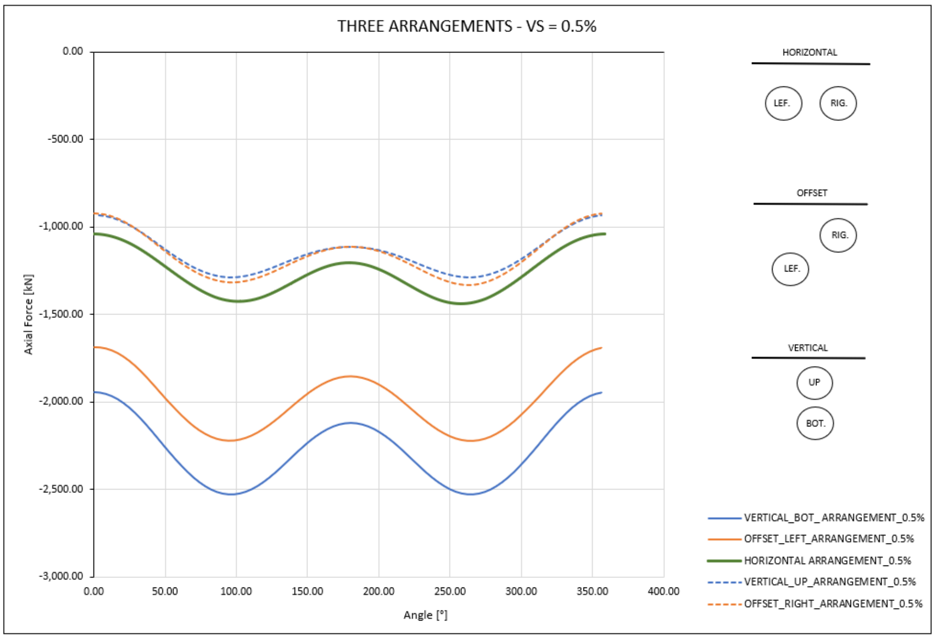

Figure 71 Bending Moment and Axial force for VS=0.5% - three layouts

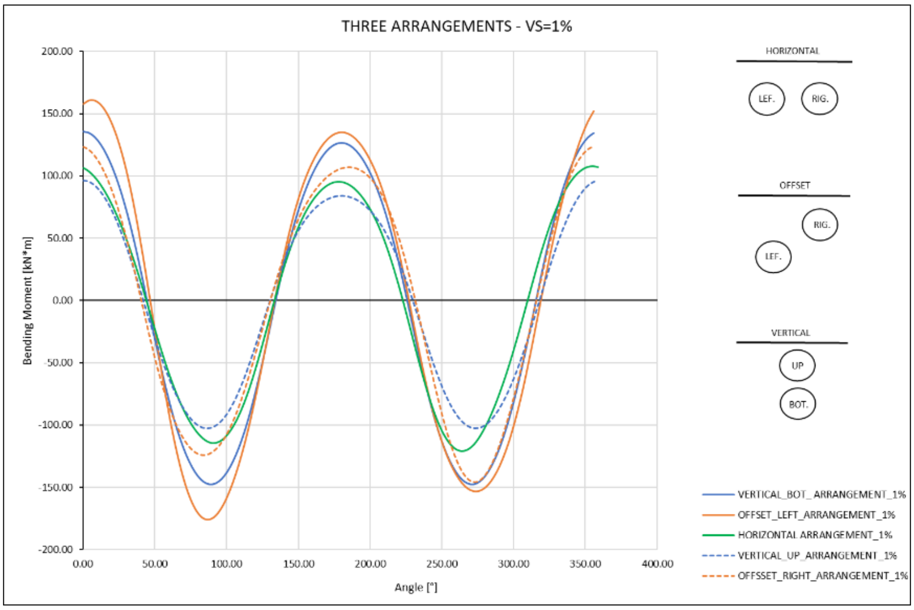

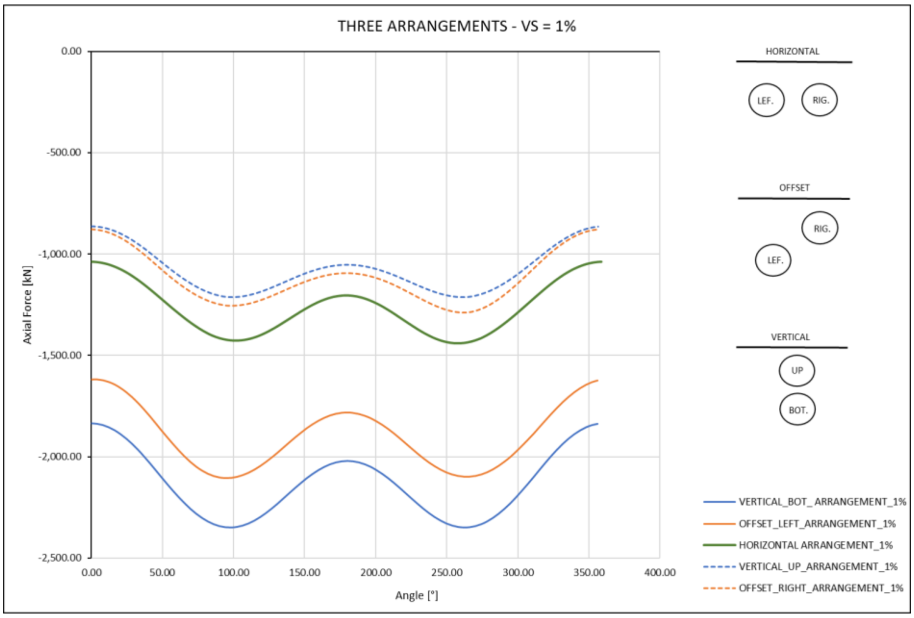

Figure 72 Bending Moment and Axial force for VS=1% - three layouts

6.3 2D Numerical Model With Vertical Alignment with PLAXIS2D

As abovementioned, the analysis is performed by the excavation of the first tunnel, the application of the lining and the excavation of the second tunnel.

The chapters are divided assuming the excavation of the upper tunnel first, then the excavation of the bottom tunnel first and at the end the comparison of the two excavation sequences.

6.3.1 Excavation of upper tunnel first

The configuration is represented in Figure 73.

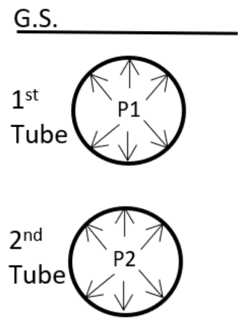

Figure 73 Scheme of excavation of upper tunnel first

Where P1 is the internal radial pressure applied on the first excavated tunnel and P2 is that one applied on the second tunnel. All these pressures are represented in the following graphs, in particular the x-axis is the normalised pressure P2 over the initial stress before the excavation, the y-axis changes based on the obtained results. Finally the P1 is represented by the different coloured lines, e.g. the blue line is the P1=0.75 bar.

Moreover, in this first analysis all the results are referred to the lining on the upper tunnel.

6.3.1.1 Axial Force N

The axial force resulting on the lining of the upper tunnel is a compressive force inside each segment, hence the whole ring results compressed. In the Table 10 are showed all the maximum axial force, considering that they are multiplied with the length of the segment (1.5 meters).

Table 10 Results of axial force- upper tunnel first

P2 [kPa]	P2/σv	P1 [kPa]	N_max [kN]	P1 [kPa]	N_max [kN]	P1 [kPa]	N_max [kN]	P1 [kPa]	N_max [kN]
Lining	0.44	75.00	691.65	100	794.11	125	909.86	150	1026.15
175.00	0.47	75.00	1068.59	100	1108.22	125	1147.84	150	1173.02
225.00	0.60	75.00	758.78	100	838.51	125	942.23	150	1048.29
275.00	0.74	75.00	694.47	100	793.84	125	905.58	150	1014.32
325.00	0.87	75.00	684.34	100	773.24	125	871.82	150	962.94

Following the Figure 74:

- The maximum values are all placed in the invert of the lining, at coordinate (0,-15.3);
- Fixing P2 value, by increasing the excavation pressure P1, the axial force increases too, due to high forces applied on the lining;
- If the second tunnel starts to excavate, the axial force decreases, by increasing the pressure P2. In fact, the maximum values of N occur at low P2. This can be due to the fact that, applying a high P2 means deconfine less the second tunnel, and this implies a low resultant stress on the upper tunnel.
- If the pressure P2 is equal to 3.25 bar, the axial force is always lower than the axial force when there is only the upper tunnel (line *Lining*);

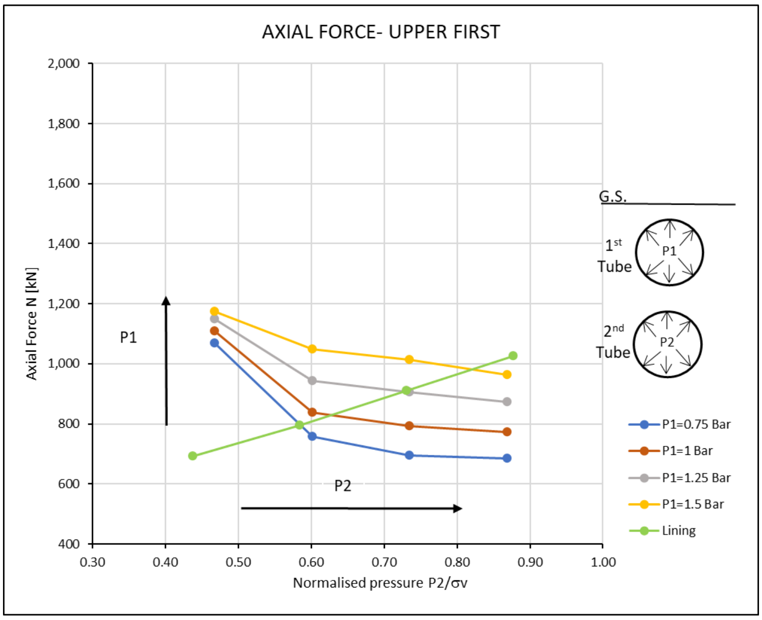

Figure 74 Axial Force - Upper first

6.3.1.2 Bending Moment M

The bending moment is subdivided in positive and negative, based on the “fibres” which tends. In general, positive moment stretches the fibres of the intradox, while the negative one deforms the extradox fibres.

The maximum values are reported in the following Table 11 where each colour refers to the pressure P1.

Table 11 Bending Moment M- Upper tunnel first

P2 [kPa]	P2/σv	P1 [kPa]	M- [kN*m]	M+ [kN*m]	P1 [kPa]	M- [kN*m]	M+ [kN*m]
Lining	0.44	75.00	-20.68	14.91	100.00	-17.62	13.40
175.00	0.47	75.00	-185.77	142.74	100.00	-205.35	155.31
225.00	0.60	75.00	-68.99	54.72	100.00	-86.38	61.18
275.00	0.74	75.00	-32.19	23.31	100.00	-44.64	28.47
325.00	0.87	75.00	-25.26	33.08	100.00	-12.61	17.37

P2 [kPa]	P2/σv	P1 [kPa]	M- [kN*m]	M+ [kN*m]	P1 [kPa]	M- [kN*m]	M+ [kN*m]
Lining	0.44	125.00	-17.73	13.14	150.00	-15.75	12.34
175.00	0.47	125.00	-220.60	164.91	150.00	-227.36	166.92
225.00	0.60	125.00	-94.38	64.16	150.00	-94.12	61.94
275.00	0.74	125.00	-48.49	30.64	150.00	-48.96	29.87
325.00	0.87	125.00	-9.46	12.59	150.00	-7.37	7.96

The graphs are represented in the Figure 76 and the Figure 77.

- The excavation of the upper tunnel only with the increasing P1, does not significantly affect the moments, despite the axial force N;
- By increasing the excavation pressure P1, both the positive and negative bending moments increase;
- By increasing the P2, however, the bending moments are reduced significantly, in some cases also of more than 95%;
- For all the P1 and P2=1.75, 2.25, 2.75 bar the maximum negative bending moment is on the invert (coordinate 0, -15.3) and the maximum positive is on the half of the gallery (coordinate -3.3; -12). While with P2=3.25 bar, there is an inversion of the coordinates of the maximum moments between positive and negative, as shown in Figure 75.

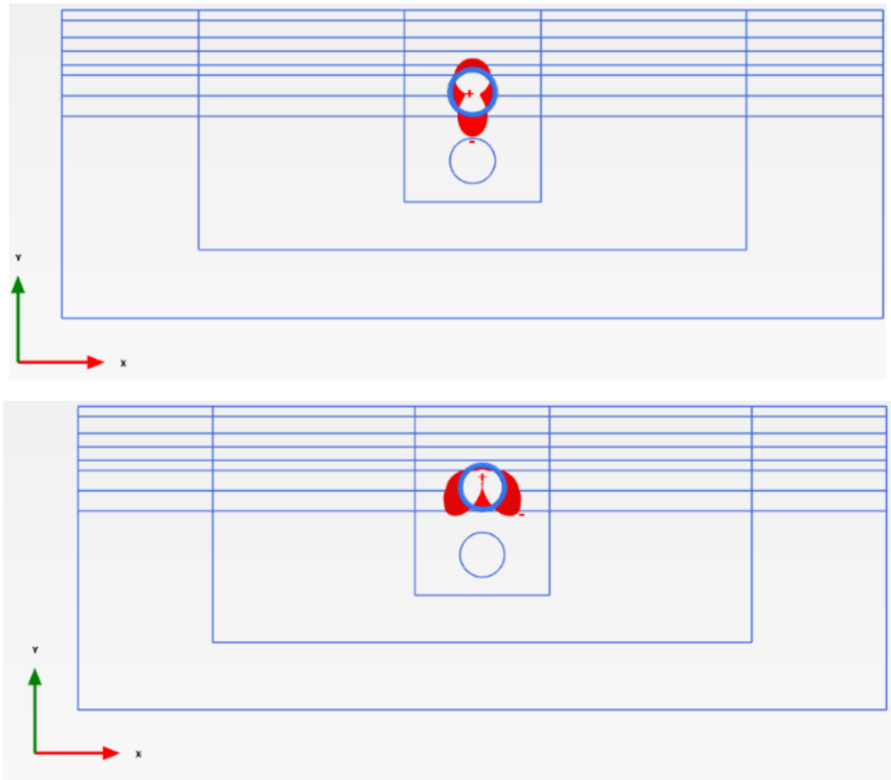

Figure 75 Distribution of moments P2=1.75,2.25,2.75 bar (up); Distribution of moments P2=3.25 bar (bottom)

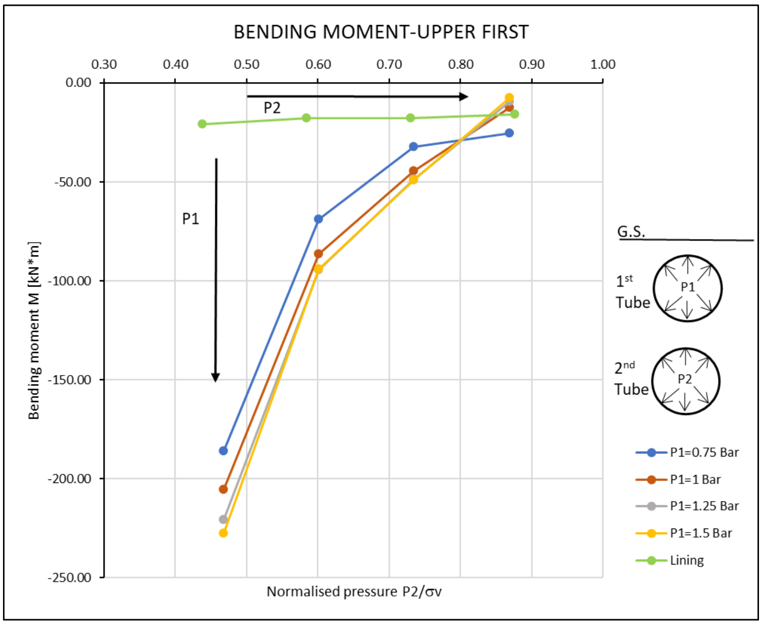

Figure 76 Negative Bending Moment - upper first

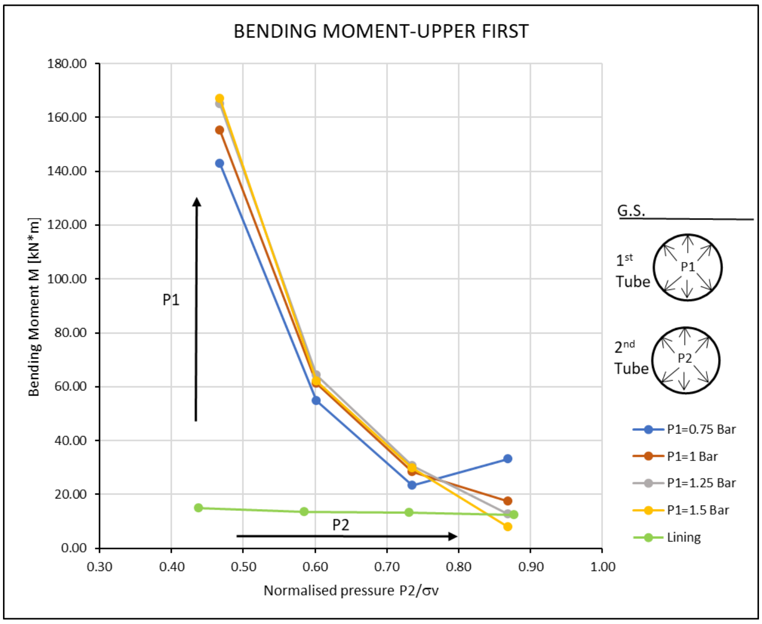

Figure 77 Positive Bending Moment - upper first

For the sake of completeness, axial forces which induce bending moments are calculated. The maximum negative bending moments correspond to the maximum axial forces, in fact the considerations are the same of N. The absolute maximum bending moment corresponds to the low P1 (0.75 bar) and maximum P2 (3.25 bar). Also the axial force which results for positive moments are calculated, however this analysis is explained in the chapter 6.3.2.6 M-N Interaction Diagram.

6.3.1.3 Eccentricity e

The eccentricity is the ratio between the bending moment and axial force. Due to the difference in sign of the moments, there are two eccentricities. The Table 12 show the maximum values: “e-“ means eccentricity due to negative moment, while “e+” means eccentricity for positive bending moment.

Table 12 Eccentricities - Upper tunnel first

P2 [kPa]	P2/σv	P1 [kPa]	e - [cm]	e + [cm]	P1 [kPa]	e - [cm]	e + [cm]
Lining	0.44	75.00	2.99	-2.51	100.00	2.22	-1.90
175.00	0.47	75.00	17.38	-21.31	100.00	18.53	-21.02
225.00	0.60	75.00	9.09	-9.19	100.00	10.30	-8.83
275.00	0.74	75.00	4.64	-3.97	100.00	5.62	-4.05
325.00	0.87	75.00	3.83	-4.86	100.00	1.67	-2.25

P2 [kPa]	P2/σv	P1 [kPa]	e - [cm]	e + [cm]	P1 [kPa]	e - [cm]	e + [cm]
Lining	0.44	125.00	2.36	-1.60	150.00	1.84	-1.33
175.00	0.47	125.00	28.83	-20.64	150.00	19.38	-19.61
225.00	0.60	125.00	10.02	-8.05	150.00	8.98	-10.29
275.00	0.74	125.00	5.35	-3.77	150.00	4.83	-3.25
325.00	0.87	125.00	1.11	-1.45	150.00	0.78	-0.83

The Figure 78 and Figure 79 show the trend of the eccentricities varying the two radial pressures. The red point on the drawing in the graphs, illustrate where they are calculated. In fact, they follow the behaviour of the moments to which they correspond.

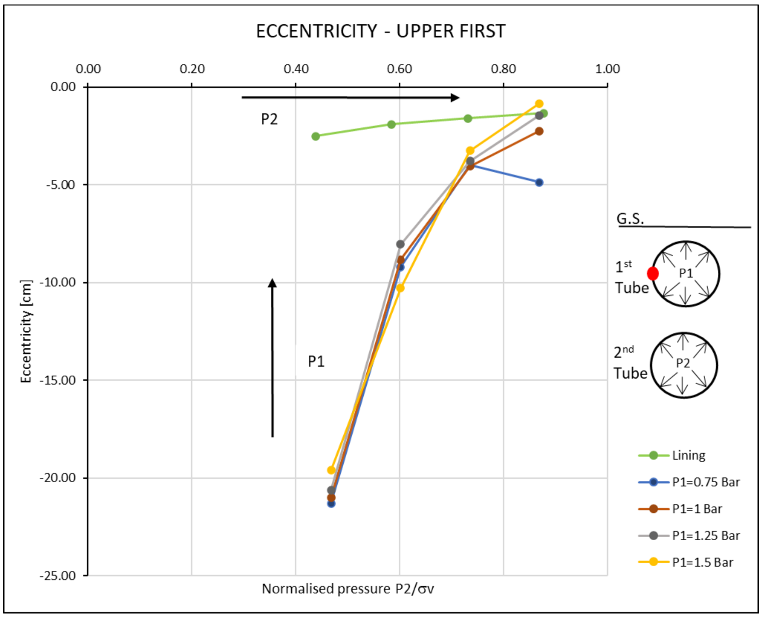

Figure 78 Eccentricity due to positive bending moments - Upper tunnel first

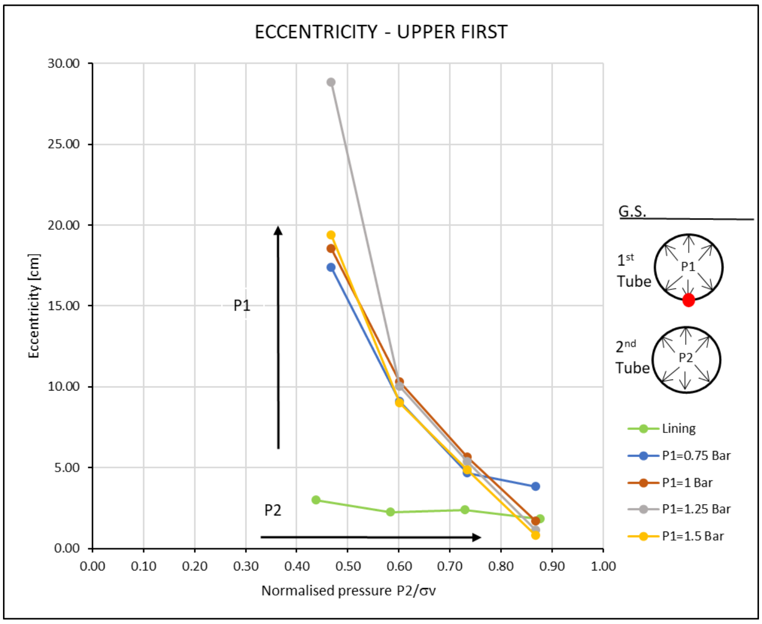

Figure 79 Eccentricity due to negative bending moments - Upper tunnel first

6.3.1.4 Vertical and Horizontal Ovalization

The ovalization explain how the lining deforms with respect to the diameter. The formula used in this thesis is:

$$ovalization_{vertical}\ [\%] = \frac{(D + u_{y,cap}) - (D + u_{y,invert})}{D}$$

$$ovalization_{horizontal}\ [\%] = \frac{(D + u_{x,right}) - (D + u_{x,left})}{D}$$

in order to taking into account the sign of the displacements. The displacement u_y or u_x can be positive or negative, due to the coordinate system on the software. In PLAXIS2D the results are plotted with the y-direction positive upwards and x-direction positive to the right.

Table 13 Vertical and Horizontal ovalization - Upper tunnel first

P2 [kPa]	P2/σv	P1 [kPa]	ova_vert [%]	ova_hor [%]	P1 [kPa]	ova_vert [%]	ova_hor [%]
Lining	0.44	75.00	0.01%	-0.02%	100.00	0.01%	-0.02%
175.00	0.47	75.00	0.11%	-0.11%	100.00	0.12%	-0.12%
225.00	0.60	75.00	0.03%	-0.03%	100.00	0.04%	-0.04%
275.00	0.74	75.00	0.01%	-0.01%	100.00	0.01%	-0.01%
325.00	0.87	75.00	-0.03%	0.03%	100.00	-0.02%	0.02%

P2 [kPa]	P2/σv	P1 [kPa]	ova_vert [%]	ova_hor [%]	P1 [kPa]	ova_vert [%]	ova_hor [%]
Lining	0.44	125.00	0.01%	-0.02%	150.00	0.01%	-0.02%
175.00	0.47	125.00	0.13%	-0.13%	150.00	0.13%	-0.13%
225.00	0.60	125.00	0.04%	-0.04%	150.00	0.04%	-0.04%
275.00	0.74	125.00	0.02%	-0.01%	150.00	0.02%	-0.01%
325.00	0.87	125.00	-0.02%	0.02%	150.00	-0.02%	0.02%

Obviously the two ovalizations are correlated each other, as the Figure 80 and Figure 81 demonstrate.

- In the vertical ovalization the negative sign means that the tunnel is pressed, while the positive sign means that the tunnel extends in y-direction;
- In horizontal ovalization the negative sign means that the tunnel is pressed, and the positive sign means that the tunnel expands in x-direction;
- It is possible to notice that in the phase of the installation of the lining, the ovalizations do not change varying the pressures P1. In this phase, the ring tends to move upwards, hence in the x-direction the relative horizontal displacement, with respect to the diameter, is reduced.
- Starting the excavation of the second tunnel down, the lining tends to elongate because of the creation of a void, as shown in Figure 82;
- By increasing the pressure P1, the ovalization increases; however P1, in particular from the value equal to 1 up to 1.5 bar, does not induce any effect on the horizontal ovalization.
- By increasing the pressure P2, both the ovalizations reduces, because of the higher pressure, the higher the soil is less deconfine, so the upper tunnel is not able to moves.
- At P2=3.25 bar, there is an inversion of the trend. In fact, the vertical direction has negative sign, which means that the lining start to be

compressed in the invert part (no more elongated as before), and this implies that along the x-direction the lining expands, as shown in Figure 83. This is probably due to the high excavation pressure of the bottom tunnel, which push the upper lining.

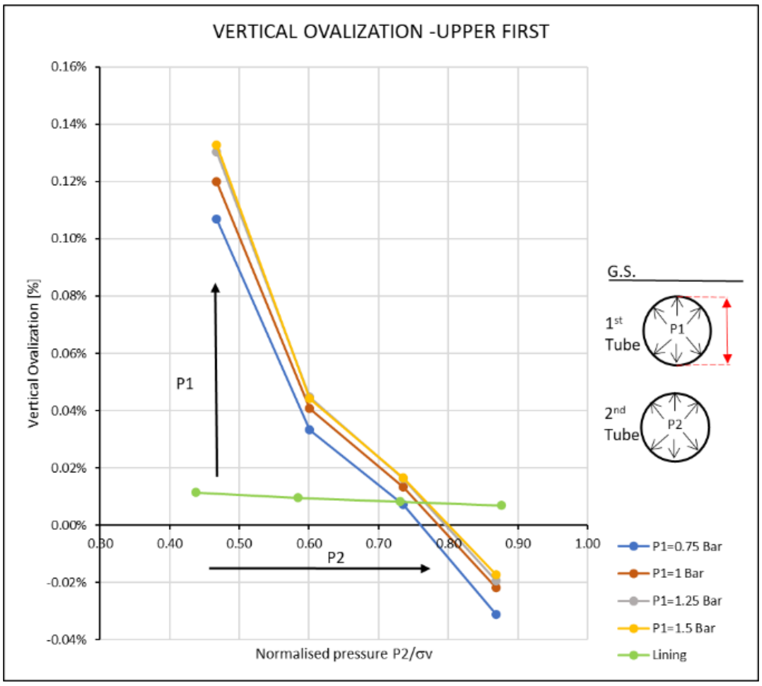

Figure 80 Vertical ovalization - Upper tunnel first

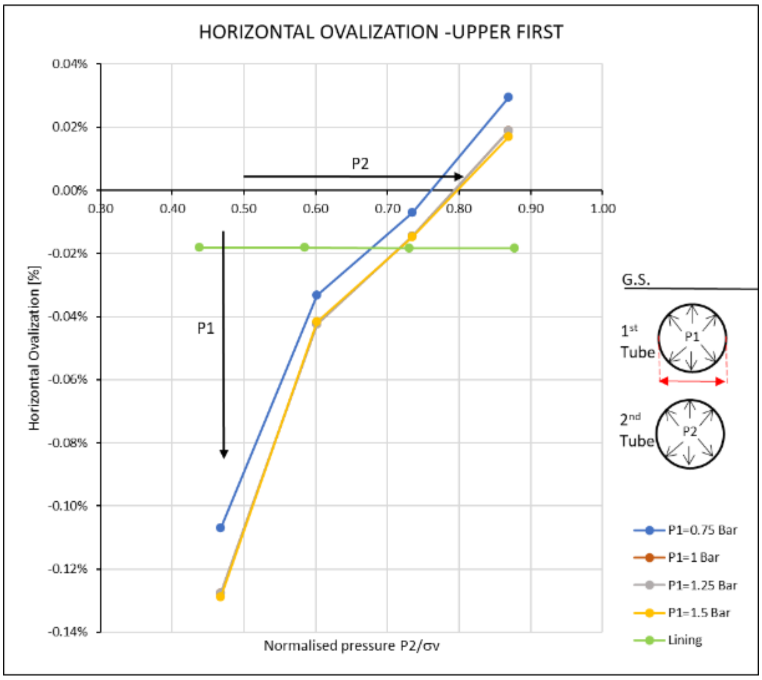

Figure 81 Horizontal ovalization - Upper tunnel first

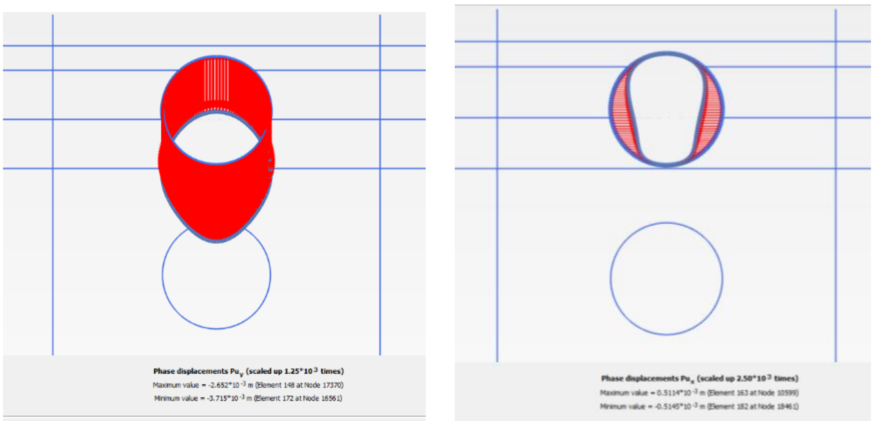

Figure 82 Zoom of the ovalization with P2=2.75 bar

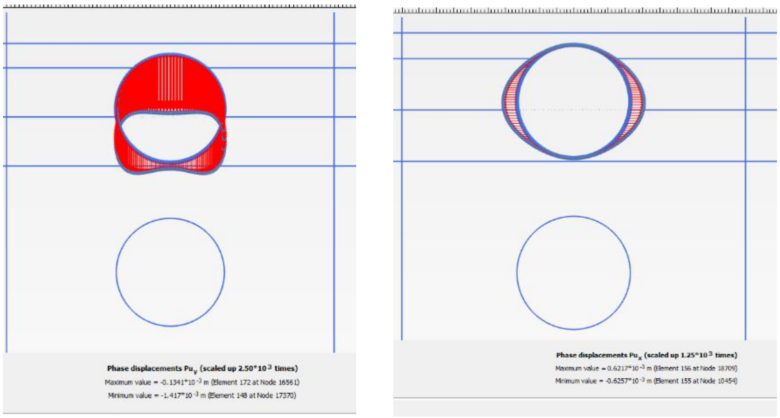

Figure 83 Zoom of the ovalization with P2=3.25 bar

6.3.1.5 Vertical Displacement

It has been analysed also only the vertical displacement of the invert of the upper tunnel. This analysis is performed in order to control the movement of the lining; this is important because in bottom part, there is the back-up of the machine during the construction, or if the upper tunnel is finished there can be facilities or trains.

Remembering the coordinate system, the y-direction is positive upwards. As shown in Table 14, positive values are present only during the installation of lining, which induce a lift of the tunnel. All the other are negatives, so the tunnel tends to move downwards, due to the void of the second tunnel.

Table 14 Vertical displacement - Upper tunnel first

P2 [kPa]	P2/σv	P1 [kPa]	uy_inv [mm]	P1 [kPa]	uy_inv [mm]	P1 [kPa]	uy_inv [mm]	P1 [kPa]	uy_inv [mm]
Lining	0.44	75.00	5.23	100.00	4.91	125.00	4.91	150.00	5.01
175.00	0.47	75.00	-33.89	100.00	-39.81	125.00	-44.70	150.00	-47.66
225.00	0.60	75.00	-7.54	100.00	-9.57	125.00	-11.08	150.00	-11.62
275.00	0.74	75.00	-2.00	100.00	-3.11	125.00	-3.88	150.00	-4.10
325.00	0.87	75.00	2.34	100.00	0.94	125.00	-0.69	150.00	-0.86

The Figure 84 shows the trend of the invert. By decreasing P1, also the vertical displacement decreases. Opposite trend, by increasing P2, in fact the vertical displacement decreases. Moreover, at the maximum excavation pressure P2 (3.25 bar), the lining reverses its trend and goes up, in particular when it is excavated at low pressures (0.75 bar), as can be seen in Figure 85.

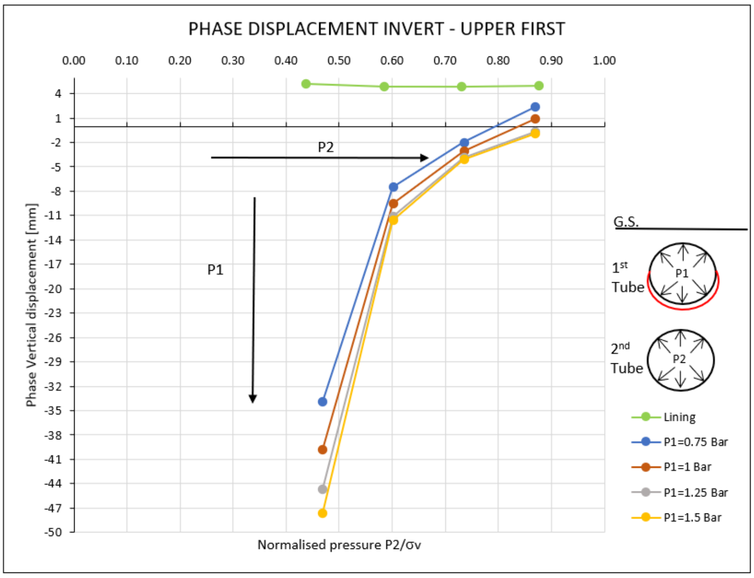

Figure 84 Phase displacement - Upper tunnel first

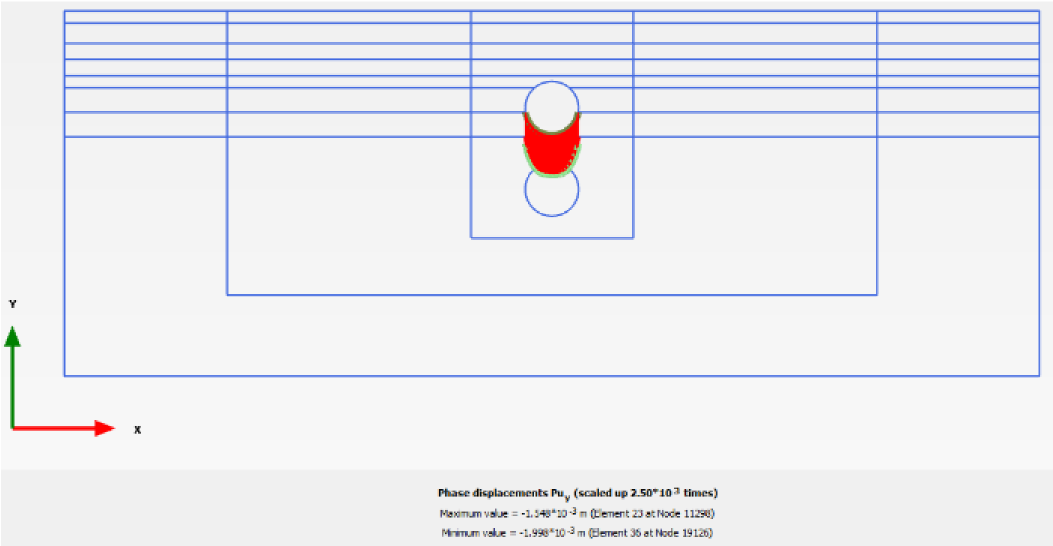

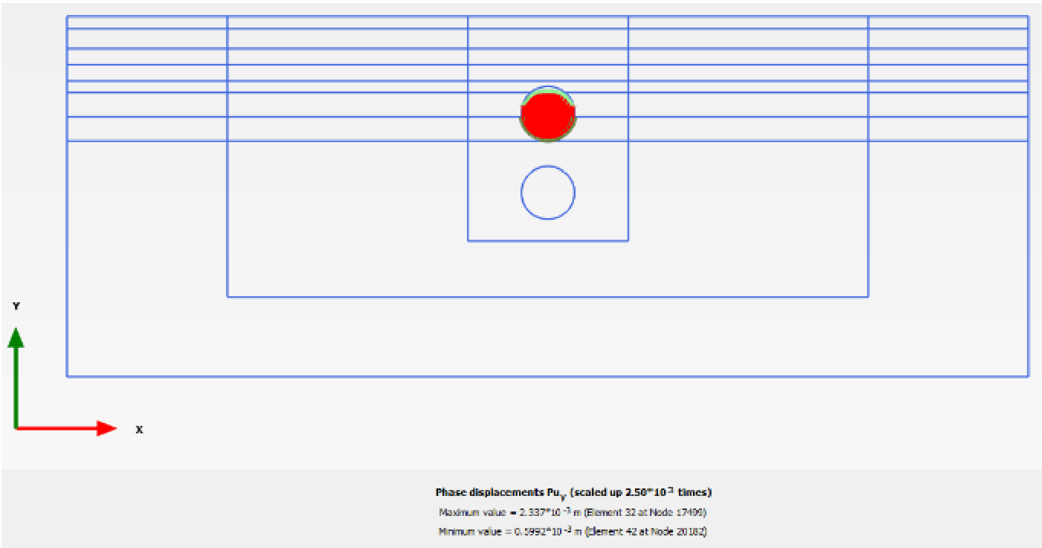

Figure 85 Example of vertical displacement of the invert with P2=2.75 bar (up) and P2=3.25 bar (bottom)

6.3.2 Excavation of bottom tunnel first

In this tunnel the situation is reversed. The configuration is represented in Figure 86.

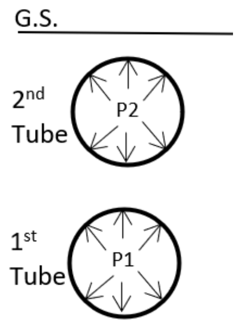

Figure 86 Scheme of excavation of bottom tunnel first

Where P1 is the internal radial pressure applied on the first excavated tunnel and P2 is that one applied on the second tube. The geometry does not change and the pressure P1 is represented by the different coloured lines, e.g. the blue line is the P1=1.75 bar.

6.3.2.1 Axial Force N

In the Table 15 the maximum values of the axial compression are presented.

Table 15 Axial Force N - Bottom tunnel first

P2 [bar]	P2/σv	P1 [bar]	N_max [kN]	P1 [bar]	N_max [kN]	P1 [bar]	N_max [kN]	P1 [bar]	N_max [kN]
Lining		175.00	1274.93	225.00	1453.59	275.00	1680.53	325.00	1913.01
75.00	0.44	175.00	1356.87	225.00	1436.11	275.00	1618.00	325.00	1809.88
100.00	0.58	175.00	1314.19	225.00	1440.09	275.00	1627.60	325.00	1828.60
125.00	0.73	175.00	1296.84	225.00	1442.05	275.00	1636.00	325.00	1841.73
150.00	0.88	175.00	1291.04	225.00	1432.73	275.00	1630.30	325.00	1832.96

By following the Figure 87 Axial Force - Bottom tunnel first:

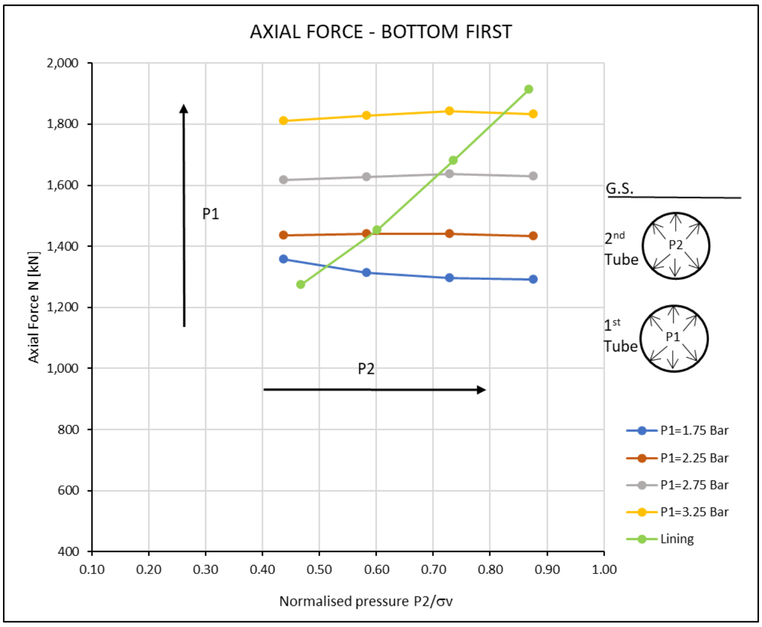

Figure 87 Axial Force - Bottom tunnel first

- The maximum values are all placed at the invert of the lining, at coordinate (0,-25.3);
- By increasing the pressure of the excavation of the first bottom tunnel P1, the effect on the lining increases.
- The excavation of the second tunnel does not have any effect on the bottom tunnel, as it is noticeable by the straight lines.
- In general the bottom tunnel has high values of axial force N due to the high depth at which it is placed respect to the upper tunnel.

6.3.2.2 Bending Moment M

The maximum values are reported in the Table 16 where each colour refers to the pressure P1.

Table 16 Bending Moment - Bottom tunnel first

P2 [bar]	P2/σv	P1 [bar]	M- [kN*m]	M+ [kN*m]	P1 [bar]	M- [kN*m]	M+ [kN*m]
Lining		175.00	-18.73	6.06	225.00	-11.50	1.88
75.00	0.44	175.00	-21.44	28.37	225.00	-62.16	35.20
100.00	0.58	175.00	-19.93	13.58	225.00	-60.62	34.31
125.00	0.73	175.00	-19.63	20.07	225.00	-50.40	28.55
150.00	0.88	175.00	-31.12	40.90	225.00	-34.77	20.08

P2 [bar]	P2/σv	P1 [bar]	M- [kN*m]	M+ [kN*m]	P1 [bar]	M- [kN*m]	M+ [kN*m]
Lining		225.00	-8.26	0.00	275.00	-7.50	0.00
75.00	0.44	225.00	-86.37	48.25	275.00	-86.16	44.56
100.00	0.58	225.00	-77.84	42.78	275.00	-78.99	40.45
125.00	0.73	225.00	-64.87	34.22	275.00	-66.89	34.61
150.00	0.88	225.00	-49.53	24.80	275.00	-51.33	26.64

The resulting moments are lower compared to the previous analysis. By increasing the excavation pressure P1, both the positive and negative bending moments increase too. Moreover, when the excavation of the upper tube starts, the effects on the bottom tunnel are beneficial because the moments reduce.

A particular consideration can be done on the blue line (P1=1.75 bar): at high excavation pressure P2 (1.5 bar) there is an increase of moments. This could be explained by that fact that the high pressure recompresses the around soil and the resulting moments on the bottom lining rise, as shown in Figure 88and Figure 89.

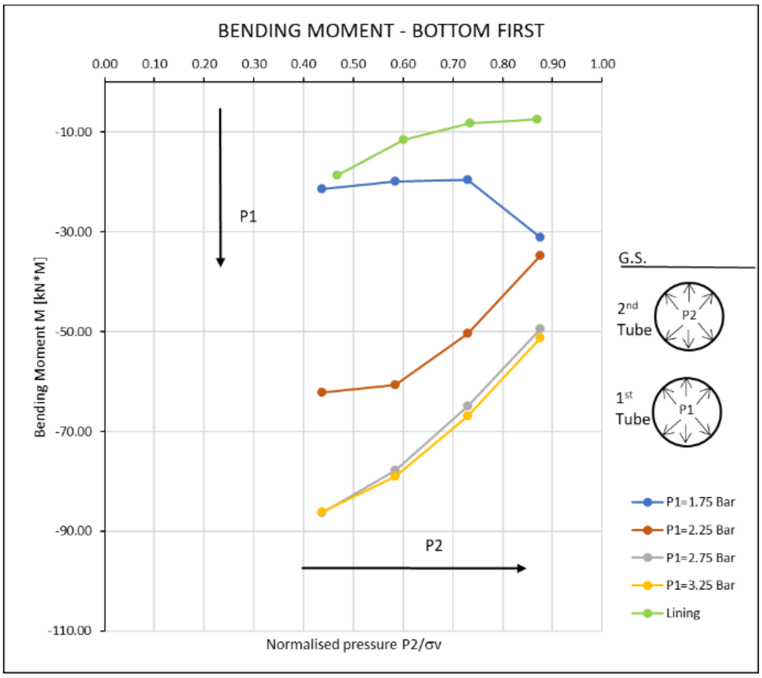

Figure 88 Negative Bending moment - bottom tunnel first

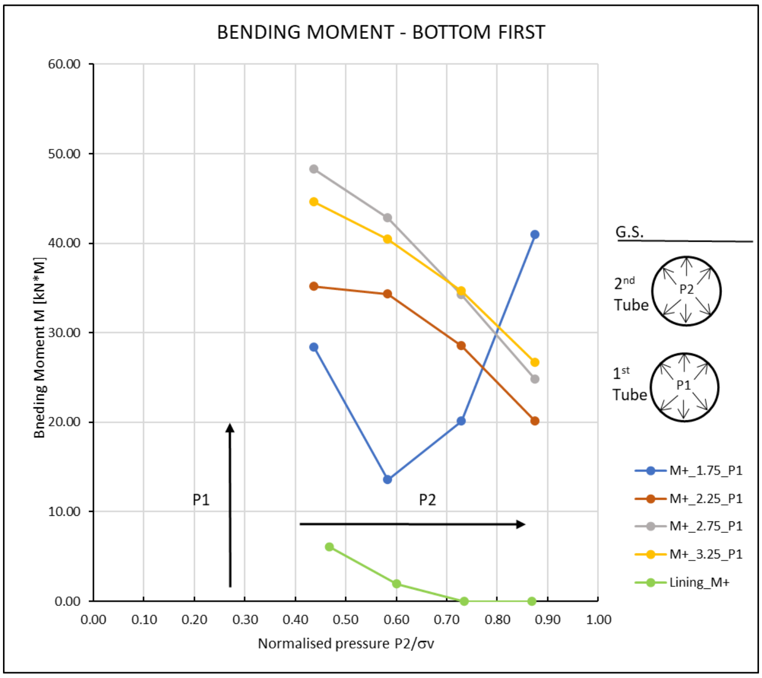

Figure 89 Positive Bending moment - bottom tunnel first

6.3.2.3 Eccentricity e

Also in this case, the eccentricities follow the behaviour of bending moments. The values of the eccentricity are lower compared to the previous case, due to the low bending moments and high axial forces.

Table 17 Eccentricities - Bottom tunnel first

P2 [bar]	P2/σv	P1 [bar]	e - [cm]	e + [cm]	P1 [bar]	e - [cm]	e + [cm]
Lining		175.00	1.47	-0.50	225.00	0.79	-0.13
75.00	0.44	175.00	1.71	-2.35	225.00	4.86	-2.76
100.00	0.58	175.00	1.52	-1.20	225.00	4.79	-2.69
125.00	0.73	175.00	1.51	-1.83	225.00	4.01	-2.22
150.00	0.88	175.00	2.68	-3.76	225.00	2.80	-1.54

P2 [bar]	P2/σv	P1 [bar]	e - [cm]	e + [cm]	P1 [bar]	e - [cm]	e + [cm]
Lining		225.00	0.55	0.01	275.00	0.43	0.02
75.00	0.44	225.00	5.91	-3.37	275.00	5.28	-2.78
100.00	0.58	225.00	5.34	-2.96	275.00	4.82	-2.48
125.00	0.73	225.00	4.46	-2.34	275.00	4.07	-2.10
150.00	0.88	225.00	3.43	-1.69	275.00	3.16	-1.60

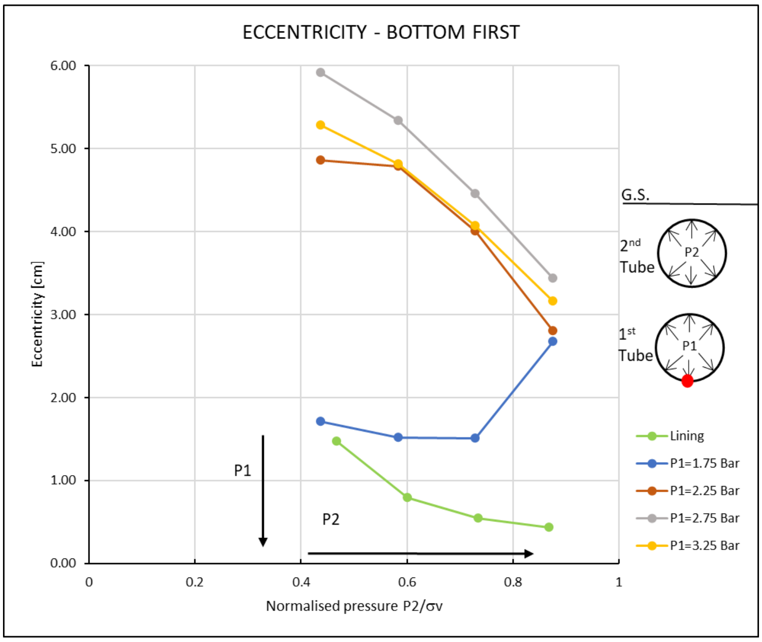

Figure 90 Eccentricity due to negative bending moment - bottom tunnel first

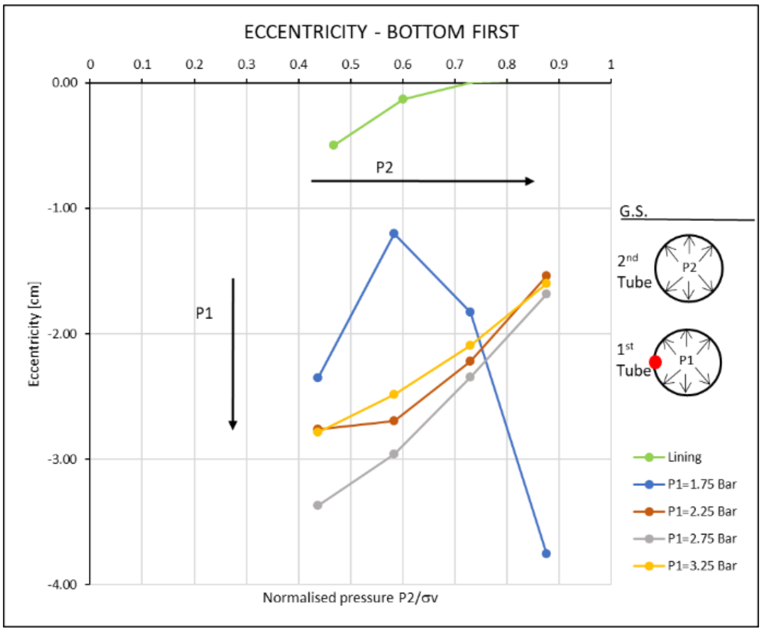

Figure 91 Eccentricity due to positive bending moment - upper tunnel first

6.3.2.4 Vertical and Horizontal Ovalization

As abovementioned, the positive sign of the vertical ovalization means the lining is stretching vertically, while the negative sign corresponds to a vertical compression of the ring. Instead the positive sign of the horizontal chord implies that the lining is getting wider, while in opposite sign that it is getting pressed.

The values are very low compared to the upper tunnel first, and this continues to demonstrate that the bottom tunnel is not affected by the excavation of the upper tunnel, if not in a positive way, especially if P2 increases.

Comment can be done on the lowest pressure P1=1.75 bar, which has an inverted behaviour with respect to the other pressures P1. With P2=0.75 bar, as shown in Figure 94, the vertical chord moves downward (negative sign) and the horizontal chord moves externally (positive sign).

Table 18 Vertical and horizontal ovalization - Bottom tunnel first

P2 [bar]	P2/σv	P1 [bar]	ova_vert [%]	ova_hor [%]	P1 [bar]	ova_vert [%]	ova_hor [%]
Lining		175.00	-0.001%	-0.011%	225.00	0.00%	-0.01%
75.00	0.44	175.00	-0.103%	0.013%	225.00	0.01%	-0.03%
100.00	0.58	175.00	-0.005%	0.003%	225.00	0.03%	-0.03%
125.00	0.73	175.00	-0.007%	0.004%	225.00	0.03%	-0.03%
150.00	0.88	175.00	-0.018%	0.014%	225.00	0.02%	-0.02%

P2 [bar]	P2/σv	P1 [bar]	ova_vert [%]	ova_hor [%]	P1 [bar]	ova_vert [%]	ova_hor [%]
Lining		225.00	-0.01%	-0.01%	275.00	-0.01%	-0.01%
75.00	0.44	225.00	0.04%	-0.04%	275.00	0.05%	-0.04%
100.00	0.58	225.00	0.04%	-0.04%	275.00	0.04%	-0.04%
125.00	0.73	225.00	0.03%	-0.03%	275.00	0.03%	-0.03%
150.00	0.88	225.00	0.03%	-0.02%	275.00	0.03%	-0.02%

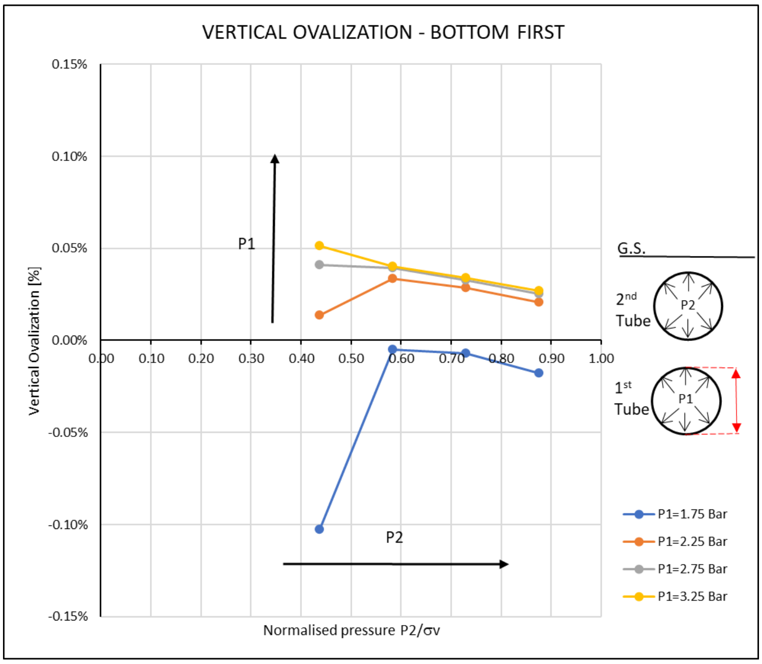

Figure 92 Vertical ovalization - Bottom tunnel first

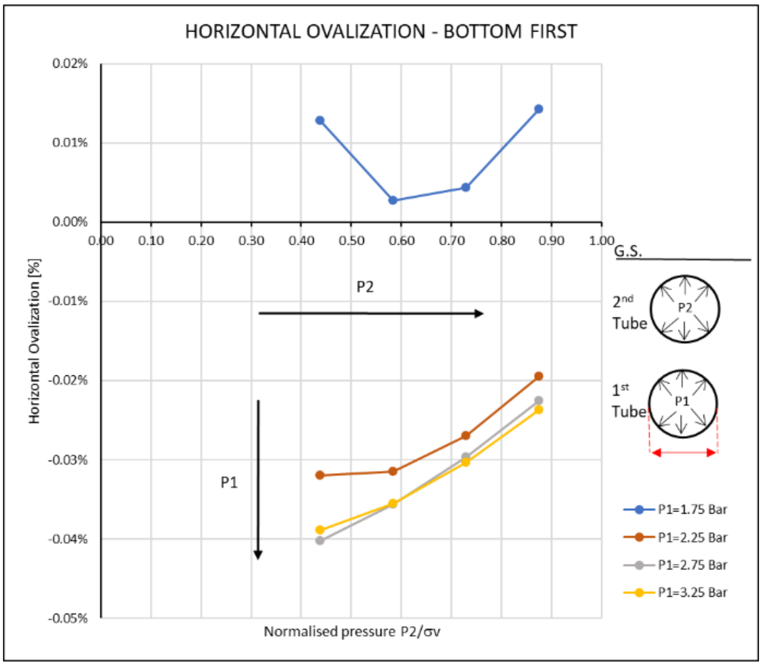

Figure 93 Horizontal ovalization - Bottom tunnel first

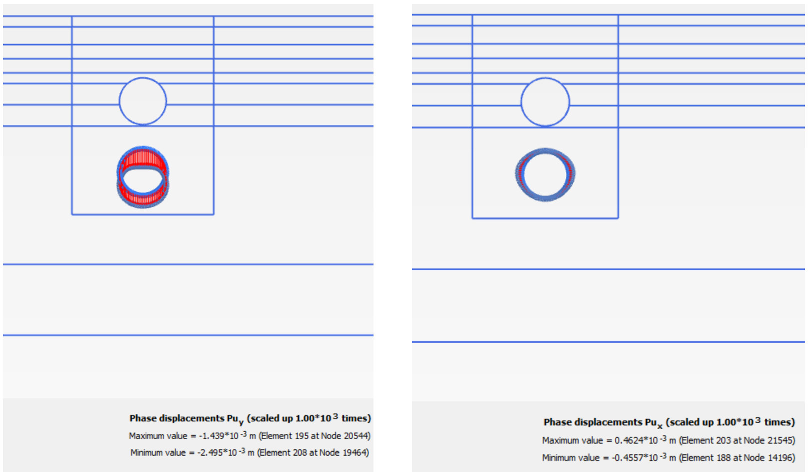

Figure 94 Zoom of ovalization for P2=0.75 bar

6.3.2.5 Vertical Displacement

The results of the vertical displacement show that the excavation of the above tunnel drives up the invert of the bottom tunnel, due to a decompression of the ground which occurs up, as it can be noticed from the positive sign of the Table 19. Only at low pressures P1 and P2, the lining moves down.

Table 19 Vertical Displacement - Bottom tunnel first

P2 [bar]	P2/σv	P1 [bar]	uy_inv [mm]	P1 [bar]	uy_inv [mm]	P1 [bar]	uy_inv [mm]	P1 [bar]	uy_inv [mm]
Lining		175.00	4.01	225.00	3.19	275.00	3.17	325.00	3.24
75.00	0.44	175.00	-1.27	225.00	2.66	275.00	3.83	325.00	4.68
100.00	0.58	175.00	-0.23	225.00	2.17	275.00	3.10	325.00	3.76
125.00	0.73	175.00	0.46	225.00	1.78	275.00	2.48	325.00	3.04
150.00	0.88	175.00	0.45	225.00	1.75	275.00	2.39	325.00	2.93

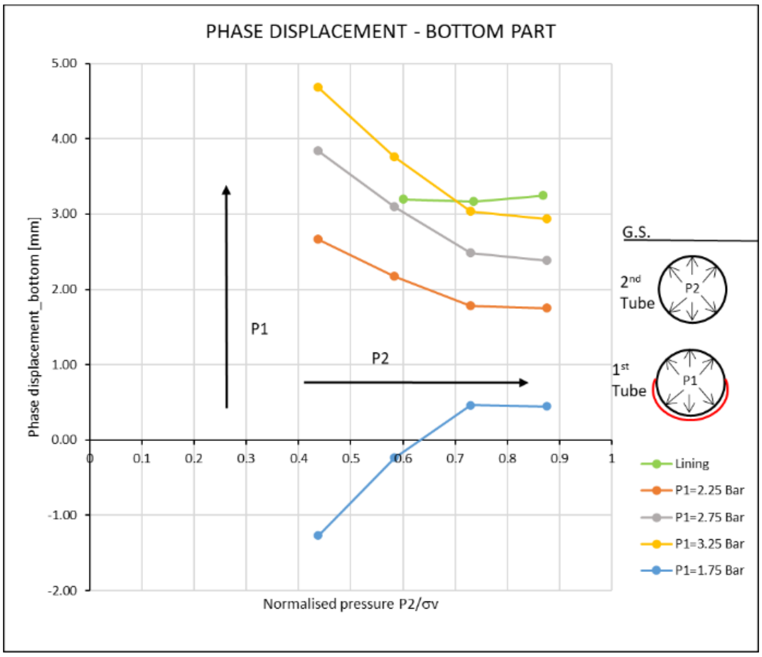

Figure 95 Vertical displacement - Bottom tunnel first

6.3.2.6 M-N Interaction Diagram

The interaction diagram allows the comparison between the actions applied on the tunnel and the strength of the tunnel lining. By all the previous chapters, the maximum values of axial force and positive and negative bending moments are plotted in the M-N dominium.

This analysis takes into account the Ultimate Limit State, as explained in the chapter 2.7.1 Ultimate Limit State.

For the construction of the M-N interaction diagram, some others information have to be described, in particular regarding rings, segments and reinforced. The concrete has a strength of C40/50, which means a cubic compressive strength of 50 MPa. The reinforcements are made with a steel yielding strength of 500 MPa.

These reinforcements are placed in circumferential and longitudinal directions in the entire rings and in longitudinal and circumferential directions for resisting to spalling and bursting phenomena.

From the Figure 96 it is possible to state that the excavation of the bottom tunnel first is safer in terms of values away from the maximum admissible values on the black curve. As demonstrate before, to excavate the bottom tunnel first result in high compression of the lining and low bending moments. While starting from top tunnel induces very high value of bending moments; in fact one point is out of the interaction curve, meaning the ULS is overpassed. This red point corresponds to the high excavation pressure P1=1.5 bar and the lower P2=1.75 bar, and it is placed on the exactly on the invert of the lining.

Finally the excavation sequence of upper tunnel first has more effects on the stresses and strains on the rings of the first tube, compared to the construction of the bottom tunnel first, which is not too much affected by the excavation of the above tube.

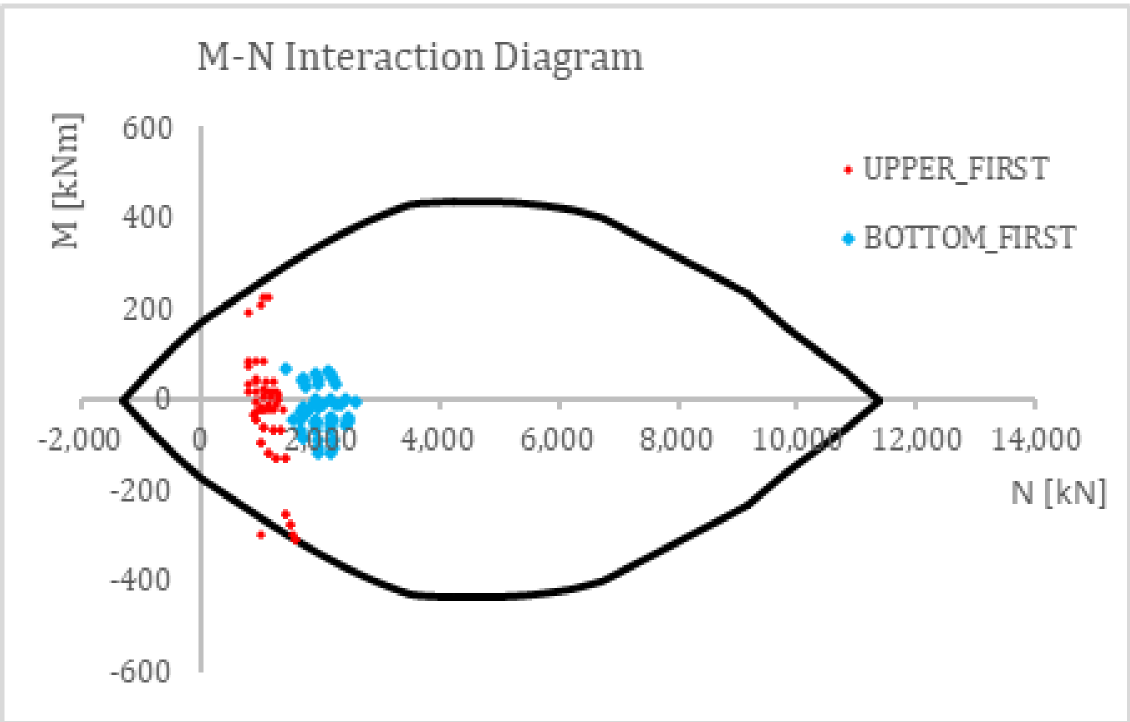

Figure 96 M-N Interaction Diagram

CONCLUSIONS

In this thesis was analysed the loads and the deformations on the segmental tunnel lining induced by the excavation of the twin tunnels performed with an Earth Pressure Balance, taking as reference the project of the fifth metro line of Bucharest, realised by the company SYSTRA SWS. In the design of M5, the two shallow tubes pass from a horizontal configuration, an offset configuration and finally vertical configuration. The reason why of the change in the alignment is due to the available space close to the stations.

The thesis focuses on the creation of numerical models to understand if the selected segmental lining is able to resist to the loads applied by the soil and those induced by the construction of a second tunnel and how it deforms under these actions. After the analysis of the numerical results, the final expectation of the thesis is to highlight what is the better construction sequence between the excavation of upper tunnel first or bottom tunnel first.

Three different numerical models are carried out: the three-dimensional model with MIDAS FEA NX, the other two models are two-dimensional with PLAXIS2D. The 3D model is able to simulate the real construction sequence, following the passage of the EPB machine up to the installation of the lining. For the 2D models, two different methods are applied for the simulation of the three-dimensionality: the method of the deconfinement and the method of application of an internal radial pressure. The method of deconfinement implies the application of a reduction coefficient on the geostatic pressure in order to have a fixed volume loss on the surface; in this thesis two values of volume loss are fixed, 0.5% and 1%. Instead, the internal radial pressures method simulates the support pressure at the face front: four different pressures are considered for each tunnel. P1 is the applied pressure on the first tunnel and P2 is the applied pressure on the second tunnel.

In the 3D models, the vertical alignment is selected for the analysis; then the first 2D model compares three layouts: horizontal, offset and vertical arrangements. The second 2D model focus on the vertical arrangement because of it is not widely used. Summarizing the remarks are:

- Based on the results achieved through the 3D model it is possible to draw some relevant conclusions as follow:
    1. The comparison between the different sequence of tunnel excavation (top tunnel excavated first or bottom tunnel excavated first) is carried out in terms of stresses in the lining. According with axis orientation in FEA NX, the stresses σ_{zz} are the one representative for the sidewalls, while the stresses σ_{xx} are the ones representative for the crow and invert .
    2. It is evident how the sequence of the excavation does not have any relevant impact in terms of vertical stresses in the lining, limited to the sidewalls. In fact stresses variations are not registered for both cases (they remain almost constant), and this is reasonable since the sidewalls are not directly affected by the ovalization of the tunnel.
    3. On the contrary, referring to the state of stresses at the crown and invert, it is evident how excavating the top tunnel first and bottom in a second stage, the latter one will induce deformations to the above tunnel with the risk of occurrence of very low compressive stresses. In other words, the already excavated tunnel above, due to the excavation of the bottom tunnel, will deform in a way that some tensile stresses could be achieved, with consequent risk of segments joints opening.
    4. If the tunnel below is excavated first and the tunnel above is excavated in a second stage in a de-tensioned soil, the tunnel above will still have enough compressive stress, minimizing again the risk

of occurrence of tensile stresses and, as consequence the risk of joints opening. On the other hand, the bottom tunnel will be obviously subjected to an increasing of the compressive stresses that need to be properly checked with the structural capacity of the lining itself.

- Among the three analysed layouts for the first 2D model, the axial force N and the bending moment M are extracted. In the horizontal configuration, the worst condition is the excavation of the second tunnel, close to the first, with a fixed volume loss of 0.5%. In the off-set layout the bending moments and the axial forces are maximum when the left bottom tunnel starts before, with the fixed volume loss of 0.5%. The vertical arrangement shows the maximum values in the bottom tunnel when the lining is installed, this can be explained by a stress-release when the upper tunnel is constructed. Plotting the three layouts together, the vertical arrangement exhibits the highest value for the induced axial force, while the moments are practically the same between vertical and offset.
- The results of the second 2D model are the axial force N, positive and negative bending moments, eccentricities, horizontal and vertical ovalization and vertical displacement of the invert.
    1. AXIAL FORCE: if the upper tunnel is constructed first, it increases with the increasing of the internal radial pressure applied on the first tunnel and it decreases with the increasing of the excavation pressure of the second tunnel. If the bottom tunnel is constructed first, the axial force increases with the increasing of the excavation pressure P1, but it does not change with the excavation of the upper tunnel.
    2. BENDING MOMENT: if the upper tunnel is constructed first, it increases with the pressure P1 and it decreases with the increasing pressure P2. The trend is the same for the construction of bottom tunnel first, however the numerical values are lower compared to the previous case.

3. ECCENTRICITY: all the resulting eccentricities follow the behaviour of the bending moment. The result of the bottom tunnel first shows lower eccentricity due the higher axial forces and lower bending moment.
4. OVALIZATION: if the upper tunnel is constructed first, the segmental tunnel lining tends to elongate in vertical direction and to shrink in horizontal direction. When the maximum support pressure on the second tunnel is applied, the behaviour of the ovalization reverses its trend: an expansion in horizontal direction and a compression in vertical direction is induced. If the bottom tunnel starts first, the ovalization is reduced by the increasing of the excavation pressure of the upper tunnel. Also in this case, the maximum values are induced when the upper tunnel is excavated first.
5. VERTICAL DISPLACEMENT OF THE INVERT: this parameter is evaluated in order to consider future infrastructures inside the tunnel. If the upper tunnel goes first, the vertical displacement increasing with the increase of the P1 pressure, and it lowers with the increasing of the bottom tunnel excavation pressure. At the highest pressure P2, there is a heave on the invert. If the bottom tunnel is constructed first, the invert goes upwards always by the increasing of the P1. It has lower value of uplifting for higher pressures P2 because the soil is more confined. When P1 and P2 have the lowest values, the invert goes down.
6. Finally, the best way to compare the two different construction sequences is the M-N interaction diagram which combines the resistances of the segmental tunnel linings with the loads. The curve is constructed considering concrete with strength of C40/50 and different orientated reinforcements. The couples M-N, resulted from

the numerical modelling activity, are increased with the partial coefficient for the ULS analysis, and plotted in the interaction diagram. It shows that starting with the construction of upper tunnel first, it induces higher bending moments and lower axial forces, which means being close to the maximum admissible safe value for the ring sections.

At the end it is possible to conclude that in terms of stresses in the lining and tunnel ovalization, it will be preferable to excavate first the bottom tunnel and after the above tunnel. This has been confirmed and validated through both 3D and 2D numerical models. Another comparative analysis of alternatives of tunnel excavation sequences has been also performed in terms of induced settlements, by (Tremaggi, 2022). In this case the optimal sequence of excavation, to minimize the effects at the ground surface, is the opposite of what has been identified through the stresses analyses, which means that preferable configuration should be to excavate first the upper tunnel and then the bottom one.

As general conclusion, if we focus mainly on the tunnels system structure and on its operation and durability during the service life, and in case the surroundings are not so sensible (not very dense urban area or buildings with low vulnerability index), it may be convenient to choose the solution which consists in excavating first the bottom tunnel and after that the top tunnel. This will allow to maximize the structural performance of the structure, discounting a local increase of surface settlements. In case the surroundings at ground surface are very sensible and densely built, the preferable solution could be to excavate first the top tunnel and after the bottom tunnel. This will have a beneficial effect on the risk of damages to the existing structures but will imply more attention on the structural design of the tunnel lining. Furthermore, in order to response to the high stress level, it is possible to increase the steel ratio to adsorb induced flexural stresses and/ or improved connection elements, like connectors or dowels between segments.

Acknowledgement

I want to thank the professor PEILA Daniele, who made me discover and passionate to the tunnel’s world.

I want to express my gratitude to the team’s company SYSTRA SWS, in particular the Engineer PALOMBA Michele, Engineer FANTINI Paolo, Engineer FERRANTI Matteo, Engineer IASIELLO Cosimo and all the master’s engineers, who sustain and support me in moments of joy and hard times, teaching me knowledge, dedication and love for this job.

Bibliography

AASHTO DCRT-1- Technical Manual for Design and Costruction of Road Tunnels. - 2010.

ACI-544.7R American Concrete Istitute Report on design and construction of fibre-reinforced precast concrete tunnel segments. - 2016.

AFTES Considerations on the Usual Method of Tunnel Lining Design. - 1993.

AFTES Reccomandations for the design, sizing and construction of a precast concrete segments installed in the rear of a tunnel boring machine. - 2005.

AFTES Recommendations for the design, production and installation of segmental rings. - 2013.

Anagnostou G. and Kovàri K. Face stability condition with Earth Pressure Balanced Shields. - [s.l.] : Tunneling and Underground Space Technology, 1996a.

Bakhshi M. e Nasri V. Practical aspects of segmental tunnel linings design. . - 2013.

Bezuijen A. and Dias T. TBM Pressure Models - Observations, Theory and Practice. - 2015.

Blom C.B.M. Design philosophy of concrete linings in tunnels in soft soils. - 2002.

DAUB Recommendations for Face Support Pressure Calculations for Shield Tunneling in Soft Ground. - 2016.

DAUB Recommendations for the design, production and installation of segmental rings. - 2014.

Do Ngoc-Anh and Dias Daniel, Oreste, Pierpaolo Three-dimensional numerical simulation of mechanized twin stacked tunnels in soft ground. - 2014.

EN Eurocode 2: Design of concrete structure - Part 1-1: General rules and rules for buildings. - 1992-1-1:2004.

Gao Shi-ming, Chen Jian-ping and Zuo Chang-qun, Wang-Wei Monitoring of Three-dimensional Additional Stress and Strain in Shield Segments of Former Tunnels in the Construction of Closely-Spaced Twin Tunnels. - 2016.

Guglielmetti Vittorio Mechanized tunnelling in urban areas: design methodology and construction control. - 2007.

ITA Working Group 2 DAMAGES OF SEGMENTAL LINING. - 2018.

ITA Working Group 2 Guidelines for the design of segmental tunnel lining. - Aprile 2019.

ITAtech Activity Group Guideline For Good Practice Of Fibre Reinforced Precast Segment - Vol. 2 : Production Aspects. - 2018.

Iyengar K.T. Two-Dimensional Theories of Anchorage Zone Stresses in Post-Tenioned Beams. - 1962.

JSCE Standard Specifications for Tunneling: Shield Tunnels. - 2007.

Loganathan N. e Poulos H. G. Pile response caused by tunneling. - 1998.

Maidl B. [et al.] Mechanised Shield Tunnelling, 2nd Edition. - 2011.

Maraveas Chrysanthos and Vrakas Apostolos Design of concrete tunnel lining for fire safety. - [s.l.] : Structural Engineering International, 2014.

Miur Wood A. M. The Circular Tunnel in Elastic Ground. - 1975.

Morgan H.D. A Contribution to the Analysis Stress in a Circular Tunnel. - 1961.

Obrzud Rafa l F. and Truty Andrzej THE HARDENING SOIL MODEL-A PRACTICAL GUIDEBOOK. - 2018.

Panet M. e Guellec P. Contribution à l'étude du soutènement d'un tunnel à l'arrière du front de taille.. - 1974.

Shah R [et al.] Influencing factors affecting the numerical simulation of the mechanized tunnel ecavation using FEM and FDM techniques. - 2017.

Technology Austrian Society for Concrete and Construction Guidelines for Concrete Segmental Lining Systems. - 2011.

Tremaggi P. 3D and 2D Numerical Models of mechanised excavation of overlapped tunnels in urban area: sensitivity analysis for the evaluation of induced settlements and building damage varying the excavation sequence. - 2022.

Wael Abd Elsamee Effect of Lining Thickness on the Behaviour and on the Distance between two adjacent circular tunnel. - 2019.

Yang Zhiyong [et al.] Study of the Construction Sequence of Overlapping Tunnels by the Shield Tunneling Method: a Case Study of the Longest Overlapping Tunnel in China. - 2020.

Figure Index

Table Index